Forschungsberichte aus dem
Institut für Nachrichtentechnik des
Karlsruher Instituts für Technologie

Jens Elsner

Interference Mitigation in Frequency Hopping Ad Hoc Networks

Band 29

Druck: Druckcooperative
Steinstraße 23
76133 Karlsruhe

ISSN: 1433-3821

Forschungsberichte aus dem Institut für Nachrichtentechnik des Karlsruher Instituts für Technologie
Herausgeber: Prof. Dr. rer. nat. Friedrich Jondral

Band 1	Marcel Kohl **Simulationsmodelle für die Bewertung von Satellitenübertragungsstrecken im 20/30 GHz Bereich**
Band 2	Christoph Delfs **Zeit-Frequenz-Signalanalyse: Lineare und quadratische Verfahren sowie vergleichende Untersuchungen zur Klassifikation von Klaviertönen**
Band 3	Gunnar Wetzker **Maximum-Likelihood Akquisition von Direct Sequence Spread-Spectrum Signalen**
Band 4	Anne Wiesler **Parametergesteuertes Software Radio für Mobilfunksysteme**
Band 5	Karl Lütjen **Systeme und Verfahren für strukturelle Musteranalysen mit Produktionsnetzen**
Band 6	Ralf Machauer **Multicode-Detektion im UMTS**
Band 7	Gunther M. A. Sessler **Schnell konvergierender Polynomial Expansion Multiuser Detektor mit niedriger Komplexität**
Band 8	Henrik Schober **Breitbandige OFDM Funkübertragung bei hohen Teilnehmergeschwindigkeiten**
Band 9	Arnd-Ragnar Rhiemeier **Modulares Software Defined Radio**
Band 10	Mustafa Mengüç Öner **Air Interface Identification for Software Radio Systems**

Forschungsberichte aus dem Institut für Nachrichtentechnik des Karlsruher Instituts für Technologie

Herausgeber: Prof. Dr. rer. nat. Friedrich Jondral

Band 11	Fatih Çapar **Dynamische Spektrumverwaltung und elektronische Echtzeitvermarktung von Funkspektren in Hotspotnetzen**
Band 12	Ihan Martoyo **Frequency Domain Equalization in CDMA Detection**
Band 13	Timo Weiß **OFDM-basiertes Spectrum Pooling**
Band 14	Wojciech Kuropatwiński-Kaiser **MIMO-Demonstrator basierend auf GSM-Komponenten**
Band 15	Piotr Rykaczewski **Quadraturempfänger für Software Defined Radios: Kompensation von Gleichlauffehlern**
Band 16	Michael Eisenacher **Optimierung von Ultra-Wideband-Signalen (UWB)**
Band 17	Clemens Klöck **Auction-based Medium Access Control**
Band 18	Martin Henkel **Architektur eines DRM-Empfängers und Basisbandalgorithmen zur Frequenzakquisition und Kanalschätzung**
Band 19	Stefan Edinger **Mehrträgerverfahren mit dynamisch-adaptiver Modulation zur unterbrechungsfreien Datenübertragung in Störfällen**
Band 20	Volker Blaschke **Multiband Cognitive Radio-Systeme**

Forschungsberichte aus dem Institut für Nachrichtentechnik des Karlsruher Instituts für Technologie
Herausgeber: Prof. Dr. rer. nat. Friedrich Jondral

Band 21	Ulrich Berthold **Dynamic Spectrum Access using OFDM-based Overlay Systems**
Band 22	Sinja Brandes **Suppression of Mutual Interference in OFDM-based Overlay Systems**
Band 23	Christian Körner **Cognitive Radio – Kanalsegmentierung und Schätzung von Periodizitäten**
Band 24	Tobias Renk **Cooperative Communications: Network Design and Incremental Relaying**
Band 25	Dennis Burgkhardt **Dynamische Reallokation von spektralen Ressourcen in einem hierarchischen Auktionssystem**
Band 26	Stefan Nagel **Portable Waveform Development for Software Defined Radios**
Band 27	Hanns-Ulrich Dehner **Interferenzuntersuchungen für inkohärente Multiband Ultra-Breitband (UWB) Übertragung**
Band 28	Maximilian Hauske **Signalverarbeitung für optoelektronische Sensoren**
Band 29	Jens Elsner **Interference Mitigation in Frequency Hopping Ad Hoc Networks**

Vorwort des Herausgebers

Der Erfolg öffentlicher Mobilfunknetze basiert darauf, dass die Endgeräte einfach sind und kostengünstig hergestellt werden können. Der Funk dient hier der Anbindung an das Festnetz, welches die Organisation des Gesamtsystems übernimmt. Funkgeräte in zellularen Netzen kommunizieren mit einer Basisstation, in *Wireless Local Area Networks* (WLANs) mit einem *Access Point*. Die Basisstationen oder die Access Points steuern das Funksystem.

In Netzen ohne Infrastruktur muss die Organisation notwendigerweise über Funk erfolgen. Es handelt sich um selbstorganisierende oder ad-hoc Netzwerke. Typische Beispiele sind drahtlose Sensornetzwerke, Netzwerke, die von Hilfs- und Rettungsorganisationen (Rotes Kreuz, Polizei, Technisches Hilfswerk) im Einsatz benutzt werden oder auch der taktische Truppenfunk. Adhoc Netzen werden, wie Zellen in einem zellularen Netz, Funkkanäle zugewiesen, auf denen sie übertragen dürfen. Die Übertragungen werden, zumindest zum Teil, vom Sender über mehrere Teilnehmer zum Empfänger transportiert (Multi Hop), d.h. es wird nach dem Relaisprinzip gearbeitet. Da ad-hoc Netze weitverzweigt sein können, kommen natürlich Fragen nach der maximal möglichen Teilnehmerzahl, die hier nicht behandelt wird[1], und nach der Zuordnung der Kanäle zu den Übertragungsstrecken auf. Diese Zuordnung muss so vorgenommen werden, dass innerhalb des Netzes eine möglichst große Übertragungskapazität, gemessen z.B. in Bit pro Sekunde, Hertz und Quadratmeter, zur Verfügung steht. Das Dilemma für den Nachrichtentechniker besteht nun darin, dass Netze informationstheoretisch nicht so ausführlich untersucht sind wie Punkt-zu-Punkt-Verbindungen (Shannontheorie).

Die Dissertation *Interference Mitigation in Frequency Hopping Ad Hoc Networks* von Jens Peter Nils Elsner liefert einen interessanten Beitrag zur Kanalnutzung in ad-hoc Netzen, den der Autor im Jahr 2011, gemeinsam mit Ralph Tanbourgi, zum Patent angemeldet hat. Dabei geht es um die Organisation großer ad-hoc Netzwerke bezüglich des Mediumzugriffs. Die angebotene Lösung besteht in der Nutzung des *Multi-Level Locally Orthogonal* (MLLO) *Frequency Hopping* (FH) mit *Parallel Rendezvous*-Protokoll. Obwohl die vorliegende Arbeit in weiten Teilen theorieorientiert ist, sind wesentliche Ergebnisse bereits in eine auf europäischer Ebene laufende Studie, die Simulatoren für künftige Cognitive Radio Netzwerke bereitstellen wird, eingeflossen.

Das in der Arbeit vorgeschlagene Prinzip des MLLO-FH ist ein in Technik und Wissenschaft vollständig neuer Ansatz zur Interferenzminimierung in ad-hoc Netzwerken. Die Leistung von Jens Elsner liegt nicht nur in der Entwicklung des Prinzips sondern insbesondere auch in dessen theoretischer Durchdringung, im Nachweis seiner Leistungsfähigkeit und in der Einbringung des Ansatzes in die Anwendung.

Karlsruhe, im Dezember 2012

Friedrich Jondral

[1] Hierzu gibt der Aufsatz *The Capacity of Wireless Networks* von P. Gupta und P. Kumar, *IEEE Transactions on Information Theory, vol. 46, 2000, pp. 388-404* Antworten.

Interference Mitigation in Frequency Hopping Ad Hoc Networks

Zur Erlangung des akademischen Grades eines

DOKTOR-INGENIEURS

von der Fakultät

Elektrotechnik und Informationstechnik

des Karlsruher Instituts für Technologie

genehmigte

DISSERTATION

von

Jens Peter Nils Elsner

geboren in

Göttingen

Tag der mündlichen Prüfung:	04. Dezember 2012
Hauptreferent:	Prof. Dr. rer. nat. Friedrich K. Jondral
Korreferenten:	Prof. Dr. Gabi Dreo Rodosek
	Prof. Dr. Jeonghoon Mo

Zusammenfassung

Funkgeräte bieten heutzutage eine hohe Flexibilität, die bis vor wenigen Jahren noch nicht technisch möglich war. Die Signalverarbeitung in Funkgeräten vor und nach der Analog-Digital-Wandlung kann nach den unter dem Begriff *Software Defined Radio* zusammengefassten Techniken extrem flexibel gestaltet werden und erlaubt es, verschiedene Funkstandards in verschiedenen Frequenzbereichen mit dem gleichen Gerät zu implementieren. In Folge dieser Entwicklung sind Architekturen entstanden, die eine große Bandbreite wählbarer Mittenfrequenzen, zum Teil über mehrere GHz im UHF-Bereich, bieten.

Diese Bandbreitenflexibilität wird bisher in existierenden Funkprotokollen nur in geringem Maße ausgenutzt. Besonders in robusten ad hoc Netzen, die eine selbstorganisierende Kommunikation zwischen vielen Netzteilnehmern ermöglichen sollen, kann diese Flexibilität große Vorteile bieten. Dies gilt insbesondere dann, wenn die ad hoc Netze in einer Funkumgebung betrieben werden, die durch Störungen und andere Systeme geprägt ist. Im Fokus dieser Arbeit stehen Techniken zur Interferenzreduktion und zur Erzielung hoher Robustheit der Datenübertragung in solchen Funknetzen. Zu diesem Zweck werden zwei bekannte Ansätze angepasst, kombiniert und analysiert: Adaptive Frequenzsprungverfahren und mehrkanaliger Medienzugriff.

Die Leistungsfähigkeit adaptiver Frequenzsprungverfahren wird zunächst mit einem Interferenzmodell beschrieben, welches auf Methoden der stochastischen Geometrie basiert. Hierbei lassen sich interne Interferenz, d.h. Selbstinterferenz des Netzes durch räumliche Frequenzwiederbenutzung, und externe Interferenz, also der Einfluss von anderen Systemen und Störern, unterscheiden. Interne Interferenz kann durch ein lokal orthogonales Frequenzsprungverfahren begrenzt werden, während der Einfluss externer Interferenz durch die Anpassung der Kanalnutzungswahrscheinlichkeiten verringert werden kann.

Der Einfluss interner Interferenz auf das Netz wird in der vorliegenden Arbeit bezüglich der Ausfallwahrscheinlichkeit einer repräsentativen Punkt-zu-Punkt-Verbindung bei fester Datenrate analytisch und simulativ charakterisiert. Zur Reduzierung des Einflusses interner Interferenz kann der Kanalzugriff so organisiert werden, dass benachbarte Übertragungen möglichst in verschiedenen Kanälen stattfinden. In Frequenzsprungnetzen ist dieser Ansatz äquivalent zur Wahl lokal orthogonaler Sprungsequenzen. Die so erreichbare mittlere Verbesserung ist bedeutend und wird im stochastischen Modell beschrieben. Um diese Verbesserung in konkreten Netzen tatsächlich zu erreichen, wird ein lokal orthogonales Mehrebenenfrequenzsprungverfahren als ein verbesserter Ansatz zur Minimierung interner Interferenz vorgestellt. Dieses lokal orthogonale Mehrebenensprungverfahren basiert auf einem verteilten Graphenfärbungsalgorithmus und ist damit für ad hoc Netze besonders geeignet.

In einem zweiten Teil wird der Einfluss externer Interferenz auf Frequenzsprungverfahren im gleichen Systemmodell beschrieben. Zur Minderung der Störeinflüsse bietet sich hier ein auf die Kanalqualitäten abgestimmtes adaptives Frequenzsprungverfahren an. Bei gegebener Störumgebung wird die Leistungsfähigkeit des optimalen adaptiven Verhaltens, welches genaue Kenntnis der Störparameter voraussetzt, mit verschiedenen suboptimalen Verfahren verglichen. Ein wesentliches Ergebnis ist, dass harte Adaptivität, also der Ausschluss von Kanälen aus der Sprungsequenz, wie er in vielen Protokollen eingesetzt wird, in den meisten relevanten Fällen Durchsätze nahe des erreichbaren Optimums erzielen kann.

Der letzte Teil der Dissertation widmet sich der Organisation des Medienzugriffes in frequenzspringenden Mehrkanalnetzen. Besonders eignet sich hier die Klasse der *Parallel Rendezvous*-Mehrkanalmedienzugriffsprotokolle. Externe und interne Interferenz werden aus Sicht des Medienzugriffes mit Hilfe eines Markov-Modells analysiert. Zur Reduzierung des Einflusses externer Interferenz wird Interferenzvermeidung auf der Protokollebene des Medienzugriffes diskutiert. Auch hier erweist sich, dass Interferenzvermeidung hohe Durchsatzgewinne gegenüber einem nicht-adaptiven Protokoll bietet. Mit zunehmender Teilnehmeranzahl und Netzwerkdurchsatz nimmt dieser relative Gewinn allerdings ab. Das neu eingeführte Mehrebenenfrequenzsprungverfahren wird ebenfalls auf der Medienzugriffsschicht evaluiert. Gegenüber bekannten Verfahren bietet es einen Durchsatzgewinn und größere Fairness beim Verbindungsaufbau durch Verminderung der internen Interferenz.

Abstract

Radio systems today exhibit a degree of flexibility that was unheard of only a few years ago. Signal processing in radio systems before and after digital-to-analog conversion can be kept very flexible with *Software Defined Radio* techniques. This offers the possibility to implement different communication standards in the same radio system, servicing different frequency bands. Software Defined Radio architectures have emerged that are able to service large swathes of spectrum, covering up to several GHz in the UHF bands.

This bandwidth flexibility is not yet used to the fullest extent in existing communication standards. Especially in robust ad hoc networks, which target self-organizing communications between many network nodes and operate under adverse spectrum conditions, such flexibility offers benefits. The focus of this work is techniques to mitigate interference and to improve the robustness of communication in such networks. To this end, two known approaches are adapted, combined and analyzed: adaptive frequency hopping and multi-channel medium access.

First, the performance of adaptive frequency hopping is analyzed with the help of an interference model that is based on stochastic geometry. One can differentiate between internal interference and external interference. Internal interference is self-interference of the network due to spatial re-use of frequencies,

while external interference is interference caused by other communication systems and jammers. Internal interference can be reduced by applying locally orthogonal frequency hopping, while the effects of external interference can be mitigated by adapting the probabilities of channel use.

The influence of internal interference on the network is characterized analytically and with the help of numerical simulations in terms of the outage probability of a point-to-point reference link at a given data rate. To reduce the influence of internal interference, the channel access can be organized in such a way that concurrent neighboring transmissions take place in different channels. In frequency hopping networks, this corresponds to choosing orthogonal hopping sequences. The significant average gain is described within the stochastic model. To actually achieve the gain within a concrete network, multi-level locally orthogonal hopping is introduced as an improved method to minimize internal interference. It turns out that multi-level locally orthogonal hopping, which is based on a distributed graph coloring algorithm, is especially suitable for ad hoc networks.

In a second part, the influence of external interference on frequency hopping networks is described within the same system model. To mitigate external interference, the frequency hopping probabilities are adapted to the channel qualities. Within a given interference environment, the optimal adaptive behavior, which requires exact knowledge of the interference, is compared to different suboptimal approaches. An important result is that hard adaptivity, i.e., the exclusion of severely disturbed channels from the hopping sequence, can achieve close to optimal performance in many relevant cases.

The final part of the dissertation is concerned with the organization of medium access in frequency hopping multi-channel networks. The class of *parallel rendezvous* protocols is found to be particularly suitable. External and internal interference are analyzed from the view point of the medium access layer with a Markov traffic model. To reduce the influence of external interference, interference avoidance on the medium access control layer is discussed. With increasing number of nodes and increasing network throughput, this relative gain, however, decreases. The introduced multi-level locally orthogonal hopping scheme is also evaluated on the medium access layer. Its benefits compared to traditional approaches are increased throughput and better link fairness and are achieved by reducing internal interference.

Contents

1

Introduction

Wireless communication technology has evolved rapidly in the last two decades and is still developing at a fast pace. Driver of this development is the need for high-speed internet access via *infrastructure-based cellular communication networks* and *wireless local area networks*. There are structural differences between those infrastructure network applications and general wireless ad hoc networks that are the focus of this thesis; these differences are described in the following.

Currently, 3GPP Long Term Evolution (LTE) [7] is being deployed in Germany and other countries as the next standard for cellular communications. LTE makes flexible use of frequency bands and operates with bandwidths of up to 20 MHz in all bands assigned to mobile network operators. In Germany, these bands are located around 900 MHz, 1800 MHz and 2.2 GHz. Data rates of up to several dozen megabit per second are supported. Wireless local area networks (WLANs) today are based on the IEEE 802.11 family of standards and have reached their fourth major generation [8]. Operating mainly in the 2.4 GHz industrial, medical and scientific (ISM) and 5 GHz bands at 40 MHz bandwidth and with relatively low power, they achieve maximum data rates in the order

This work contains material from prior conference and journal publications [1–6], ©2010 - 2012 IEEE. Reprinted, with permission. Specifically, Chapter 2 is based on [1–3], Chapter 3 on [4, 5] and Chapter 4 contains material from [6].

of hundreds of megabit per second. LTE employs centralized coordination of resources, a defining feature of cellular communications. The decisions on how to best serve the users are made by the base stations. Today, IEEE 802.11 is mostly used in the same cellular-like manner, which is supported by its infrastructure mode. Each 802.11 network operates in a single frequency channel; this channel is determined by the base station.[2]

Hierarchical network topologies with centralized resource assignment and single channel operation are key features found in today's wireless communication standards that find application in consumer products. In contrast, *wireless ad hoc networks* have a flat hierarchy and need to employ distributed resource allocation. Such networks have received much research attention, but this research has, until now, resulted in only a small number of products or applications. The reasons are obvious: Wireless networks are today used primarily as access networks to the internet; flat or locally flat[3] hierarchies that exchange information between all nodes are common only in certain applications. Three areas of potential application stand out: Military communication networks, automotive networks, and wireless sensor networks.

For sensor networks and short range communication, so called *wireless personal area networks*, IEEE provides the 802.15.1 (*Bluetooth*) [9] and 802.15.4 (*ZigBee* and others) [10] families of standards, which mainly target the 2.4 GHz bands. While the first releases of Bluetooth featured frequency hopping channel access, the type of systems that will be considered in the following chapters, later releases rely on an IEEE 802.11 sublayer to facilitate high data rates. In this thesis, the focus lies on the properties of wireless ad hoc networks with a high number of users and channels, similar to networks 802.15.1 and 802.15.4 can create on a small scale. Following the recent development of spectrally very flexible wireless transceivers, networks are investigated, where each node

- has a large tuning bandwidth,
- employs frequency hopping (FH) code division multiple access (CDMA) to increase robustness, and
- is able to coordinate transmissions over multiple channels.

[2] The *ad hoc mode* defined by 802.11 is rarely used and limited to a single channel as well.
[3] In locally flat topologies, one or more nodes might serve as a gateway node to a backbone network and hence attract more traffic than other nodes.

These characteristics lend themselves especially to applications in military communications and robust sensor networks. A combination of frequency hopping and multi-channel medium access is a good choice for robust large scale ad hoc networks.

1.1 Wireless Ad Hoc Networks

A wireless ad hoc network is a collection of nodes that can exchange data wirelessly with each other. Its defining trait is the absence of a predefined communication schedule and topology: Every node can, in principle, send data to any other node, possibly over multiple hops, resulting in the most complex wireless network. Self-organization is necessary to set up the network and to adapt to changing network conditions.

The concept of a self-organizing network with a multitude of nodes is intriguing from both an application and a research perspective. The idea is that nodes with arbitrary positions, which need to operate in harsh spectrum environments, create a network with a self-organizing topology and, independently, are able to exchange information while pursuing an ”optimal” data rate. This concept offers the fascinating possibility of being connected at any time, even without a centralized infrastructure. From a theoretical perspective, wireless networks – as opposed to the point-to-point link that has been well described by Shannon [11] – are not yet well understood. Giving a good characterization of the performance and the performance limits of this most general type of wireless network is to information theory what a ”theory of everything” is to physics.[4]

1.1.1 Channelization and Frequency Hopping: Theoretical and practical aspects

Information-theoretic motivation

From a theoretical point of view, there are two main reasons to limit the transmission bandwidth and subdivide available bandwidth into channels when mul-

[4]As in the case of physics, an open question is whether such a general theory exists or – if it indeed does exist – will be useful in practice. Without a doubt, however, wireless ad hoc networks constitute the most complex type of wireless systems.

tiple links share the same spectrum:

- A decreasing gap to capacity at low signal-to-noise ratios (SNRs) and, more importantly,
- the possibility to reduce the influence of co-channel interference, i.e., interference between neighboring channels, via filtering and frequency planning.

Consider the well-known formula by Shannon for the possible error-free transmission data rate C across a band-limited channel under the influence of additive white Gaussian noise [11]

$$C = B \log_2 \left(1 + \frac{P}{N_0 B}\right), \tag{1.1}$$

with channel bandwidth B, signal power at the receiver P and (one-sided) noise power density N_0. The first observation is that for unlimited bandwidth, $\lim_{B\to\infty} C = \frac{P}{N_0} \log_2 e < \infty$: Even with unlimited bandwidth, the capacity does not increase without bounds.

For a given bandwidth and signal power, and hence a certain signal-to-noise ratio $\mathrm{SNR}_0 = \frac{P}{N_0 B}$, we are interested in what fraction ζ of the bandwidth is needed to support a certain data rate $(1-\gamma)C \leq C$. The term $1-\gamma$ is then the fractional relative capacity and γC the gap to capacity. As it turns out, $1-\gamma$ is independent of the actual bandwidth and can be written as

$$1 - \gamma = \zeta \frac{\log_2\left(1 + \zeta^{-1}\mathrm{SNR}_0\right)}{\log_2\left(1 + \mathrm{SNR}_0\right)}. \tag{1.2}$$

The relationship between $1-\gamma$ and ζ for different SNR_0 values is shown in Fig. 1.1. It can be observed that, for $\mathrm{SNR}_0 \to \infty$, capacity is linear in bandwidth. At low SNR values, e.g., for $\mathrm{SNR}_0 = -3\,\mathrm{dB}$ giving up a fraction of bandwidth does not decrease capacity as much. Communication systems that transmit data over longer distances have to deal with low to medium SNR conditions and operate their links in a power-limited regime. It follows that, in order to ensure efficient use of spectrum in a network of such systems, splitting up the available operating spectrum via channelization leads to a higher aggregate (sum) capacity. This is shown in the right hand side of Fig. 1.1 for a simple example, assuming equivalent SNR_0 in each link. The aggregate capacity increases with the number of channels M, while the individual channel capacity

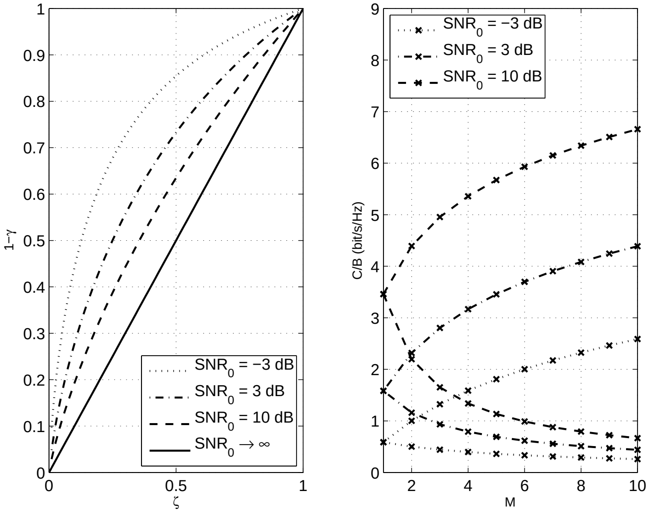

Figure 1.1: On the left hand side: Fractional bandwidth ζ versus fractional relative capacity $1-\gamma$ for various SNR_0. On the right hand side: Aggregate capacity per bandwidth of all channels (rising) and single channel capacity per bandwidth (falling) versus number of channels M for various SNR_0.

naturally decreases. Again, note that for lower SNR_0, increasing the number of channels does not significantly decrease the individual channel capacity.

In a network, where multiple transmissions are carried out concurrently and spatial re-use of frequencies is employed, the wanted signal at one node creates interference at another. The arising non-trivial trade-off between wanted signal power and interference depends heavily on the network geometry and traffic pattern. Quantifying this trade-off under sensible additional assumptions and evaluating ways to minimize interference is the subject of this thesis.

Both aspects, efficient use of spectrum and interference avoidance, motivate research into multi-channel, frequency hopping ad hoc networks. There is much to be gained by bandlimiting transmissions, so that any practical wireless ad hoc network covering larger areas should have a frequency division multiple access (FDMA) component.

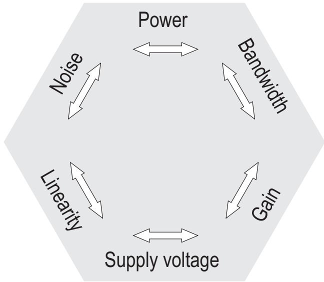

Figure 1.2: Trade-offs in radio frequency (RF) design: The RF design hexagon [12, p. 5]

High frequency engineering issues: In-band versus out-band

As seen, in certain situations it is not beneficial even from a theoretical viewpoint to use high bandwidth in point-to-point links that are part of a greater communication network. Other important factors in favor of lower bandwidth are the implementation and design costs of high frequency bandwidth at each terminal. In high frequency circuit design, several typical trade-offs exist. All of the quantities shown in Fig. 1.2 can be directly or indirectly traded against each other to some extent. Well known trade-offs are the gain/bandwidth trade-off encountered in amplifiers and the noise/bandwidth trade-off in signal processing due to thermal noise.

Fig. 1.3 shows a power consumption/frequency/bandwidth trade-off example in the receiver of an integrated state-of-the-art low power CMOS transceiver [13] for software-defined radio (SDR) applications. It is capable of servicing a frequency range from 100 MHz to 6 GHz with a noise figure of 2.5 dB (at 100 MHz) to 7 dB (at 6 GHz). The transceiver chip provides several bandwidth modes and, as such, is capable of being compliant to all relevant current wireless standards such as LTE and WLAN[5]. As shown in Fig. 1.3, increasing channel bandwidth or carrier frequency leads to higher power consumption of the receiver: In CMOS circuits the dynamic power consumption depends linearly on their switching frequency. Higher channel bandwidths also lead to higher necessary data rates after A/D conversion, thus increasing power consumption throughout the processing chain.

[5] See [13, Tab. 1, p. 2802] for a full list of target applications.

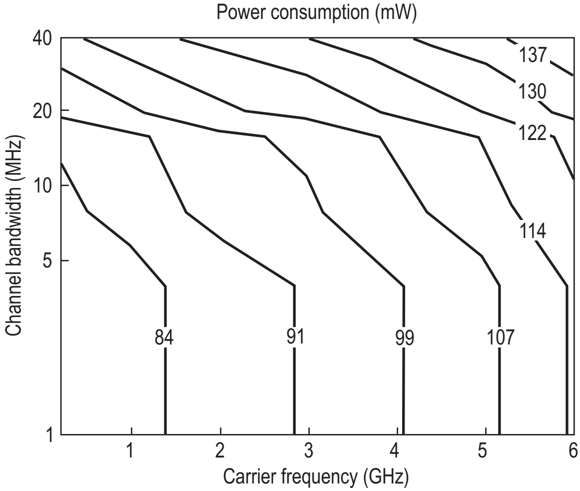

Figure 1.3: Power/frequency/channel bandwidth trade-off in the receiver chain of a state-of-the-art SDR transceiver [13]

Smaller channel bandwidth is also beneficial to decrease susceptibility to interference. If communication links are subject to interference from external sources, e.g., emissions of other communication systems or deliberate jamming attempts, a higher channel bandwidth increases the vulnerability to such interference. Out-of-band interference can be easily reduced using analog filters, while in-band interference has a direct influence on the signal-to-interference ratio. It can only marginally be mitigated[6] by signal processing in the digital domain.

Current SDR hardware

Fig. 1.4 shows the operating bandwidth of tactical communication systems available or under development today.[7] Depending on the design, the channel

[6]The bottleneck is the dynamic range offered by the A/D converter.

[7]Technical specifications are taken from publicly available product notes and press releases by *Rohde und Schwarz* (RS), *Thales Group* and *Ultra Electronics*. All information is provided without liability and for illustrative purposes only. Trademarks mentioned are the property of their respective owners. *Streitkräftegemeinsame verbundfähige Funkgeräteausstattung* (SV-

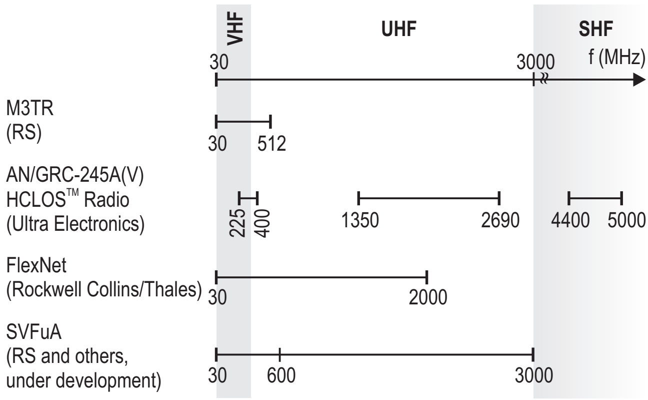

Figure 1.4: Operating bandwidth of state-of-the-art tactical communication systems in the VHF, UHF and SHF bands

bandwidth of the listed communication systems can be as wide as 5 MHz, while still providing appropriate co-site filtering. In light of the very spectrum agile radio frequency hardware available or under development for military communications and even in the low-cost SDR segment[8], frequency hopping can be potentially applied very effectively. Today's hardware can easily service large swathes of the VHF, UHF and SHF spectrum. If the hardware supports packet-based (slow) frequency hopping, huge frequency diversity can be achieved by spreading the transmission over hundreds of megahertz.

The operating (tuning) bandwidth of a node can exceed the system (radio frequency) bandwidth by orders of magnitude. In, for example, a television band overlay network the operating bandwidth is between 400 MHz and 800 MHz, while the system bandwidth is equivalent to the TV channel bandwidth, 8 MHz. The capacity of wireless ad hoc networks can be significantly increased by making use of these additional degrees of freedom available in frequency-agile (and hence multi-channel) ad hoc networks to mitigate interference.

FuA) is the German national SDR program, currently under development by RS and various other companies.

[8] See for the example the *Universal Software Radio Peripheral* product line of *Ettus Research LLC* [14] that offers high frequency front-ends tunable over a wide range of frequencies, from DC to 5 GHz.

Shared spectrum and overlay networks

Another aspect, especially relevant in overlay networks, is the minimization of interference to a primary spectrum user.

In overlay networks, devices using different transmission standards share the spectrum. Due to the limited amount of spectrum available and a multitude of new wireless applications, spectrum sharing is on the rise, especially in the UHF bands. A common requirement for secondary users is to ensure minimum interference with primary users. A *primary spectrum user* is a spectrum user that has prioritized access, as, e.g., mandated by a regulatory agency, and must not be interfered with. If the primary user characteristics are known, e.g., through additional information collected and stored in a database [15], the great flexibility of today's hardware makes it possible to minimize the impact of spectrum sharing on the primary users. Such concepts are being implemented and monitored today in the United States of America by the Federal Communications Commission's White Space Database Administration [16]. The prioritization of spectrum access is, however, not the focus of this work. In the following chapters we are only concerned with minimizing the impact of interference on our own network.[9]

1.1.2 Multi-channel MAC operation

Wireless networks with a high number of nodes that are scattered over a large area necessarily require a multi-channel medium access control (MAC) architecture, as data transmission of many nodes in a single channel is an obvious bottleneck for performance. Multi-channel MAC protocols that organize the medium access across multiple channels are more complex than single channel protocols as the state of the network cannot be inferred at each node by only observing a single channel. Multi-channel MAC protocols allow scaling the total network throughput with the number of available channels. In large scale networks, while frequency hopping is optional, multi-channel MAC operation is not. A combination of both approaches can increase the robustness and flexibility of the network if the inter-channel quality varies. This diversity gain is bought at the expense of increased demand on synchronization and channel switching overhead.

[9] Since interference is reciprocal, the concepts can, with appropriate modifications, of course be applied to shared spectrum overlay networks as well. They are also relevant for research that can be summarized under the umbrella term *cognitive radio* [17, 18].

1.2 Context and related work

Up until today, no theory is available that can easily describe all relevant properties of arbitrarily large wireless networks. Classical Shannon theory that treats each occurring link as a point-to-point connection is, due to the combinatorial nature of possible network interactions, limited to small networks. An evaluation of the capacity region, especially in multi-channel networks, is possible with current computers for only up to 6 or 7 nodes [19, 20]: The number of possible interactions in the network increases exponentially with the number of nodes. Another significant drawback of Shannon theory is that it cannot account for delay or changes in the network topology and hence does not offer a lot of practical insight. Computational intractability and practical shortcomings motivate the search for new network models[10].

A seminal publication that sparked interest in *scaling laws*, i.e., the asymptotic behavior of large networks, was published by Gupta and Kumar in 2000 [22]. Drawing on the fact that transmissions take up "interference space" they showed using a geometrical argument that the end-to-end throughput with increasing node density in any large network converges to zero. Building on this negative result, it has been shown that mobility can increase capacity [23] and that, in multi-channel networks, a low number of interfaces (one or two) does not necessarily limit the capacity of the network [22, 24]. Scaling laws, however, are of limited practical use as they only state results for asymptotically infinite node density.

A new approach that can capture the properties of networks with arbitrary density is based on stochastic geometry. The idea is to model node positions by means of a stochastic process. Expressions can then be derived by averaging over all possible spatial configurations. Depending on the assumed distribution of positions, the resulting expressions are even analytically tractable. Instead of trying to model all interactions between nodes, one is satisfied with results that characterize the *average* performance over all possible spatial network configurations.

Relevant recent introductory and advanced literature that applies stochastic geometry to wireless networks are a tutorial paper and a monograph by Haenggi et al. [25, 26], a monograph by Baccelli and Blaszczyszyn [27], a tutorial paper

[10] Refer to the magazine article by Andrews et al. [21] for a recent overview and discussion of research directions in information theory.

and a monograph by Weber et al. [28], [29] and an overview paper summarizing current developments by Andrews et al. [30].

In the next two chapters of this work, a network model based on a homogeneous Poisson point process is used to describe interference trade-offs in FH-CDMA networks. In a relevant prior publication, Andrews et al. [31] give an overview and discuss the use of spread spectrum, i.e., low spectral efficiency waveforms in ad hoc networks. The pros and cons of employing high spectral efficiency modulation (high data rate, but susceptibility to interference) and low spectral efficiency (low data rate, increased robustness) are discussed. A central idea not touched upon in [31] however, or by the references therein, is the physical necessity to use multiple channels in larger networks. Furthermore, interference avoidance by adapting hopping sequences, a central theme of this thesis, is also not discussed.

Frequency hopping is a well-known and proven technique for increasing the robustness of transmissions. An overview of the history and applications can be found in the book by Simon et al. [32]. More recent notable publications include works by Popovski et al. [33, 34] and Stabellini et al. [35]. The publications propose and discuss frequency hopping techniques, but do so outside of a stochastic geometry framework and without a link to multi-channel MACs.

MACs for wireless ad hoc networks have been extensively studied, see, e.g. [36] for an overview. Central to our MAC analysis is the Markov traffic model for a multi-channel ad hoc network introduced by Mo et al. in [37].

1.3 Organization

Chapters 2 and 3 discuss *internal* and *external* interference as well as strategies for countering their influence within a simple stochastic network model, where node positions are assumed to follow a homogeneous Poisson point process. Internal interference, i.e., self-interference caused by unwanted network transmissions due to spatial re-use of frequencies, can be avoided in FH-CDMA networks by orthogonalizing the hopping sequences, if network geometry allows this. The problem is cast as a graph coloring problem and possible performance gains are shown. For a given network, an algorithm is provided that achieves local orthogonalization in a practical setting.

External interference is the influence of external systems on the channel qualities. By adapting the hopping sequences, it is possible to mitigate its influence.

Chapter 3 derives, within the given system model, the optimum probability distribution. Suboptimal but practically relevant strategies are compared to this optimal performance bound.

Chapter 4 highlights design problems in MAC protocols for multi-channel frequency hopping networks. The performance of interference avoidance techniques is analyzed in a MAC layer model. Finally, Chapter 5 summarizes the work, highlights the contributions and gives an overview of further research directions.

The three main chapters treat different aspects of frequency hopping systems. As they use different system models, they are written to be self-contained, so that each chapter can be read separately from the others. Together, they offer a broad view of the physical layer and MAC layer issues of frequency hopping systems operating under interference.

2

Mitigating Internal Interference

Internal interference is interference caused by the unwanted signals of concurrent transmissions from other network nodes in the same physical channel. In large wireless networks with significantly more transmitting nodes than available channels, the same channels have to be used in different parts of the network. Internal interference then necessarily degrades performance. Techniques to mitigate internal interference by transmission coordination are therefore of special interest, as interference leaks through space more easily than through frequency and time [30].

In cellular networks, reduction of internal interference is achieved by careful frequency planning and verification measurements[11]. As the base station positions are known, the cells can be fine-tuned by adapting transmission power and antenna directions and choosing appropriate downlink and uplink channels. This minimizes the interference of different base stations at the mobile terminals. The interference at the base stations can also be managed through

[11] See [38] for an in-depth description of propagation models and frequency planning techniques.

frequency planning due to the fact that mobile terminals have much lower transmission power than base stations[12].

In ad hoc networks, managing internal interference is much more difficult as there is no pre-defined traffic structure or geometry. Both facts complicate frequency planning. Due to the power-law properties of path loss attenuation, internal interference is dominated by unwanted transmission of other nearby nodes in the same channel. A strategy to avoid internal interference in a network of frequency hopping code division multiple access (FH-CDMA) systems is hence the spatial orthogonalization of transmission hop sets.

This chapter deals with the performance gains that can be achieved by such scheduling of transmissions within a geometrical model, where the node positions are given by a homogeneous Poisson point process (PPP). We consider the following research questions:

- What are the possible spatial average gains of adaptive hopping with local orthogonalization?
- For a given network, what is a practical hopping strategy if local orthogonalization is not possible due to network geometry?

In prior related works based on PPP models, Weber et al. compare FH-CDMA and direct sequence spread spectrum (DSSS) CDMA systems under a power constraint with equivalent total occupied bandwidth [31, 40, 41].[13] They find that FH-CDMA systems have an advantage in terms of transmission capacity[14], a metric closely related to spectral area efficiency. Hence, it is more beneficial to avoid interference in ad hoc networks than to mitigate it with the help of channel coding.

Within the same model, Weber et al. [42] derive the transmission capacity for a network employing interference cancellation. They find that interference cancellation is beneficial overall, but high cancellation efficiency is needed. Furthermore, if cancellation efficiency is high, it is sufficient to only cancel the closest interferer to achieve a large gain[15]. Jindal et al. answer the question as

[12] The maximum transmission power for mobile terminals is 23 ± 2 dBm, while base stations of macro cells typically transmit with $43-48$ dBm [39, pp. 266-268].

[13] DSSS-CDMA systems implement extremely low rate channel coding via pseudo-random spreading of the transmitted symbols.

[14] The transmission capacity is the expected number of successful transmissions per unit area, formally defined in (2.3).

[15] The same also holds for FDMA under certain conditions, see [43].

to how to split a given operating bandwidth to maximize spectral area efficiency [44].

All these prior works assume that a transmission over full bandwidth with low spectral efficiency is possible. Thus, the comparison between low spectral efficiency transmissions over high bandwidth (low spectral density) and high spectral efficiency transmissions over smaller bandwidth (high spectral density) is reasonable. This comparison is indeed fair if the operation bandwidth is relatively small, e.g., up to 40 MHz. With growing bandwidth, however, it becomes increasingly difficult and costly to design and operate DSSS-CDMA systems due to the required signal dynamic range and radio frequency engineering constraints[16]. Designing and operating DSSS-CDMA systems at acceptable costs over an operating bandwidth of a few hundred MHz, as envisioned here, is entirely impossible. This needs to be borne in mind when interpreting the results of the aforementioned works. In contrast to these prior works, the bandwidth split under the assumption that the network locally coordinates transmissions in a frequency division multiple access (FDMA) fashion by adapting the hopping sequences is considered here.

The next sections build on the cited results by Weber, Jindal et al. to show the principal limits of FH-CDMA networks capable of locally organizing channels in terms of the transmission capacity metric in the interference-limited regime[17]. A contribution is the application of Brooks' theorem[18] [45] in the transmission capacity framework.

The remainder of this chapter is structured as follows. In Section 2.1, the system model is introduced. Section 2.2 restates results for naïve (non-adaptive) FH-CDMA by Jindal et al. [44] for comparison. The transmission capacity of networks with local FDMA scheduling is derived in Section 2.3 and compared with the no scheduling case. Finally, Section 2.4 focuses on a practical algorithm for implementing local FDMA scheduling for a given ad hoc network. Section 2.5 provides concluding remarks.

[16]Radio frequency design becomes generally more difficult with higher bandwidth (see also Section 1.1.1): Oscillators need to be more stable and hence have better phase noise properties.

[17]We neglect thermal noise and interference, this will be the topic of Chapter 3.

[18]See also Appendix B.

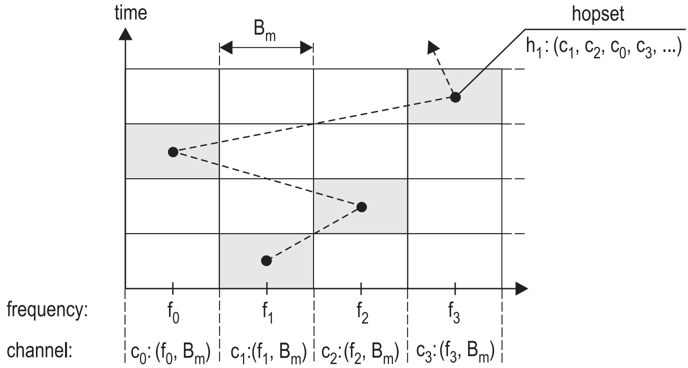

Figure 2.1: Illustration of frequencies, channels and hopsets.

2.1 System model

2.1.1 Geometry, channel and receiver model

The wireless network considered consists of nodes assumed to be distributed in the plane. The operating bandwidth B is the total bandwidth available for communication and is split into M orthogonal channels of system bandwidth $B_m = \frac{B}{M}$. The system bandwidth is the high frequency bandwidth of a single node, and each node i transmits in only one channel $m_i \in \mathbb{M}$, $\mathbb{M} = \{1, \ldots, M\}$.

We assume that slotted ALOHA is used to access the channel[19] at each node. The set of active transmitters in a certain time slot is modeled by a homogeneous marked PPP $\Phi = \{(X_i, m_i)\}$ of intensity λ, where the $X_i \in \mathbb{R}^2$ denote the locations of transmitters and the $m_i \in \mathbb{M}$ are the marks attached to the X_i, indicating the associated channel.

In frequency hopping systems, one can differentiate, as shown in Figure 2.1, *frequencies*, *channels* and *hopsets*[20]. A frequency is a physical center frequency of a channel. A channel is a pointer to a (center) frequency with an associated bandwidth, and a hopset is a time-indexed set of channels. In order

[19] ALOHA channel access is described and analyzed in, e.g., [46]. This simple model of synchronized but uncoordinated medium access is appropriate for simple networks or to model the network-wide RTS/CTS phase of a more sophisticated MAC protocol as described in Chapter 4.

[20] The terms *hopset* and *hopping sequence* are used interchangeably in this thesis.

to evaluate FH-CDMA with locally orthogonal hopping, the interference situation at a certain time instance is evaluated, i.e., one considers a network snapshot. Furthermore, it is presumed that the channels are accessed with equal probability, i.e., that the channels of transmitting nodes are determined by (pseudo-)-random hopsets.

We define $\Phi_m = \{(X_i, m_i) | X_i \in \Phi,\, m_i = m\}$ as the point process containing only those transmitters which transmit in channel m. According to the hopset properties, we assume that, even though the marks are not assigned independently, they are assigned with equal probability, i.e., the distribution of marks of all points is uniform. We can then well approximate Φ_m as a (non-homogeneous) Poisson point process and the intensity of Φ_m can be denoted as $\lambda_m = \lambda / M$.

The performance of the network is evaluated with the help of a (hypothetical) *typical* transmission[21] between a reference transmitter and reference receiver in each channel. All channels have an identical interference profile, so it is sufficient to consider one reference pair. The reference receiver is placed at the origin and the reference transmitter r units away at position $\mathbf{x}$. Each transmitter, both the reference transmitter and interferers, transmits with power ρ and hence spectral power density $\frac{\rho}{B_m} = \frac{\rho M}{B}$ in a channel.

The transmitted signals are attenuated by path loss and may also be subject to Rayleigh fading. The path loss between two points $\mathbf{x}', \mathbf{y}' \in \mathbb{R}^2$ is given by $\|\mathbf{x}' - \mathbf{y}'\|^{-\alpha}$, with $\alpha > 2$.[22] We assume that any interference can be treated as white noise, i.e., that appropriate pre-whitening measures have been taken at the receivers.

The instantaneous signal-to-interference-and-noise ratio (SINR) at the probe

[21] In the following, only transmitters will be considered. For a PPP made up of nodes that can act as transmitters or receivers, the typical transmission in homogeneous PPPs can also be justified with Slivnyak's Theorem (see [47, p. 95] or [48]) as follows: The PPP is thinned into transmitting and receiving nodes. All transmitters choose their destination nodes, and the destination is interpreted as a point mark. Then, a typical transmitter is picked; the statistics are not affected by conditioning of the marked PPP on a specific point. This approach relies on the independence of marks.

[22] Note that this two-dimensional model is not valid for $\alpha = 2$, as the interference contributions from an infinite number of nodes in the plane lead to infinite interference power. Mathematically, the corresponding integral diverges, see [49]. Furthermore, it is only valid for distances $r > 1$.

receiver in channel m is given as

$$\begin{aligned} \mathrm{SINR}_m &= \frac{\rho\, G_0 r^{-\alpha}}{N_m + \sum_{\Phi_m \setminus \{\mathbf{x}\}} \rho\, G_i \|X_i\|^{-\alpha}} \\ &= \frac{G_0}{\mathrm{NSR}_m + r^{\alpha} \sum_{\Phi_m \setminus \{\mathbf{x}\}} G_i \|X_i\|^{-\alpha}}, \end{aligned} \tag{2.1}$$

where N_m is the thermal noise level in channel m, $\mathrm{NSR}_m = \frac{N_m}{\rho r^{-\alpha}}$ is the mean noise-to-signal ratio in channel m.[23] The variables G_0 and G_i are independently and exponentially distributed with unit mean and capture the random fluctuations in the received power due to Rayleigh fading at the probe receiver. Setting $G_0 = G_i = 1$, (2.1) reduces to a path loss model.

The outage probability of the typical link in channel m is given by the reduced Palm probability [27]:

$$\begin{aligned} q_m &= P^{!\mathbf{x}} \left[\mathrm{SINR}_m < \beta\right] \\ &= P \left[\mathrm{SINR}_m < \beta\right], \end{aligned} \tag{2.2}$$

where β is the required SINR threshold and $P^{!\mathbf{x}}$ is the probability measure with respect to the point process $\Phi_m \cup \{\mathbf{x}\}$ without counting the point $\mathbf{x}$, as the probe transmitter does not contribute to the interference seen by the probe receiver. The second equality of (2.2) follows from Slivnyak's Theorem, which states that $P^{!\mathbf{x}}[\cdot] = P[\Phi \in \cdot]$, if Φ is a PPP [27]. The outage probability q_m is a function of the SINR, and hence of all model parameters of (2.1). It is monotonically increasing with the density of active transmissions λ.

A measure that relates the outage probability to the number of attempted transmissions is the transmission capacity (TC) [28]. The TC is the density of concurrent transmissions weighted by the success probability associated with this density, i.e., for a single channel:

Definition (Transmission capacity)**.**

$$c_m(\lambda) = \lambda_m (1 - q_m(\lambda_m)) \tag{2.3}$$

The transmission capacity is a measure of the spatial goodput and gives the number of nodes transmitting successfully in a unit area at a given time. With the data rate of a single packet and the channel bandwidth, the area spectral efficiency can be directly calculated from the TC.

[23] Note that the interference comes from all nodes of Φ_m, except for the desired transmitter at position $\mathbf{x}$.

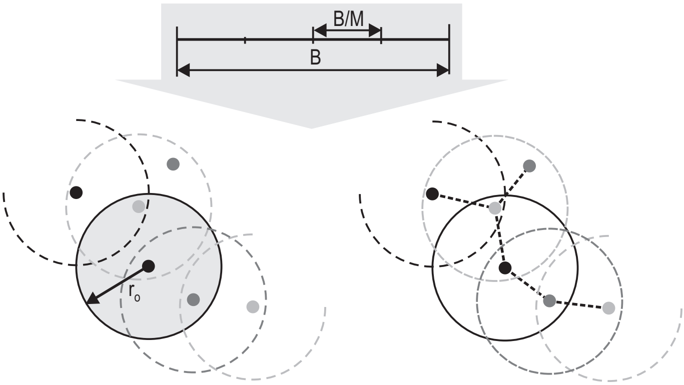

Figure 2.2: Bandwidth partitioning and scheduling

2.1.2 Local FDMA scheduling

For a given network, the optimum channel assignment minimizes the overall interference between nodes. Channel assignment problems have been well studied for fixed cellular networks, see e.g. [50–52], and are in general known to be *NP-hard*[24], although efficient algorithms exist to find close-to-optimal solutions with global knowledge of the network state. In ad hoc networks, nodes have to rely on local information and make local decisions. For the stochastic network model, it is assumed that the network protocol is capable of orthogonalizing the transmissions of all neighbors around the reference receiver in an orthogonalization radius r_o. Concurrent transmissions in the same area thereby take place on different channels, resulting in a guard zone free of interfering transmitters. Fig. 2.2 shows the bandwidth partitioning and resulting scheduling; each transmitter in the vicinity is assigned a different channel.

For a fixed operating bandwidth B, more channels mean less interference as more neighbors can be orthogonalized and less interference comes from all other nodes since their activity is split onto M channels. On the other hand, less spectrum is available for a point-to-point link, resulting in a higher outage probability for a given data rate. In the following sections, we will quantify this trade-off and find the optimum number of channels M for the path loss and Rayleigh fading model.

[24]For an introduction to algorithmic complexity see [53].

Formally, one can describe local FDMA scheduling as follows. Let Φ' be a marked point process with points and marks (X_i', m_i') and let $d(X_i', r_o)$ be the disc with radius r_o centered at X_i', where X_i' has the mark m_i'. Furthermore, let $\Phi'(\cdot, m_i')$ denote Φ' on a given area, counting only points with mark m_i'. Then, a set of marks m_i' needs to be found such that

$$\forall X_i' \in \Phi' : P\left[\Phi'(d(X_i', r_o), m_i') \setminus (X_i', m_i') = \emptyset\right] = 1 - \varepsilon_o \tag{2.4}$$

holds. In other words, a mark (channel) is only used once with probability $1-\varepsilon_o$ within all disc of radius r_o around all points X_i'. Depending on the properties of Φ', this might be possible for $\varepsilon_o = 0$ if the number of points per area is bounded. In the case of a PPP approximation, ε_o converges to 0 fast with the number of available channels as we will see later.

2.2 Transmission capacity with naïve FH-CDMA

First, we will derive the relationship between system bandwidth, operating bandwidth and transmission capacity under internal interference for a network which needs to support a (minimum) data rate R_m at a (maximum) distance r in each point-to-point connection *without* local scheduling (naïve FH-CDMA). We assume a Shannon capacity relationship between SINR and R_m. There is an optimal split of the operating bandwidth M_{opt} for which outage is minimized, independently of λ. The transmission capacity of the network is the goodput of the associated node density.

The SINR experienced by the reference receiver in a channel m can be written as, see (2.1),

$$\mathrm{SINR}_m = \frac{G_0}{\mathrm{NSR}_m + r^\alpha \sum_{\Phi_m \setminus \{\mathbf{x}\}} G_i \|X_i\|^{-\alpha}},$$

where $\mathrm{NSR}_m = \frac{N_0 B_m}{\rho r^{-\alpha}}$ denotes the noise-to-signal ratio in channel m.

In channel m the outage probability q_m for a transmission rate R_m, assuming

Shannon capacity, is

$$
\begin{aligned}
q_m(\lambda_m) &= P\left[B_m \log_2(1+\mathrm{SINR}_m) \leq R_m\right] \\
&= P\left[\mathrm{SINR}_m^{-1} > \underbrace{\frac{1}{2^{\frac{R_m}{B_m}}-1}}_{=:1/\beta}\right].
\end{aligned}
\tag{2.5}
$$

2.2.1 Path loss only model

For the path loss only model, we set $G_0 = G_i = 1$. Making use of symmetry, the two-dimensional PPP of Φ_m can be mapped to a one-dimensional PPP with unit intensity Φ_u [28] and SINR^{-1} hence written as:

$$
\mathrm{SINR}^{-1} = \underbrace{\frac{N_0 B_m}{\rho r^{-\alpha}}}_{\mathrm{NSR}_m} + (\pi r^2 \lambda_m)^{\frac{\alpha}{2}} \underbrace{\sum_{i\in\Phi_u} T_i^{-\frac{\alpha}{2}}}_{Z_\alpha},
\tag{2.6}
$$

where T_i is the distance to the origin of the interferer i. It follows for $q_m(\lambda_m)$:

$$
q_m(\lambda_m, R_m) = P\left[Z_\alpha > (\pi r^2 \lambda_m)^{-\frac{\alpha}{2}} \left(\underbrace{\frac{1}{\beta} - \mathrm{NSR}_m}_{\theta_m}\right)\right].
\tag{2.7}
$$

Let $\overline{F}_{Z_\alpha}$ denote the complementary cumulative distribution function of Z_α. Then,

$$
q_m(\lambda_m) = \overline{F}_{Z_\alpha}((\pi r^2 \lambda_m)^{-\frac{\alpha}{2}} \theta_m).
\tag{2.8}
$$

The optimal system bandwidth of each channel is given by minimizing the outage probability over the number of channels:

$$
M_{\mathrm{opt}} = \arg\min_M q_m(\lambda_m, R_m)
\tag{2.9}
$$

Inserting (2.8) and assuming a symmetric distribution of nodes[25] to channels with $\lambda_m = \frac{\lambda}{M}$ and $B_m = \frac{B}{M}$ yields

$$\begin{aligned} M_{\text{opt}} &= \arg\min_M \left(\overline{F}_{Z_\alpha}\left(\frac{\theta_m}{(\pi r^2 \lambda_m)^{\frac{\alpha}{2}}} \right) \right) \\ &= \arg\max_M \left(\frac{\theta_m}{(\pi r^2 \lambda_m)^{\frac{\alpha}{2}}} \right) \\ &= \arg\max_M \left(M^{\frac{\alpha}{2}} \left(\underbrace{\frac{1}{2^{\frac{R_m}{B}M} - 1}}_{1/\beta} - \underbrace{\frac{N_0 B}{\rho r^{-\alpha} M}}_{\text{NSR}_m} \right) \right) \end{aligned} \tag{2.10}$$

This optimization problem is solvable in closed form for the interference-limited regime (thermal noise is assumed negligible, $\text{NSR}_m \to 0$) [44]. It follows

$$M_{\text{opt}} = \frac{B}{R_m} \underbrace{\log_2 \exp(\frac{\alpha}{2} + \mathscr{W}(-\frac{\alpha}{2}\exp(-\frac{\alpha}{2})))}_{b_{\text{opt}}} \tag{2.11}$$

where $\mathscr{W}$ denotes the principal branch of the Lambert-W function. The optimal split[26] hence depends on the path loss exponent α, desired supportable rate R_m and operating bandwidth B.

This is, under the given path loss model assumptions, the optimum operating bandwidth split for an FH-CDMA ad hoc network to minimize outage at a given point-to-point data rate. The split corresponds to an SINR threshold β of

$$\beta_{\text{opt}} = 2^{b_{\text{opt}}} - 1 \tag{2.12}$$

and a spectral efficiency in all links of b_{opt}.

In a multi-channel network, the total transmission capacity is given by, see (2.3),

$$c(\varepsilon) = \sum_{m=1}^{M} c_m(\varepsilon)\,, \tag{2.13}$$

[25] The symmetric distribution to channels is justified due to the homogeneous PPP model and equal background noise in each channel.

[26] Assuming B or R_m are adjusted so that M_{opt} is an integer, otherwise the optimal M will be the ceiling or floor of the expression.

where $\lambda_m = q_m^{-1}(\varepsilon)$, i.e., the densities in each channel are chosen such that a given outage probability ε is achieved.

Using (2.8), (2.11) we can then write,

$$c(\varepsilon) = \frac{\overline{F}_{Z_\alpha}^{-1}(\varepsilon)^{-\frac{2}{\alpha}}}{\pi r^2}(1-\varepsilon)\beta_{\text{opt}}^{-\frac{2}{\alpha}} \underbrace{\frac{B}{R_m} b_{\text{opt}}}_{M_{\text{opt}}} . \tag{2.14}$$

The transmission capacity in (2.14) scales linearly with operating bandwidth. In multi-channel ad hoc networks, the ratio $\frac{R_m}{B}$ will typically be small, resulting in a high number of channels. In the interference-limited regime, the transmission capacity can be made arbitrarily large by extending the operating bandwidth.

In general, the transmission capacity (2.14) cannot be explicitly stated as a closed-form expression. A special case is $\alpha = 4$, where the transmission capacity is, $Q(z) = P[Z \leq z]$ for $Z \sim N(0,1)$, [28]

$$c(\varepsilon) = \frac{\sqrt{2/\pi} Q^{-1}((1+\varepsilon)/2)}{\pi r^2 \sqrt{\beta_{\text{opt}}}}(1-\varepsilon)M_{\text{opt}} . \tag{2.15}$$

This case will be used for comparison.

2.2.2 Rayleigh fading model

For the Rayleigh fading model (2.16) one has to take into account the fading coefficients G_0, G_i. SINR^{-1} can be written as

$$\text{SINR}^{-1} = \frac{1}{G_0}\left(\frac{N_0 B_m}{\rho r^{-\alpha}} + (\pi r^2 \lambda_m)^{\frac{\alpha}{2}} \underbrace{\sum_{i\in\Phi_u} (G_i T_i)^{-\frac{\alpha}{2}}}_{Z'_\alpha}\right) , \tag{2.16}$$

where T_i is the distance to the origin of the interferer i. As we see, the structure of optimization problem is the same, leading to the same optimum number of channels M_{opt}. This is due to the fact that geometry and fading define Z'_α, but Z'_α remains independent of m. Hence, fading results in an instantaneous scaling of the SINR but does not affect the optimum bandwidth split in the interference-limited regime, $\text{NSR}_m \to 0$.

2.3 Transmission capacity with locally orthogonal hopping

2.3.1 Feasibility of Orthogonalization

An important initial question regards the feasibility of orthogonalization according to (2.4) of N neighbors when M channels are available. This corresponds to a graph vertex coloring problem with M colors in an infinite random graph. Only if orthogonalization is feasible anywhere in the network with high probability, can the reference link be regarded as accurately describing the performance of the whole network. By Brooks' theorem [45], successful orthogonalization (coloring) of a graph with node (vertex) set $\{X_i\}$ is feasible with M channels (colors), if the maximum number of neighbors $\max\{N_i\}$ (maximum degree) is less than M. Obviously, this can only be the case for a finite number of nodes in a given area. Hence, the PPP Φ is conditioned on having K nodes on an area of interest $A \subset \mathbb{R}^2$, where $\frac{K}{A} = \lambda$. Given a PPP with intensity λ, the numbers of neighbors N_i of each node i are identically and independently Poisson distributed with parameter $\pi r_o^2 \lambda$. In other words, the expected number of neighbors λ_n for a node from a PPP with density λ is[27]

$$\lambda_n = \pi r_o^2 \lambda \,. \tag{2.17}$$

A sufficient condition for feasibility of orthogonalization with probability greater than $1-\varepsilon_o$ is that the maximum of the set of Poisson random variables describing the number of neighbors N_i of each node X_i is not greater than or equal to the number of colors available:

$$P\left[\max\{N_1, N_2, ..., N_K\} \leq M-1\right] > 1-\varepsilon_o \,. \tag{2.18}$$

By making use of the independence of the random variables, this condition yields

$$\begin{aligned} 1-\varepsilon_o(M) &< \Big(\sum_{i=0}^{M-1} \exp(-\lambda_n)\frac{\lambda_n^i}{i!}\Big)^K \\ &= \Gamma_r(M,\lambda_n)^K \,. \end{aligned} \tag{2.19}$$

[27] We will use both λ and λ_n in the following: The meaning of λ_n is intuitive, while λ allows to compare performance results easily with results from literature.

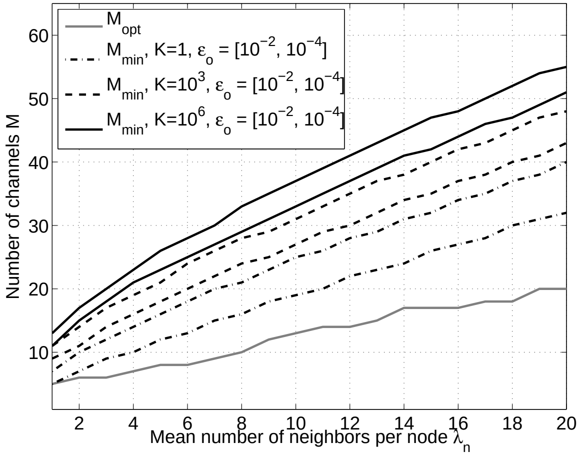

Figure 2.3: Number of channels M required to allow orthogonalization in a network of K nodes with probability ε_o and number of channels minimizing point-to-point outage M_{opt} in the local scheduling case. M_{opt} is determined via Monte Carlo simulations for $R_m/B = 0.1$, $\alpha = 4$ and $r = 10$.

where $\Gamma_r(s,x) = \frac{\Gamma(M,\lambda_n)}{\Gamma(M)}$ is the regularized gamma function. As M grows, $\varepsilon_o(M)$ rapidly converges to 0. In fact, denoting $\exp(x) = \sum_{i=0}^{M-1} \frac{x^i}{i!} + R_M(x)$, $\varepsilon_o(M)$ can be upper bounded by

$$\begin{aligned}
\varepsilon_o(M) &= 1 - (\sum_{i=0}^{M-1} \exp(-\lambda_n)\frac{\lambda_n^i}{i!})^K \\
&= 1 - (1 - \exp(-\lambda_n)R_M(\lambda_n))^K \qquad (2.20)\\
&\leq 1 - (1 - \exp(-\lambda_n)\frac{2\lambda_n^M}{M!})^K
\end{aligned}$$

for $M \geq 2\lambda_n - 2$ (making use of $R_M(x) \leq 2\frac{|x|^M}{M!}$, proof by bounding the remainder term of the exponential series).

Given an area A, λ, $\varepsilon_o > 0$ and r_o, the minimum number of channels $M_{\min}$ needed for FDMA orthogonalization within radius r_o can be obtained by solving (2.19) for M, according to

$$M_{\min} = \Gamma_r^{-1}\left((1-\varepsilon_o)^{\frac{1}{K}}, \lambda_n\right). \tag{2.21}$$

Fig. 2.3 shows the number of channels needed for various K and ε_o. Somewhat surprisingly, even for a large number of nodes K and small ε_o, the required minimum number of channels grows slowly. This is one of the properties of the distribution of the maximum of a set of independent Poisson random variables.[28]

2.3.2 Outage and Transmission Capacity

Let us now assume that the network uses M channels and is agile enough to coordinate the transmission of neighboring nodes to avoid interference within its intended transmission range $r = r_o$ in such a way that it always finds an orthogonalization if it is feasible. The assumption is reasonable: if nodes can communicate directly, they can also effectively exchange their transmission schedule.

The probability $1-\varepsilon_o(M)$ of a feasible orthogonalization in a network with K nodes and M channels is upper bounded by (2.19). If the probability of network orthogonalization is high, a representative measure is the probability of a locally feasible orthogonalization. This is the probability p_o that not more than $M-1$ nodes lie within the orthogonalization range of the reference node:

$$\begin{aligned} p_\text{o} &= \sum_{i=0}^{M-1} \exp(-\lambda_n)\frac{\lambda_n^i}{i!} \\ &= \sum_{i=0}^{M-1} \exp(-\pi r_o^2\lambda)\frac{\left(\pi r_o^2\lambda\right)^i}{i!}. \end{aligned} \tag{2.22}$$

For the following considerations, it is hence assumed that *MAC scheduling can eliminate* $M-1$ *near interferers in the transmission range* r, by assigning them to different frequency channels.

Similar to the no scheduling case, closed form solutions of such an interference field do not exist. We will derive upper and lower bounds on the outage probability.

[28] The statistics are further examined in a recent publication by Briggs et al. [54].

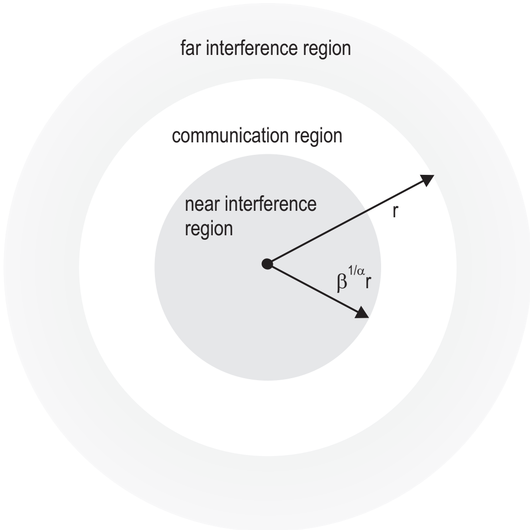

Figure 2.4: $\beta \leq 1$: The communication region is greater or equal to the near interference region.

The outage event can be decomposed by considering the communication region, the near interference region and the far interference region [28]. The communication region and the near interference region are discs of radius r and $r_s = \beta^{\frac{1}{\alpha}} r$, respectively. The far interference region is the area outside the near interference region. Interfering nodes inside the near interference region directly cause outage. Interfering nodes in the far interference region can cause outage, if the aggregate interference exceeds $\frac{1}{\beta}$.

The overall trade-off to be examined can be characterized as follows: A higher number of channels increases the feasibility of orthogonalization and reduces the total number of interferers in a channel, but at the same time increases power spectral density of each interferer and reduces the usable point-to-point bandwidth, which still needs to support the same data rate.

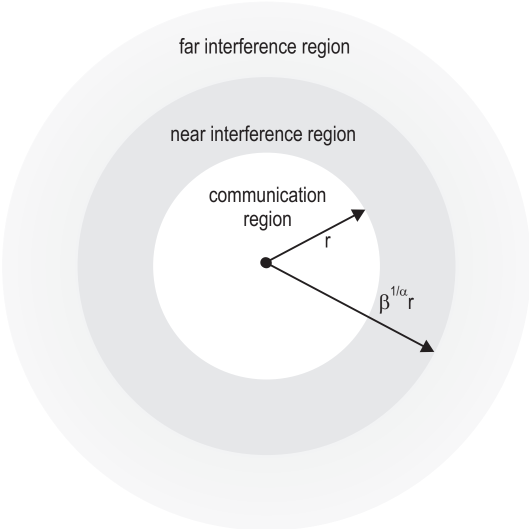

Figure 2.5: $\beta > 1$: The communication region is smaller than the near interference region. The near interference region thus extends beyond the communication range.

As shown in Fig. 2.4 and 2.5, two cases have to be differentiated. For $\beta > 1$, the near interference range is greater than the communication range. For $\beta \leq 1$, the communication range is greater than the near interference range. For both cases, we derive bounds on outage for a given number of channels and show the associated transmission capacity in relation to the no scheduling case.

2.3.3 Low spectral efficiency - the spreading case: $\beta \leq 1$, $\frac{R_m}{B} M \leq 1$

From $2^{\frac{R_m}{B}M} - 1 = \beta \leq 1$, it immediately follows $\frac{R_m}{B}M \leq 1$. In this case, the communication region is greater than the near interference region. The outage probability $q(\lambda)$ can be decomposed into outage due to infeasible orthogonalization around the reference receiver and outage due to far interferers. Equivalently, for successful transmission with probability $1 - q(\lambda)$,

$$\begin{aligned} 1 - q(\lambda) = p_o(\lambda) P\left[Y_r(\lambda) \leq \beta^{-1}\right] + (1 - p_o(\lambda)) \\ P\left[\text{no non-orth. node within } r_s\right] P\left[Y_{r_s}(\lambda) \leq \beta^{-1}\right] \end{aligned} \tag{2.23}$$

must hold, where $Y_r(\lambda)$ is the amount of interference created by nodes that are at least r units away from the reference receiver. Given that orthogonalization has failed at the reference receiver, $P[\text{no non-orth. node within } r_s]$ is the probability of ”no non-orthogonalized node in near interference region” and $P\left[Y_{r_s}(\lambda) \leq \beta^{-1}\right]$ is the probability of ”the aggregate interference from the far field starting at r_s not exceeding $\frac{1}{\beta}$”.

Lower Bound: If the second term in (2.23) is neglected, a lower bound on the success probability $1 - q$ is obtained, according to

$$1 - q(\lambda) > p_o(\lambda) P\left[Y_r(\lambda) \leq \beta^{-1}\right] \tag{2.24}$$

The term $P[Y_r(\lambda) \leq \beta^{-1}]$ can further be lower bounded using the Markov inequality[29] $cP[X \geq c] \leq E[X]$, yielding [28]

$$P\left[Y_r(\lambda) \leq \beta^{-1}\right] \geq 1 - \frac{\lambda}{M} \frac{2\pi r^2}{\alpha - 2} \beta. \tag{2.25}$$

Note that this bound is loose for small M. For $M \to 1$, it follows that $p_o = 0$ and thus the right side of (2.23) is replaced by $P\left[\text{no node within } r_s\right] P\left[Y_{r_s}(\lambda) \leq \beta^{-1}\right]$.

Upper Bound: An upper bound on the success probability can be derived by assuming that the next $M - 1$ neighbors of the reference receiver can always be orthogonalized and just taking into account nodes in the near interference region. In this case, a transmission is successful if no more than $M - 1$ nodes are found in the near interference region. $P\left[Y_{r_s}(\lambda) \leq \beta^{-1}\right]$ can hence be upper bounded by

$$P\left[Y_{r_s}(\lambda) \leq \beta^{-1}\right] \leq \sum_{i=0}^{M-1} \exp(-\lambda_s) \frac{\lambda_s^i}{i!}, \tag{2.26}$$

where $\lambda_s = \lambda \pi (\beta^{\frac{1}{\alpha}} r)^2$. An upper bound on the transmission capacity is given by numerically solving (2.26) for λ and multiplying this density with the given probability of success according to (2.3).

[29] The Markov inequality holds for positive random variables X with finite expectation $E[X]$. See, e.g., [55, p. 183].

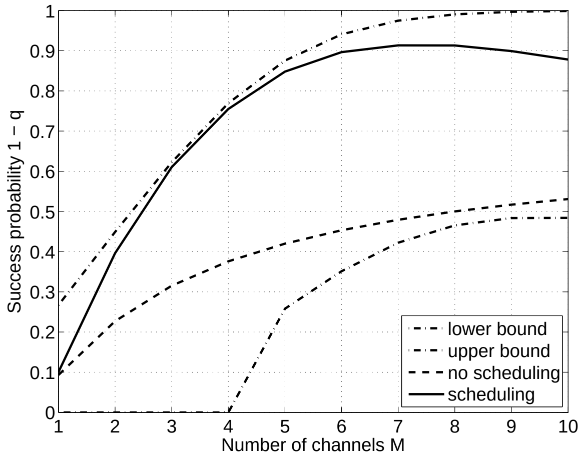

Figure 2.6: Success probability for $\beta \leq 1$: $R_m/B = 0.1$, $\lambda_n = 5$, $\alpha = 4$, $r = 10$.

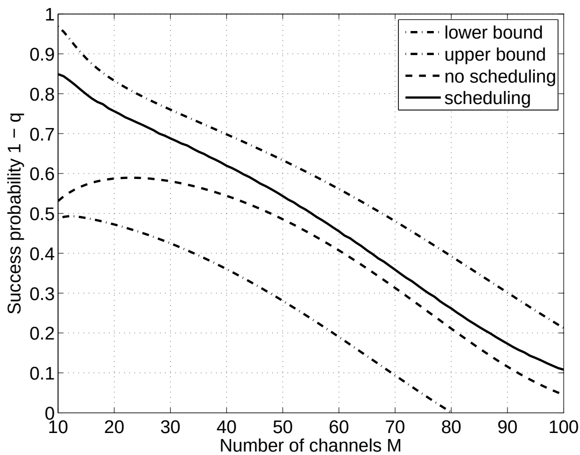

Figure 2.7: Success probability for $\beta \geq 1$: $R_m/B = 0.1$, $\lambda_n = 5$, $\alpha = 4$, $r = 10$.

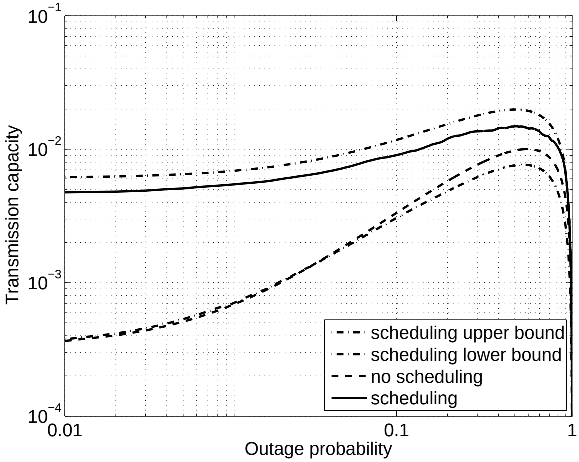

Figure 2.8: Transmission capacity for $K = 10^3$, $\varepsilon_o = 10^{-2}$, $R_m/B = 0.1$, $\alpha = 4$, $r = 10$.

Fig. 2.6 shows the outage probability computed via Monte Carlo simulation, the lower bound (2.24), the upper bound based on (2.26) as well as the exact outage probability for the no scheduling case.

2.3.4 High spectral efficiency: $\beta > 1$, $\frac{R_m}{B}M > 1$

In the high spectral efficiency regime, the interference region exceeds the communication region. In this case, outage can be due to an orthogonalization failure, to the presence of at least one node within the annulus with radii $r_s = \beta^{\frac{1}{\alpha}} r$ and r, or to the aggregate interference from the far field exceeding $\frac{1}{\beta}$. The success probability is

$$1 - q(\lambda) = p_o(\lambda) P\left[\text{no node in annulus}\right] P\left[Y_{r_s}(\lambda) \leq \beta^{-1}\right], \tag{2.27}$$

where $P[\text{no node in annulus}] = e^{-\frac{\lambda}{M}\pi(r_s^2 - r^2)}$.

Lower bound: We obtain a lower bound on $P\left[Y_{r_s}(\lambda) \leq \beta^{-1}\right]$ by using the Markov inequality, yielding (see 2.25)

$$1 - q(\lambda) \geq p_o(\lambda)\left[1 - \frac{\lambda}{M}\frac{2\pi r^2}{\alpha - 2}\beta^{\frac{2}{\alpha}}\right] e^{-\frac{\lambda}{M}\pi(r_s^2 - r^2)}. \tag{2.28}$$

Upper Bound: An upper bound on the transmission capacity for $\beta > 1$ is obtained by assuming $p_o(\lambda) = 1$ and neglecting far field interference. In this case, the success probability $1 - q(\lambda)$ depends only on nodes situated in the annulus with inner radius r and outer radius r_s:

$$1 - q(\lambda) \leq e^{-\frac{\lambda}{M}\pi(r_s^2 - r^2)} \tag{2.29}$$

Fig. 2.7 shows the outage probability computed via Monte Carlo simulation, the lower bound (2.28), the upper bound based on (2.29) as well as the exact outage probability for the no scheduling case.

2.3.5 Discussion

Fig. 2.7 and 2.6 show that, for a fixed low number of neighbors λ_n in communication range, local scheduling offers the maximum gain at a lower number of channels and hence lower spectral efficiencies. The dominating interferers are orthogonalized via FDMA and need not be avoided randomly. If high spectral efficiencies are employed, the gain of local scheduling diminishes quickly due to the fact that the dominating interferers are no longer in communication range.

Fig. 2.8 shows the transmission capacity of local scheduling in dependence of the outage probability and a comparison to the no scheduling case. For the no scheduling case, the number of channels is chosen according to (2.10). For the scheduling case, the optimum number of channels M_{opt} minimizing point-to-point outage is always less than the number of channels required for feasible network orthogonalization, cf. Fig. (2.3). Accordingly, the minimum number of channels for feasible network orthogonalization was chosen in Fig. 2.8. High allowable outage probabilities lead to a high number of channels and high spectral efficiencies. An important fact to note is that the optimum number of channels minimizing link outage M_{opt} now depends on the node density λ, which is not the case in the no scheduling case. The overall gain in terms of transmission capacity is a factor of 1.35 to 13, depending on the allowable outage.

2.4 Averaging interference: Multi-level locally orthogonal hopping

The previous sections were concerned with the performance of local FDMA averaged over all possible spatial configurations of the network. For a concrete realization of a network, an algorithm has to be given to achieve local orthogonalization. In order to be practical in an ad hoc network, this algorithm has to work in a distributed fashion.[30]

Recall that we differentiate *frequencies*, *channels* and *hopsets*. A frequency is a physical center frequency of a channel; a channel is a pointer to a frequency with an associated bandwidth, and a hopset is a time-indexed set of channels.

As already discussed, multiple access interference is dominated by nearby nodes transmitting in the same channel. In locally orthogonal frequency hopping, neighboring nodes try to mitigate interference by choosing orthogonal hopsets. If there are M orthogonal channels, exactly M orthogonal hopping sequences exist. Orthogonal hopping creates a spatial ordering that minimizes interference if there are enough channels available at every node in the network, i.e., if $\forall n : |\mathcal{N}_n| \leq M$ is true, where $\mathcal{N}_n$ is the set of nodes that are in the neighborhood of node n. If the number of nodes in a neighborhood exceeds the number of orthogonal hopping sequences, repeated collisions of hopping sequences follow. Unwanted collisions in the same channel can also occur if a certain node attracts more traffic than others, e.g., because the node acts as a gateway due to its spatial or hierarchical position.

[30] Note that in the following we are concerned with mitigating the influence of internal interference by better distributing channel access according to the local network geometry. Not discussed are methods to counter interference by making the packet itself more robust, e.g., by adaptive modulation and channel coding or interference cancellation. Adaptive coding and modulation and other mechanisms will, of course, be required in a practical protocol.

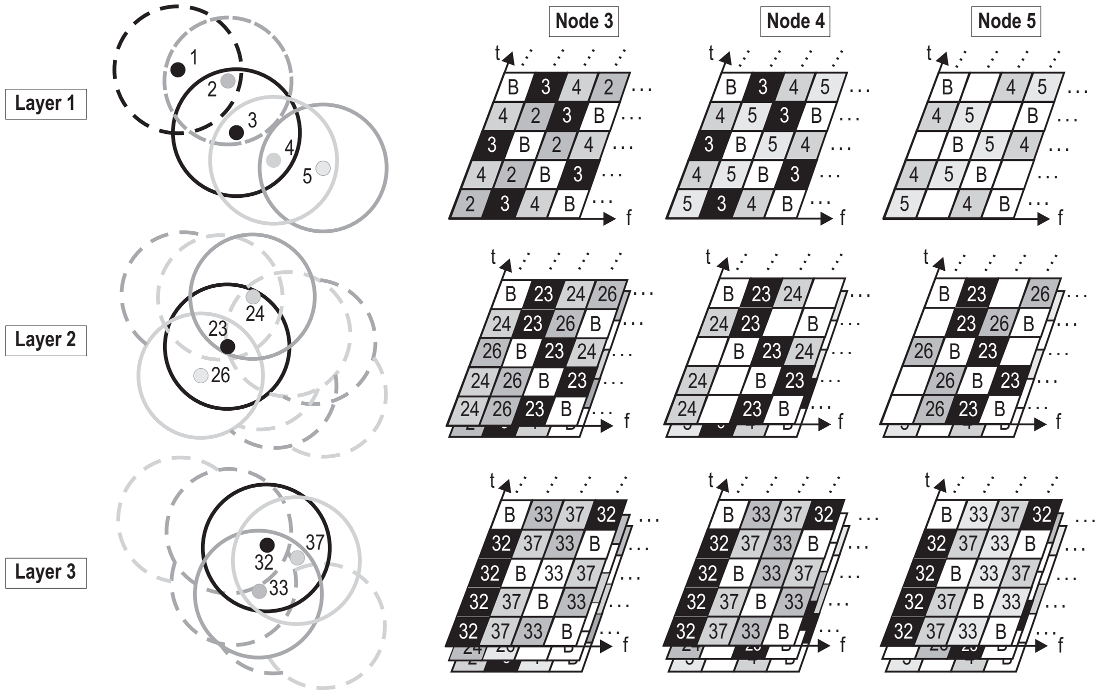

Figure 2.9: Principle of multi-level locally orthogonal frequency hopping

Introducing another hopping layer, i.e., another set of orthogonal hopping sequences that are weakly correlated with the first set, allows the order to be broken where necessary to resolve these deterministic collisions. The interference of this new layer is then, from the perspective of any other layer, distributed fairly across all channels, while no interference occurs from nodes within the same layer.

Fig. 2.9 illustrates the principle of multi-level locally orthogonal (MLLO) frequency hopping for part of a network with a total of 11 nodes on three layers and four available channels. The figure shows the channel choice in the neighborhood of nodes 3, 4 and 5. As seen in the figure, the hopping sequences within a layer are locally orthogonal, i.e., no node occupies the same channel within the neighborhood indicated by gray shaded circles. As there are more nodes than channels, more than one layer exists. A possible[31] broadcast channel, indicated by B and following a broadcast hopset, is the same on all layers. Of interest is now an algorithm to reach a hopset (and hence channel[32]) assignment according to the described MLLO-FH-CDMA scheme in a large scale ad hoc network.

Note that if the number of hopping layers L is equivalent to the number of nodes N, this scheme corresponds to standard FH-CDMA. If $L = 1$, it corresponds to orthogonal hopping. Also, in a certain time slot, a specific channel in a certain layer is part of exactly one hopset.

2.4.1 Hopset assignment with distributed graph coloring

In a large scale ad hoc network, decisions about hopset assignment have to be made locally as every node has only a limited view of the network.

Globally, the hopset assignment problem can be interpreted as a graph vertex coloring problem of an undirected graph $\mathscr{G}$. Each network node is a graph vertex. Two vertices are connected by an edge of $\mathscr{G}$ if the corresponding network nodes *can be in conflict* with each other, i.e., if they are in a neighborhood. The vertex colors denote channels. For a given layer, a proper coloring of the conflict graph $\mathscr{G}$ corresponds to a valid channel assignment that allows for locally orthogonal hopping.

[31] In multi-channel networks, several approaches for neighborhood discovery and transmission negotiation exist, some of which require a common broadcast channel. E.g., for asynchronous split phase protocols, a shared channel is needed. Details are discussed in Chapter 4.

[32] A *hopset assignment* allocates channels to nodes for all times.

A fast converging distributed algorithm has to be given to reach a proper hopset assignment according to the MLLO hopping scheme. The algorithm should converge to a solution that partitions the (not necessarily colorable) graph $\mathscr{G}$ into a number of colorable subgraphs $\mathscr{G}_1, \ldots, \mathscr{G}_L$ corresponding to the hopping layers. The number of layers should be as small as possible to ensure a maximum of regularity and hence reduce multiple access interference (MAI).

Two approaches for building the interference graph can be considered.

Receive channel scheduling for uncoordinated medium access

With receive channel scheduling, the receive channels are allocated in such a way that they are locally orthogonal. Transmitting nodes then choose the transmit hopset according to the receive hopset of the intended receiver. The corresponding conflicts are defined as follows: All nodes within the neighborhood $\mathscr{N}_i$ are in conflict with a node i, the position of node i is X_i. The vertex set of the interference graph $\mathscr{G}$ is hence $\{X_1, \ldots, X_i\}$. An edge is placed between two vertices X_i, X_j, if $j \in \mathscr{N}_i$ or $i \in \mathscr{N}_j$, i.e., if i may receive signals from j or j may receive signals from i.

Transmit and receive channel scheduling for CSMA/CA-type medium access

If the protocol allows for coordination of medium access, conflicts at both the transmitter and the receiver can be considered. In contrast to receive scheduling, this strategy is dynamic in the sense that it makes short-time allocations based on the knowledge of the actual transmission schedules. Here, a transmitter at position X_i^{tx} is in conflict with all (unintended) receivers in its neighborhood $\mathscr{N}_i^{\text{tx}}$ and a receiver at position X_i^{rx} is in conflict with all (unintended) transmitters in its neighborhood $\mathscr{N}_i^{\text{rx}}$. The additional labeling of the neighborhood is necessary to indicate the type of nodes (receivers or transmitters) creating a conflict. For instance, $\mathscr{N}_i^{\text{rx}}$ is the set of transmitters in the neighborhood of the receiver at position X_i^{rx}. The vertex set of the interference graph $\mathscr{G}$ is composed of all transmitter-receiver position pairs $\{(X_i^{\text{tx}}, X_i^{\text{rx}})\}$. An edge between two vertices $(X_i^{\text{tx}}, X_i^{\text{rx}})$, $(X_j^{\text{tx}}, X_j^{\text{rx}})$ is drawn, if $X_i^{\text{tx}} \in \mathscr{N}_j^{\text{rx}}$ or $X_i^{\text{rx}} \in \mathscr{N}_j^{\text{tx}}$.

Fig. 2.10 shows the two approaches to create an interference graph.

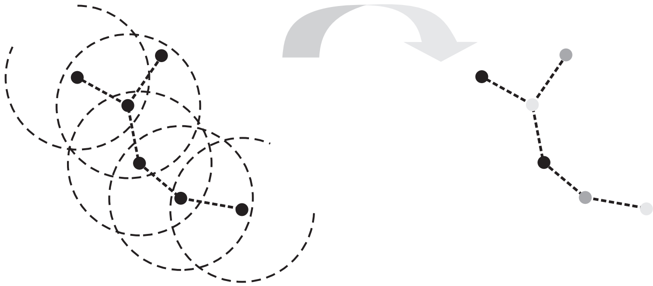

(a) Conflict graph for receive channel scheduling

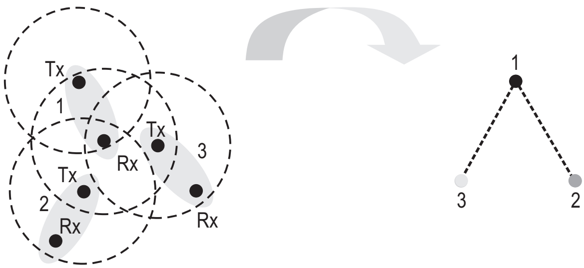

(b) Conflict graph for transmit and receive channel scheduling, numbers denote transmitter and receiver pairs, i.e., 1 shows N_1^{tx} and N_1^{rx}.

Figure 2.10: Interference graphs

Transmit and receive channel scheduling will naturally lead to better interference avoidance than receive channel scheduling, as the actual physical conflicts are considered. However, it requires a possibly network-wide negotiation phase before each transmit phase. Receive channel scheduling has the advantage that no re-negotiation of channels is needed, even if the communication partner changes, meaning it creates less protocol overhead. It can be a good choice for static or slowly changing network topologies: For receive channel scheduling, the interference graph only depends on the network topology, and not the actual traffic patterns. Hence, the slower the network topology changes, the less updates of the interference graph are required.

In the following, we will focus on receive channel scheduling, but note that the principal approach is the same if transmit and receive scheduling for CSMA/CA-type medium access is employed.[33]

[33] The CSMA/CA scheme is evaluated in a more complete MAC model in Chapter 4. It also

Distributed multi-level coloring for receive channel scheduling

With M channels and M corresponding hopsets, a layer $\mathcal{G}_i$ is surely colorable if any node in that layer has no more than $M-1$ conflicts (Greedy coloring)[34].

As an example of an algorithm leading to a proper MLLO hopset assignment, the following algorithm[35] shown in Fig. 2.11 is proposed, extending [56, 57]:

Each node, denoted by subscript n, selects a certain hopset $c_n(t)$ at time t in a layer $\mathcal{G}_i$ according to a probability distribution $p_n(t)$, kept by each node. Each node furthermore keeps a hop sequence collision counter $k_n(t)$ and a collision-free counter $\overline{k}_n(t)$.

- Upon entering the network, a node starts with a receive hopping sequence uncorrelated to all layers. This allows the quality of all channels and the neighborhood to be acquired.
- Once the neighborhood is known, the node starts in the first layer and initializes $p_n(t)$ to a discrete uniform distribution over all possible hopsets, i.e, $p_n(t) = \left[\frac{1}{M}, \ldots, \frac{1}{M}\right]^{\mathrm{T}}$.
- The probability distribution $p_n(t)$ is evolved according to the update rule (2.30).
- Each time a node experiences a conflict, $k_n(t)$ is increased and $\overline{k}_n(t)$ is reset to zero.
- If a node has no conflict, $\overline{k}_n(t)$ is increased and $k_n(t)$ is reset to zero.
- If the collision counter of a node exceeds a threshold $\zeta \in \mathbb{N}$, $k_n(t) > \zeta$, the node moves up a layer and resets $p_n(t)$ to a discrete uniform distribution.
- If the collision-free counter of a node exceeds a threshold $\varepsilon \in \mathbb{N}$, $\overline{k}_n(t) > \varepsilon$, and the node is not in the first layer, the layer below is checked. If there are less than M nodes in the neighborhood on the layer below, the node moves down a layer and sets $p_n(t)$ to a discrete uniform distribution.

requires the separation into transmit- and receive hopsets.

[34] For most graphs, even M neighbors result in a surely colorable graph, cf. Brooks' Theorem [45].

[35] Of course, other distributed coloring algorithms can be used to implement MLLO hopping as well.

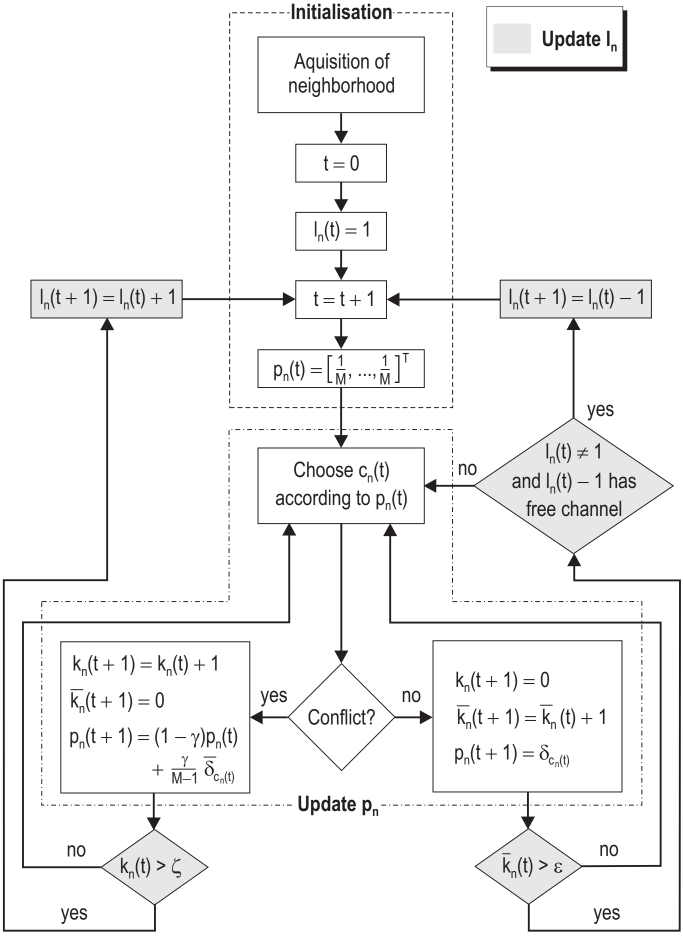

Figure 2.11: Distributed multi-level coloring algorithm. Not shown are packet error threshold τ and randomization of layer changes.

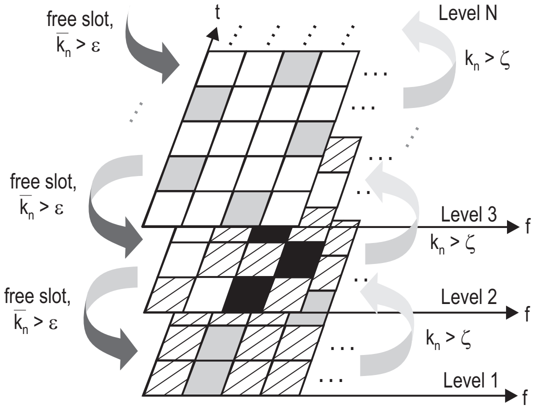

Figure 2.12: Illustration of changing layers

- If the packet error rate exceeds a threshold τ, the node chooses a hop sequence uncorrelated to all layers.

The update rule for channel selection is

$$p_n(t+1) = \begin{cases} \delta_{c_n(t)} & ,\forall i \in \mathcal{N}_n : c_n(t) \neq c_i(t) \\ (1-\gamma)p_n(t) + \frac{\gamma}{M-1}\bar{\delta}_{c_n(t)} & ,\text{otherwise} \end{cases} \tag{2.30}$$

where $\delta_{c_n(t)}$ denotes the vector of length M with a one at position $c_n(t)$ and a zero at all other positions (for example, if $c_n(t) = 1$, then $\delta_1 = [1, 0, \ldots, 0]^{\mathrm{T}}$); $\bar{\delta}_{c_n(t)}$ denotes the vector of length M with a zero at position $c_n(t)$ and a one in all other positions.

As seen in Fig. 2.11, the algorithm can be partitioned into initialization, updating of the hopset probability density, and updating of the current layer.

The algorithm is parameterized by the resistance to change a hopset $\gamma \in (0,1)$ if in conflict on the same layer, the resistance given in number of collisions to move up a layer $\zeta \in \mathbb{N}$, the resistance to move down a layer $\varepsilon \in \mathbb{N}$ given in number of non-collisions and a bail-out threshold τ. At each node, ζ and ε should be randomized to avoid deterministic collisions. This can be done, for example, by only changing layers if thresholds are exceeded with a certain probability $p' < 1$.

We note that this algorithm will lead to an MLLO hopset assignment, but not necessarily to a global optimum. The resulting assignment might not be globally optimal, since interference is also influenced by the *activity* and *position* of nodes inside and outside the neighborhood. The real, physical interference graph can be thought of as being complete (fully connected, since every node influences every other node) and weighted by the interference potential. We approximate this real interference graph above by assuming a finite distance of influence. The method described here can - and should - be extended in a practical protocol by including the channel quality (e.g., by measuring the per channel packet error rate determined by position and activity of other nodes) due to non-decodable internal or external interference at each node when choosing a channel and layer. The protocol should tend to group very active and close nodes in a neighborhood in the same layer to reduce MAI.

In the algorithm, nodes exposed to stronger interference due to their position or activity resort to uncorrelated hopping if a packet error rate threshold of τ is exceeded. Note that if $\tau = 0$, the scheme again corresponds to standard FH-CDMA. The switching between layers according to the algorithm is illustrated in Fig. 2.12.

2.4.2 Analysis

In the following, we shall evaluate the improvement of MLLO hopping compared to uncoordinated FH-CDMA using a simplified scenario. Let $\Pi^{(N)}$ be a Binomial point process with N nodes on a bounded region W, i.e., $\Pi^{(N)} = \{X_0, X_1, \ldots, X_{N-1}\}$, where all the $X_i \in W \subset \mathbb{R}^2$ are the positions of the nodes. An interference graph is then constructed by drawing edges between all pairs X_i, X_j, with $i \neq j$. Such a construction models the interference situation in a neighborhood, where every node's transmission creates excessive interference to the other nodes, directly creating outage.

We further introduce the following quantities:

- The activity indicators, denoting the probability of transmission of a node, are given by $\{a_0, a_1, \ldots, a_{N-1}\}$, where the $a_i \in \{0, 1\}$ are pairwise identically and independently distributed boolean random variables and have mean $\bar{a}$. If $a_i = 1$ a node is active and trying to access a channel, if $a_i = 0$ it is not active.
- The collision indicators are given by boolean random variables $\{\kappa_{ij}\}$, with $i, j = 0, \ldots, N-1$, $i \neq j$. The event $\kappa_{ij} = 1$ indicates that nodes

at positions X_i and X_j are in conflict, i.e., they have chosen the same channel. The complementary event is indicated by $\kappa_{ij} = 0$.[36]

By considering the a_i as marks associated with the points X_i, we define by $\tilde{\Pi}^{(N)} = \{(X_0, a_0), (X_1, a_1), \ldots, (X_{N-1}, a_{N-1})\}$ the marked Binomial point process. To investigate the interference situation within this network, it is necessary to consider the network from the viewpoint of a specific point. Therefore, we condition $\tilde{\Pi}^{(N)}$ on having the point X_0 in the origin and are interested in the interference situation at this node. When a point process with distribution P is conditioned on having a point in the origin without counting it, the reduced Palm distribution $P^{!o}$ must be used to further analyze the point process. From Slivnyak's theorem [47, p. 95], it follows that $P^{!o}[\tilde{\Pi}^{(N)}(W)] = P^{o}[\tilde{\Pi}^{(N)}(W) \setminus X_0] = P[\tilde{\Pi}^{(N-1)}]$ for a Binomial process. This means, the statistics of $\tilde{\Pi}^{(N)}$ on an area W, conditioned on having a point in the origin without counting it, are the same as the statistics of $\tilde{\Pi}^{(N-1)}$. The node in the origin with position X_0 is referred to as the reference node[37].

The comparison between MLLO hopping and FH-CDMA will be based on the mean number of conflicts the reference node experiences[38]. The conflicts are analyzed in the following.

Case FH-CDMA

The average number of conflicts Δ_{FH} at X_0 is calculated as

$$\begin{aligned} \Delta_{\mathrm{FH}} &= E^{!o}\left[\sum_{i=0}^{N-1} a_0 a_i \kappa_{0i}\right] \\ &= E\left[\sum_{i=1}^{N-1} a_0 a_i \kappa_{0i}\right], \end{aligned} \tag{2.31}$$

[36] Note that the collision indicators κ_{ij} are independent of the activity indicators a_i.
[37] Due to lack of stationarity of the Binomial point process, the point X_0 is not typical in the sense that all other points have the same view of the process. However, since, in our calculations, distances will not be involved in any way, the point X_0 will reflect the characteristics of all points of the process.
[38] This will not quantify the actual interference situation at the nodes but will allow a simple comparison of the two schemes. The analysis of the number of conflicts can be taken as a rough measure to quantify the improvement of MLLO hopping compared to uncoordinated FH-CDMA.

where the expectation is over all uncertainties $a_0, \ldots, a_{N-1}$ and $\kappa_{0,1}, \ldots, \kappa_{0,N-1}$. The second equation follows by application of Slivnyak's theorem. Taking the expectation yields

$$\begin{aligned}\Delta_{\mathrm{FH}} &= E[a_0] \sum_{i=1}^{N-1} E[a_i] E[\kappa_{0i}] \\ &= \frac{\bar{a}^2}{M}(N-1),\end{aligned} \tag{2.32}$$

since $E[\kappa_{0i}] = 1 \times P\{X_i$ chooses the same channel as $X_0\} = 1/M$ in the uncoordinated FH-CDMA case.

Case MLLO-FH-CDMA

Again let $\mathcal{G}_k$ denote the k-th layer in our simplified scenario, where $\mathcal{G}_0$ is the lowest layer. Since in every layer $\mathcal{G}_k$ the nodes have orthogonal channels, it is necessary to require that $|\mathcal{G}_k| \leq M$ for all k, where $|\mathcal{G}_k|$ denotes the number of nodes in layer $\mathcal{G}_k$. Furthermore, the following assumptions concerning the scheduling algorithm are made:

1. At the time the algorithm has found a solution, the nodes of $\Pi^{(N)}$ are distributed to the layers $\mathcal{G}_k$ in a bottom-up way, i.e., according to the sequential assignment rule $X_i \in \mathcal{G}_k$, if and only if $|\mathcal{G}_0| = \ldots = |\mathcal{G}_{k-1}| = M$ and $|\mathcal{G}_k| < M$, where $\mathcal{G}_K$ is the highest non-empty layer.
2. The order of the assignments is assumed to be random and all nodes are equally likely to end up in a certain layer. In other words, there is no incentive for a certain node i with position X_i to choose a certain layer $\mathcal{G}_k$ and hence the probability of the event "node i with position X_i is in $\mathcal{G}_k$ after the algorithm converges" is equal for all nodes.

We consider again the average number of conflicts at the reference node with position X_0. After the scheduling process, two cases concerning the assignment of reference node to a layer $\mathcal{G}_{k_0}$ emerge, depending on whether the layer $|\mathcal{G}_{k_0}| < M$ or $|\mathcal{G}_{k_0}| = M$.

Case $|\mathcal{G}_{k_0}| = M$: Here, it is required that $N \geq M$. Without loss of generality, the remaining nodes within the same layer $\mathcal{G}_{k_0}$ are labeled $X_1, \ldots, X_{M-1}$. These nodes do not create conflict with node X_0 and we write $\kappa_{0i} = 0$ for $i = 1, \ldots, M-1$. We now consider the other layers $\mathcal{G}_k$ for which $|\mathcal{G}_k| = M$, according to assumption 1. Here, in each of these layers there will always be a node creating a conflict with X_0, since in each of these layers, M nodes are orthogonal on M channels. If for the highest layer $|\mathscr{G}_K| < M$, there is no deterministic collision with the reference node at position X_0. The probability of a collision depends on the number of nodes within this last layer $\mathscr{G}_k$, according to

$$P\left[\bigvee_{i:X_i\in\mathscr{G}_K}(\kappa_{0i}=1)\right] = \frac{|\mathscr{G}_K|}{M}, \tag{2.33}$$

where $\bigvee$ denotes the existential quantifier connected with a logical *or* for all items indexed (in this case all nodes from the highest layer).

Hence, one can write[39]

$$\begin{aligned} E^{!o}&\left[\sum_{i=1}^{N-1} a_0 a_i \kappa_{0i} \middle| |\mathscr{G}_{k_0}| = M\right] \\ &= \sum_{\substack{k:|\mathscr{G}_k|=M\\ k\neq k_0,K}} E[a_0]E\left[\bigvee_{i:X_i\in\mathscr{G}_k}(a_i\kappa_{0i}=1)\right] \\ &\quad + E[a_0]E\left[\bigvee_{i:X_i\in\mathscr{G}_K}(a_i\kappa_{0i}=1)\right]. \end{aligned} \tag{2.34}$$

With the observations stated above that conflicts from full layers only depend on node activity and has to be weighted for the highest, non-empty layer $\mathscr{G}_K$, we conclude that $E\left[\vee_{i:X_i\in\mathscr{G}_k}(a_i\kappa_{0i}=1)\right] = E[a_i]$ and $E\left[\vee_{i:X_i\in\mathscr{G}_K}(a_i\kappa_{0i}=1)\right] = E[a_i]|\mathscr{G}_K|/M = E[a_i](N \bmod M)/M$. We can rewrite (2.34) as

$$\begin{aligned} E^{!o}\left[\sum_{i=0}^{N-1} a_0 a_i \kappa_{0i} \middle| |\mathscr{G}_{k_0}| = M\right] &= \bar{a}^2\left(\left\lfloor\frac{N}{M}\right\rfloor - 1\right) + \bar{a}^2\frac{|\mathscr{G}_K|}{M} \\ &= \bar{a}^2\left(\left\lfloor\frac{N}{M}\right\rfloor + \frac{N \bmod M}{M} - 1\right) \\ &= \bar{a}^2\left(\frac{N}{M} - 1\right). \end{aligned} \tag{2.35}$$

[39] Note that the sum $\sum_{\substack{k:|\mathscr{G}_k|=M\\ k\neq k_0,K}} \cdot$ runs over all layers, except for the layer of the reference node and $\mathscr{G}_{\mathscr{K}}$. It hence runs over $\lfloor\frac{N}{M}\rfloor - 1$ elements.

Case $|\mathscr{G}_{k_0}| < M$: Here, conflicts deterministically emerge from the lower (full) layers $\mathscr{G}_k$, since $|\mathscr{G}_k| = M$ for all $k < k_0$. We thus can write

$$E^{!o}\left[\sum_{i=1}^{N-1} a_0 a_i \kappa_{0i} \middle| |\mathscr{G}_{k_0}| < M\right] = \bar{a}^2 \left\lfloor \frac{N}{M} \right\rfloor. \tag{2.36}$$

Based on the assumption 2, one can determine the probabilities of the two cases as follows: Given the final distribution of the nodes at position X_i to the layers $\mathscr{G}_k$, the probability of reference node at X_0 being in a layer $\mathscr{G}_k$ with $|\mathscr{G}_k| = M$ is equivalent to the probability of the event $|\mathscr{G}_{k_0}| = M$. Hence, we write

$$P\left[|\mathscr{G}_{k_0}| = M\right] = \frac{\text{Number of Possibilities}}{\text{Number of Nodes}} = \frac{M\left\lfloor \frac{N}{M} \right\rfloor}{N}. \tag{2.37}$$

Accordingly, the complementary event has probability

$$P\left[|\mathscr{G}_{k_0}| < M\right] = 1 - \frac{M\left\lfloor \frac{N}{M} \right\rfloor}{N}. \tag{2.38}$$

Combining (2.35)-(2.38), we conclude that

$$\begin{aligned}
\Delta_{\text{MLLO}} &= E^{!o}\left[\sum_i a_0 a_i \kappa_{0i}\right] \\
&= \bar{a}^2 \left(\left(\frac{N}{M} - 1\right) \frac{M\left\lfloor \frac{N}{M} \right\rfloor}{N} \left\lfloor \frac{N}{M} \right\rfloor \left(1 - \frac{M\left\lfloor \frac{N}{M} \right\rfloor}{N}\right)\right) \\
&= \bar{a}^2 \left\lfloor \frac{N}{M} \right\rfloor \left(2 - \frac{M}{N}\left(1 + \left\lfloor \frac{N}{M} \right\rfloor\right)\right).
\end{aligned} \tag{2.39}$$

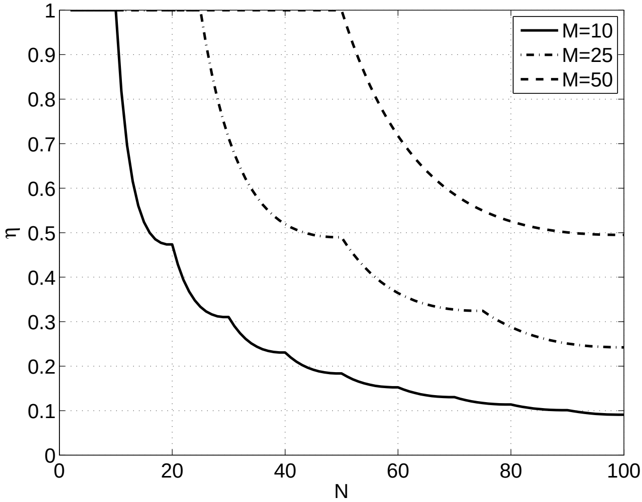

Figure 2.13: Relative gain of MLLO-FH-CDMA in terms of relative reduction of average conflicts for a number of nodes N and a number of channels M.

To analyze the performance of MLLO-FH-CDMA compared to uncoordinated FH-CDMA, the relative improvement in terms of reduction of average conflicts, i.e., $\eta = 1 - \frac{\Delta_{\text{MLLO}}}{\Delta_{\text{FH}}}$, is shown in Fig. 2.13. Note that η is independent of $\bar{a}$. For $N/M \leq 1$, the relative improvement is 1, since all nodes are situated in one layer only and thus are orthogonalized. As the ratio N/M grows, the performance of MLLO becomes similar to that of uncoordinated FH-CDMA.

2.4.3 Simulations

To evaluate the outage probabilities of MLLO-FH-CDMA in a large network, it is necessary to make assumptions regarding the traffic model and geometry of the network.

We assume that communication partners are chosen uniformly within the neighborhood and that each node transmits with probability $\bar{a}$, reflecting the overall network activity. A packet is deemed decodable if the SINR threshold $\beta > 1$ is exceeded. The path loss exponent is assumed to be $\alpha = 4$, fading is not

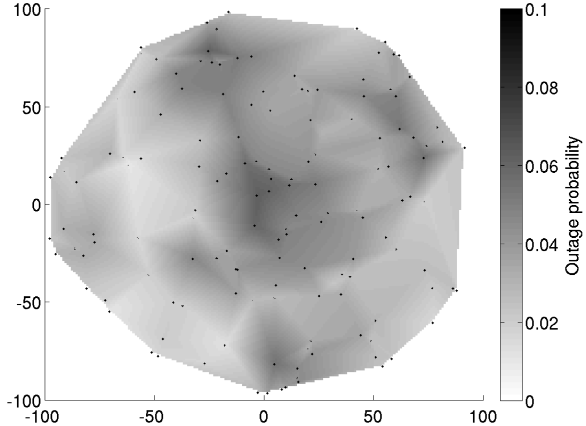

(a) Standard FH-CDMA

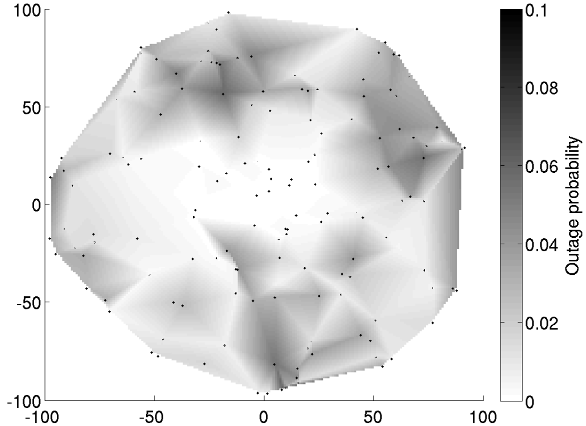

(b) MLLO-FH-CDMA

Figure 2.14: Resulting outage probabilities for a scenario of 150 nodes.

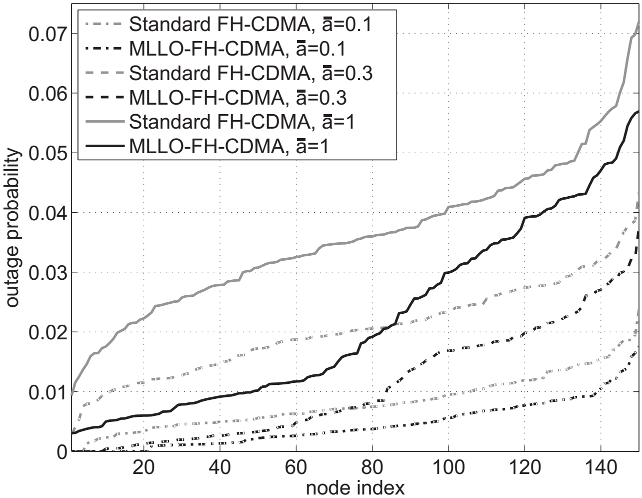

Figure 2.15: Ordered outage probabilities for the spatial configuration shown in Fig. 2.14.

considered[40].

Fig. 2.14 shows the resulting outage probabilities of FH-CDMA and MLLO-FH-CDMA, derived by spatially interpolating the packet error rates at each node. The results are averaged over 10,000 possible network states for a realization of a Binomial point process with 150 nodes using $M = 50$ channels on a disc with radius $R_{\text{sim}} = 100$ units. All nodes within distance $r = 25$ units of each other are assumed to be in a neighborhood. Fig. 2.15 shows the corresponding ordered outage probabilities for the same spatial configuration and various activity levels. The threshold values τ were chosen as 0.05, 0.03, and 0.01, respectively. As can be seen, the absolute gain of MLLO-FH-CDMA increases with network activity, while the relative gain is approximately constant. The outage probability is especially reduced in the center of the network, where the overall outage probability is high in case of uncoordinated FH-CDMA.

[40] Including fading effects in the simulation does not change the behavior, MAI is reduced on average.

2.5 Summary

As shown in the analysis, it is very beneficial to employ local FDMA scheduling in large scale dense ad hoc networks. Local FDMA scheduling yields significant gains and is less complex in implementation than interference canceling techniques, for example. The concrete physical layer modulation design was not touched upon, as most physical layer modulation techniques can readily be combined with frequency hopping and local FDMA scheduling. An efficient protocol design for multi-channel ad hoc networks should incorporate a combination of dynamic frequency planning and adaptive link spectral efficiencies.

Multi-level locally orthogonal FH-CDMA was introduced as a method for reducing MAI in large scale ad hoc networks. A possible algorithm for implementing MLLO hopping has been given and verified using simulations. In homogeneous node configurations, hot spots arising from local competition for channels are avoided by averaging the interference. The gain of the proposed method in a concrete implementation will largely depend on the traffic patterns of the nodes and the geometry; it is fair to assume that geometrically clustered and very active interference limited networks will likely benefit most by introducing the geometrical ordering through hopping layers.

A point not addressed here is the actual method of channel access. Depending on the application, channel access could be random or reservation based. Furthermore, it is likely that not single nodes, but groups of nodes will share a hopping sequence to facilitate point-to-multipoint communication in clustered networks. Both issues need to be addressed in the design of frequency hopping multi-channel networks. MLLO hopping can be beneficial, especially in scenarios where self-interference limits performance.

3

Mitigating External Interference

Having analyzed the possible gains of reducing internal interference by means of adaptive frequency planning in Chapter 2, we will now consider the influence of *external interference* on the network. External interference is interference caused by signal sources that are not part of the network. It can stem from other communication systems operating in the same bandwidth or, in an electronic warfare context, from deliberate jamming of frequencies. To achieve maximal robustness, the network needs to adapt to this interference.

In this chapter, we consider, within a geometrical model based on a homogeneous Poisson point process (PPP), an adaptive synchronous slow frequency hopping code division multiple access (FH-CDMA) system capable of adapting channel access probabilities (and hence, the hopping pattern) according to the external interference experienced in the channels and internal interference generated by other nodes. Due to fast variations in the spatial configuration of transmitting nodes[41] adaptation takes into account the *expected* spatial interference. The questions to be answered are the following:

[41] Such variations naturally arise when nodes change from transmitting mode to receiving mode and vice-versa, or when the network exhibits some mobility.

- What are the highest possible gains of adaptive FH-CDMA when compared to non-adaptive FH-CDMA?
- What are the gains of practical suboptimal strategies?

The optimum channel assignment that balances internal (network) interference due to spatial reuse and external interference is derived analytically for a path loss and for a Rayleigh fading model. The performances of the resulting hopping strategies are then compared to various suboptimal hopping strategies such as non-adaptive hopping and min-max allocation with constant quality of service (QoS).

For prior related work addressing the properties of an interference field of a homogeneous PPP spatial node configuration, see [28, 40, 44] and references therein. To the best of the author's knowledge, external interference as described here has not yet been considered in literature.

The remainder of this chapter is structured as follows. Section 3.1 introduces the system model. The transmission capacity of networks under external interference is derived in Section 3.2 for a Rayleigh fading and for a path loss interference model. Section 3.3 compares the considered strategies, while Section 3.4 provides concluding remarks.

3.1 System model

3.1.1 Geometry, channel and receiver model

A network consists of nodes distributed in the plane. The total operating bandwidth B available for communication is split into M orthogonal channels of equal bandwidth. At each time instance a subset of nodes transmits in a certain channel $m \in \mathbb{M} = \{1, \ldots, M\}$. Assuming that there is no listening period before accessing the channel and that channel access is uncoordinated among the nodes, i.e., that slotted ALOHA[42] is employed, we model the transmitter positions by a homogeneous independently marked PPP $\Phi = \{(X_i, m_i)\}$ of intensity λ, where the $X_i \in \mathbb{R}^2$ denote the locations of transmitters and the m_i are the marks attached to the X_i, indicating the associated channel. Each node

[42] For a description of ALOHA channel access see, e.g., [46]. This simple model of synchronized but uncoordinated medium access is appropriate for simple networks or to model the network-wide RTS/CTS phase of a more sophisticated MAC protocol as described in Chapter 4.

transmits only in one channel $m \in \mathbb{M}$, this channel has the system bandwidth of a single node.

In frequency hopping systems, we can differentiate *frequencies*, *channels* and *hopsets*[43], see Fig. 2.1. A frequency is a physical center frequency of a channel. A channel is a pointer to a frequency with an associated bandwidth, and a hopset is a time-indexed set of channels.

To evaluate the performance of adaptive FH-CDMA, we make the following assumptions. First, the interference situation in the network is evaluated at a certain time instance, i.e., an interference snapshot is considered. Second, in this snapshot, the channel access according to the hopping sequences of transmitting nodes can be described by a discrete probability distribution, the *channel access probabilities*[44]. Hence, we assume that, at the time of transmission, each transmitter randomly chooses a channel according to the channel access probabilities $\mathbf{p} = (p_1, \ldots, p_M) \in [0,1]^M, ||\mathbf{p}||_1 = 1$ for transmitting its message. For convenience, we define $\Phi_m = \{(X_i, m_i) | X_i \in \Phi, m_i = m\}$ as the point process counting only those transmitters which transmit in channel m. Due to uncoordinated, and hence independent, transmissions every Φ_m is also a Poisson point process and the intensity of Φ_m can be denoted by

$$\lambda_m = p_m \lambda \,. \tag{3.1}$$

Each transmitter has an associated receiver at a distance[45] r and transmits with power ρ. The transmitted signals are attenuated by path loss and may also be subject to Rayleigh fading. The path loss between two points $\mathbf{x}', \mathbf{y}' \in \mathbb{R}^2$ is given by $\|\mathbf{x}' - \mathbf{y}'\|^{-\alpha}$, with $\alpha > 2$.[46] We assume that any interference can be treated as white noise, i.e., that appropriate pre-whitening measures have been taken at the receivers.

[43] The terms *hopset* and *hopping sequence* are used interchangeably in this thesis.

[44] The concrete way how the hop sequences that follow these probability distributions are generated is not of interest; creating random numbers according to a given discrete probability distribution is trivial. For an application to frequency hopping as considered here see, e.g., Stabellini et al. [35].

[45] This assumption poses a restriction on the system model but allows for analytical tractability. The effect of r being different for every transmitter-receiver pair on the results is investigated with numerical simulations (see Fig. 3.7). Recently, the influence of including the receivers in the PPP has been investigated in [58].

[46] Note that this two-dimensional model is not valid for $\alpha = 2$, as the interference contributions from an infinite number of nodes in the plane lead to infinite interference power. Mathematically, the corresponding integral diverges, see [49]. Furthermore, it is valid only for distances $r > 1$.

Due to the homogeneity of the PPP, the resulting interference field obeys the same statistics at any point in the plane. This allows characterization of the performance of the whole network by the performance of a *typical* transmission. Therefore, we place a probe receiver at the origin and an associated probe transmitter r units away at location $\mathbf{x}$. The instantaneous signal-to-interference-and-noise ratio (SINR) at the probe receiver in channel m is given as

$$\begin{aligned}\mathrm{SINR}_m &= \frac{\rho\, G_0 r^{-\alpha}}{G_N N_m + \sum_{\Phi_m\setminus\{\mathbf{x}\}} \rho\, G_i \|X_i\|^{-\alpha}} \\ &= \frac{G_0}{G_N\, \mathrm{NSR}_m + r^{\alpha} \sum_{\Phi_m\setminus\{\mathbf{x}\}} G_i \|X_i\|^{-\alpha}},\end{aligned} \tag{3.2}$$

where N_m is the noise level in channel m due to the external interference, $\mathrm{NSR}_m = \frac{N_m}{\rho r^{-\alpha}}$ is the mean noise to signal ratio in channel m. The variables G_0, G_N and G_i are independently and exponentially distributed with unit mean and capture the random fluctuations in the received power due to Rayleigh fading at the probe receiver. By setting $G_N = G_0 = G_i = 1$, (3.2) reduces to the path loss model.

The outage probability of the probe link operating in channel m is given by the reduced Palm probability [27][47]

$$\begin{aligned}q_m(\lambda_m) &= P^{!\mathbf{x}}\left[\mathrm{SINR}_m < \beta\right] \\ &= P\left[\mathrm{SINR}_m < \beta\right],\end{aligned} \tag{3.3}$$

where β is the required SINR threshold and $P^{!\mathbf{x}}$ is the probability measure with respect to the point process $\Phi_m \cup \{\mathbf{x}\}$ without counting the point $\mathbf{x}$, as the probe transmitter does not contribute to the interference seen by the probe receiver. The second equality of (3.3) follows from Slivnyak's Theorem, which states that $P^{!\mathbf{x}}[\cdot] = P[\Phi \in \cdot]$, if Φ is a PPP [27]. We define the outage probability as

Definition (Average outage probability)**.**

$$q(\lambda, \mathbf{p}) = \sum_{m=1}^{M} p_m q_m(p_m \lambda), \tag{3.4}$$

i.e., we consider the *average* outage probability associated with the channel access probabilities $\mathbf{p}$. This expression is the spatial *and temporal* average outage probability of a node given channel access probabilities $\mathbf{p}$.

[47] The outage probability q_m is of course a function of all model parameters. As we are mainly interested in its dependency on the variable parameter λ_m, we write $q_m(\lambda_m)$.

Our primary metric of interest is the transmission capacity (TC) [28], which is the density of concurrent transmissions weighted by the success probability associated with this density, i.e.,

Definition (Transmission capacity)**.**

$$c(\lambda, \mathbf{p}) = \lambda(1 - q(\lambda, \mathbf{p})) \tag{3.5}$$

It is easy to see that for two $\mathbf{p}_1 \neq \mathbf{p}_2$, $c(\lambda, \mathbf{p}_1) \neq c(\lambda, \mathbf{p}_2)$ in general, since $q(\lambda, \mathbf{p}_1) \neq q(\lambda, \mathbf{p}_2)$. Therefore, the value of $c(\lambda, \mathbf{p})$ depends on how the channel access probabilities $\mathbf{p}$ are chosen.

3.1.2 Optimizing channel access: Balancing internal and external interference

Internal interference in a channel is the aggregated interference generated by other nodes of the same network transmitting in the same channel. External interference is interference generated by sources outside the network. Both interference sources affect the outage probability of a transmission in a certain channel.

Our degree of freedom is the channel access probability distribution $\mathbf{p}$. If we choose to increase the load on one channel by assigning more probability mass to it, we will increase the outage probability in that channel but simultaneously reduce the load of the other channels. We are now looking for the optimum distribution $\mathbf{p}_{\text{opt}}$ that maximizes the TC and hence balances internal and external interference.

Definition. *We define by $\mathbf{p}_{opt}$ the channel access probabilities for which the average outage probability $q(\lambda)$ is minimal for a given λ.*

Lemma 1. *The average outage probability $q(\lambda)$ is a strictly monotonically increasing function of λ if $\mathbf{p} = \mathbf{p}_{opt}$ at every λ.*

Proof. Proof by contradiction: Suppose that $q(\lambda_1, \mathbf{p}_1) \geq q(\lambda_2, \mathbf{p}_2)$ for some arbitrary $\lambda_1 < \lambda_2$. From the definition of $\mathbf{p}_{\text{opt}}$ it follows that both $q(\lambda_1, \mathbf{p}_1)$ and $q(\lambda_2, \mathbf{p}_2)$ are minimal at λ_1 and λ_2, respectively. Analyzing $\frac{\partial q_m(\lambda p_m)}{\partial \lambda}|_{\lambda=\lambda_2}$ we see that this is, due to the nature of q_m, always positive for fixed $\mathbf{p} = \mathbf{p}_2$. Thus, going "backwards" from λ_2 to a point λ, we have $q(\lambda, \mathbf{p}_2) < q(\lambda_2, \mathbf{p}_2)$. After reaching the point $\lambda = \lambda_1$, we observe that $q(\lambda_1, \mathbf{p}_2) < q(\lambda_2, \mathbf{p}_2)$. Using the initial assumption, we finally have

$$q(\lambda_1, \mathbf{p}_2) < q(\lambda_2, \mathbf{p}_2) < q(\lambda_1, \mathbf{p}_1),$$

which is a contradiction to the assumption that $\mathbf{p}_1$ is optimal and hence, $q(\lambda_1, \mathbf{p}_1)$ is minimal. Therefore, $q(\lambda_1, \mathbf{p}_1) < q(\lambda_2, \mathbf{p}_2)$ always holds. □

Lemma 2. *The maximization of $\lambda(q)$ for a given q is equivalent to minimizing $q(\lambda)$ for a given λ.*

Proof. From Lemma 1 we know that the average outage probability $q(\lambda)$ with $\mathbf{p} = \mathbf{p}_{\text{opt}}$ is a strictly monotonically increasing function of λ. Hence, for any pair (λ', q') generated by $\mathbf{p}_{\text{opt}}$, we have that $\lambda' = \max_{\mathbf{p}}\{\lambda(q', \mathbf{p})\}$ and $q' = \min_{\mathbf{p}}\{q(\lambda', \mathbf{p})\}$ and the Lemma follows. □

Using Lemma 2 we can now transform the problem of maximizing the TC into the problem of minimizing the average outage probability $q(\lambda, \mathbf{p})$ over $\mathbf{p}$ given some λ.

3.1.3 Optimization problem 1: Maximizing transmission capacity

The first problem strives to minimize the average outage probability $q(\lambda, \mathbf{p})$ from (3.4) as follows:

$$\begin{aligned} \mathbf{p}_{\text{opt}} = \arg\min_{\mathbf{p}} & \sum_{m=1}^{M} p_m q_m(p_m \lambda) \\ \text{s.t. } & \|\mathbf{p}\|_1 = 1, \\ & \forall m \in \mathbb{M}: \; p_m \geq 0. \end{aligned} \tag{P1}$$

According to Lemma 2, the solution of (P1) yields the maximal transmission capacity of (3.5). If all functions $q_m(\lambda_m)$ are convex, the problem can be solved with convex optimization [59, pp. 20ff]. If the $q_m(\lambda_m)$ are non-convex, the optimization problem can generally only be solved heuristically. Due to their nature as cumulative density functions, the $q_m(\lambda_m)$ are monotonically increasing in λ_m, however not necessarily convex[48].

[48] For very high λ_m, outage occurs with probability converging to one. In a scenario with high

3.1.4 Optimization problem 2: Maximizing transmission capacity under constant QoS

Practical systems will strive to have the same expected packet error probability, every time a channel is accessed, hence assuring constant QoS. An optimization approach that achieves constant QoS is based on minimizing the maximum weighted outage probability associated with the M channels:

$$\begin{aligned} \mathbf{p}_{\text{opt, QoS}} &= \arg\min_{\mathbf{p}} \max_{m} p_m q_m(p_m \lambda) \\ \text{s.t. } &\|\mathbf{p}\|_1 = 1, \\ &\forall m \in \mathbb{M}: \; p_m \geq 0. \end{aligned} \tag{P2}$$

From [59, Theorem 2.4.1], we know that for the global minimum of (P2), $\forall i, j \in \mathbb{M} : \lambda_i q_i(\lambda_i) = \lambda_j q_j(\lambda_j) = \text{const}$ holds: The access probability weighted packet error probability in every channel remains constant. The solution of (P2) hence yields the *transmission capacity under constant QoS*. Due to the monotonicity of $\lambda_m q_m(\lambda_m)$, this optimization problem has a unique global minimum and efficient algorithms exist to solve it numerically [59, pp. 31ff].

3.2 Transmission capacity under external interference

In the following, we consider well known outage functions q_m arising from a path loss only interference field and from a Rayleigh block fading interference field. With the help of these outage functions, we are then able to calculate the average outage probability according to (3.4) and the *transmission capacity* (3.5).

For the pure path loss model with $\alpha = 4$, q_m is given by [28]

$$q_m^{\text{pl}}(\lambda_m) = 2Q\left(\lambda_m \xi_m^{\text{pl}}\right) - 1, \tag{3.6}$$

density λ, one channel can take all the excess interference, so that the density in the remaining channels is adjusted to levels at which communication is still possible. This (pathological) scenario is avoided in the following analysis by restricting the optimization to the convex domain of the objective function.

where

$$\xi_m^{\mathrm{pl}} = \sqrt{\frac{\pi}{2}}\frac{\pi r^2}{\sqrt{\gamma_m}} \tag{3.7}$$

and

$$\gamma_m = \begin{cases} \frac{1}{\beta} - \mathrm{NSR}_m & , \frac{1}{\beta} - \mathrm{NSR}_m > 0 \\ 0 & , \text{otherwise.} \end{cases} \tag{3.8}$$

The γ_m can be interpreted as the quality levels of the channels: The larger γ_m, the less external interference the corresponding channel has to bear. If γ_m is zero, communication in that channel is impossible.

Similarly, for the Rayleigh block fading model, q_m is given by [26]

$$q_m^{\mathrm{rl}}(\lambda_m) = 1 - e^{-\lambda_m \Delta \xi_m^{\mathrm{rl}}}, \tag{3.9}$$

where

$$\Delta = 2\pi^2 \frac{r^2 \beta^{2/\alpha}}{\alpha \sin 2\pi/\alpha} \tag{3.10}$$

and

$$\xi_m^{\mathrm{rl}} = \begin{cases} \frac{1}{1+\beta \mathrm{NSR}_m} & , g_N \sim \mathrm{Exp}(1) \\ e^{-\beta \mathrm{NSR}_m} & , g_N = 1, \end{cases} \tag{3.11}$$

where $\sim \mathrm{Exp}(1)$ denotes that g_N is distributed according to an exponential distribution with expected value 1.

3.2.1 Optimal strategy for path loss only model $q_m = q_m^{\mathrm{pl}}$

The adaptive channel allocation minimizes the outage probability by adapting p_m and hence λ_m according to the quality level γ_m of the respective channels[49]. The problem (P1) can be written as

$$\min_{\mathbf{p}} \sum_{m=1}^{M} p_m q_m(p_m \lambda) = \min_{p_o, p_{L+1}, \ldots, p_M} p_o + \sum_{m=L+1}^{M} p_m q_m(p_m \lambda) \tag{3.12}$$

$$\text{s.t. } p_o + \sum_{m=L+1}^{M} p_m = 1, \quad \forall m \in \{L+1, \ldots, M\} : p_o, p_m \geq 0,$$

[49] To the best of the author's knowledge, such a soft-hopping scheme was first suggested by Stabellini et al. in [35]. In the following, we will derive the optimum channel probabilities for our given geometry.

where $1,\dots,L$ are the indices[50] of channels for which $\gamma_m = 0$ and hence $q(\lambda_m) = 1$, and p_o is the accumulated channel access probability assigned to these channels. The probability p_o can be interpreted as the optimum back-off probability needed to maximize transmission capacity by reducing internal interference. The corresponding back-off intensity is given by $\lambda_o = p_o\lambda$.

The optimizing problem (3.12) is generally non-linear and non-convex with non-linear non-convex monotonically increasing objective function and linear equality and inequality constraints. If the function q can be expressed analytically, as in the two cases considered here, the objective function of (P1) can be tested for convexity by showing positive semi-definiteness of the Hessian matrix. Additional constraints for small λ_m, and hence total λ, can then assure convexity. In the following, we will derive the optimum solution under these additional constrains, focusing on small λ and thus small (practically relevant) outage probabilities. We note three relevant observations:

Lemma 3. *The optimization problem* (P1) *with $q_m = q_m^{pl}$ and $\alpha = 4$ is convex, if $\forall m \in \mathbb{M} : 0 \le \lambda_m \le \frac{\sqrt{2}}{\xi_m^{pl}}$.*

Proof. We examine the convexity of $c^{\mathrm{pl}} = \sum \lambda_m q^{\mathrm{pl}}(\lambda_m)$. Taking the second partial derivative with respect to λ_m, we find

$$\frac{\partial^2 c^{\mathrm{pl}}}{\partial \lambda_m^2} = \begin{cases} \frac{2}{\pi}\xi_m^{\mathrm{pl}} e^{-\frac{1}{2}(\xi_m^{\mathrm{pl}}\lambda_m)^2}(2-\lambda_m^2(\xi_m^{\mathrm{pl}})^2) & ,i=j, \\ 0 & ,i \neq j. \end{cases} \tag{3.13}$$

The Hessian matrix $\mathbf{H}$ of the objective function thus has positive elements only for $i = j$, $i \ge L+1$, and zeros elsewhere. For $\mathbf{H}$ to be positive semi-definite and hence q_m to be convex, $0 < \lambda_m \le \frac{\sqrt{2}}{\xi_m^{\mathrm{pl}}}$ must hold. ☐

Lemma 4. *The optimization over p_o can be performed separately after finding the solution for $p_{L+1},\dots,p_M$.*

Proof. Optimization over $p_{L+1},\dots,p_M$ of the objective function of (3.12) results in a function that depends on p_o. The minimum of this function is also the global minimum. ☐

Lemma 5. *A necessary condition for an extremum of (P1) with $q_m = q_m^{pl}$ is that $\forall i \in \{L+1,\dots,M\} : q_m(\lambda_i,\gamma_i) = \tau = const$, $0 \le \tau \le 1$.*

[50] A reordering might be necessary.

Proof. Let $f_i(\lambda_i) = \frac{\gamma_i}{(\pi r^2 \lambda_i)^{\frac{\alpha}{2}}}$ and $f_j(\lambda_j) = \frac{\gamma_j}{(\pi r^2 \lambda_j)^{\frac{\alpha}{2}}}$. Assume we have an extremum of the objective function of (P1) in the convex region with associated solution $\lambda_1, \ldots, \lambda_M$. Consider two λ_i and λ_j of the solution for which $\gamma_i \neq 0, \gamma_j \neq 0$. We can write

$$k = \sum \lambda_m q^{\mathrm{pl}}(\lambda_m, \gamma_m) = \lambda_i q^{\mathrm{pl}}(f_i(\lambda_i)) + \lambda_j q^{\mathrm{pl}}(f_j(\lambda_j)) + \mathscr{R}, \tag{3.14}$$

where $\mathscr{R}$ are all terms independent of λ_i, λ_j. At the solution, the constraint $\sum \lambda_m = \lambda$ has to be fulfilled, so we can set $\lambda_i + \lambda_j = \lambda'$ and write (3.14) in terms of λ_i. Furthermore, we know that at an extremum the partial derivative with respect to λ_i has to be zero:

$$\begin{aligned} \frac{\partial k}{\partial \lambda_i} = q^{\mathrm{pl}}(f_i(\lambda_i)) + \frac{\alpha}{2}(q^{\mathrm{pl}})'(f_j(\lambda' - \lambda_i)) f_j(\lambda' - \lambda_i) \\ - q^{\mathrm{pl}}(f_j(\lambda' - \lambda_i)) - \frac{\alpha}{2}(q^{\mathrm{pl}})'(f_i(\lambda_i)) f_i(\lambda_i) = 0 \end{aligned} \tag{3.15}$$

$f_i(\lambda_i) = f_j(\lambda' - \lambda_j)$ is a solution to this equation; we assumed convexity (and strict convexity for $\lambda_{L+1}, \ldots, \lambda_M$) of the objective function, hence it is the only solution. Since this is the case for arbitrary i and j, all $f_m(\lambda_m)$ are equal and the Lemma follows. □

Since $q(\lambda_m)$ is strictly monotonically increasing with respect to λ_m, for a given p_o minimizing $q(\lambda_m)$ is equivalent to minimizing its argument. Given this fact and Lemma 4 and Lemma 5, the optimization problem over $p_{L+1}, \ldots, p_M$ for a given p_o can hence be written as

$$\begin{aligned} \mathbf{p}_{\mathrm{opt}}(p_o) = \arg \min_{p_{L+1},\cdots,p_M} \tau \\ \text{s.t. } \tau - \frac{\gamma_m}{(p_m \lambda)^{\frac{\alpha}{2}}} = 0, \quad m = L+1, \ldots, M, \\ p_o + \sum_{m=L+1}^{M} p_m = 1, \\ \forall m \in \{L+1, \ldots, M\} : p_o, p_m \geq 0. \end{aligned} \tag{3.16}$$

The problem in (3.16) is a convex optimization problem with linear objective function, convex equality constraints and linear inequality constraints. This optimization problem can be analytically solved with the help of Karush-Kuhn-Tucker (KKT) conditions[51]. Using Lemma 3, we have the following result:

[51] See e.g. [59, Section 2.1] for an introduction.

Theorem 1 (TC with optimal strategy, path loss only)**.** *The solution of the optimization problem* (P1) *with* $q_m = q_m^{pl}$ *in the convex region is given by*

$$p_m^*(\lambda_o) = \frac{\gamma_m^{\frac{2}{\alpha}}}{\sum\limits_{m=L+1}^{M} \gamma_m^{\frac{2}{\alpha}}}(1 - p_o) \text{ for } m = L+1, \ldots, M. \tag{3.17}$$

and $p_m^* = \frac{p_o}{M-L}$ *for* $m = 1, \ldots, L$.

Proof. The solution follows by solving the standard KKT equations. □

Note that (3.17) holds for all α, it is necessarily a local optimum. Furthermore, it is a global optimum for all values of α if conditions on the per channel density, similar to those of Lemma 3, are met. In the case of $\alpha = 4$, convexity of the problem (and hence a global optimum) is assured by Lemma 3. To determine p_o, we numerically solve (3.12) with the $p_m^*(p_o)$ given in Theorem 1.

From the structure of (3.17), we see that the optimal strategy assigns probability to the channels proportional to the $\frac{2}{\alpha}$-th power of γ_m. The smaller γ_m, the worse the channel. From (3.8), we see that for $\rho \to \infty$ (self-interference limited networks) or $\eta_i = \eta_j, \forall i, j$, the optimal strategy is equivalent to the naïve strategy (see Section 3.3) , i.e., to assigning the same probability to each channel.

3.2.2 Optimal strategy for Rayleigh fading model $q = q^{\text{rl}}$

Analogously to the path loss case, we state the following observation (see (3.10)):

Lemma 6. *The optimization problem* (P1) *with* $q_m = q_m^{rl}$ *is convex, if* $\forall m \in \mathbb{M}$: $\lambda_m \Delta \leq 2$.

Proof. We examine the convexity of $c^{\text{rl}} = \sum \lambda_m q^{\text{rl}}(\lambda_m)$. The elements of the Hessian matrix $\mathbf{H}$ are given by

$$\frac{\partial^2 c^{\text{rl}}}{\partial \lambda_i \partial \lambda_j} = \begin{cases} \lambda^2 \Delta \xi_i^{\text{rl}} e^{-\lambda_i \Delta}(2 - \lambda_i \Delta) & , i = j \\ 0 & , i \neq j. \end{cases} \tag{3.18}$$

The matrix $\mathbf{H}$ is positive semi-definite if all minors are non-negative. From (3.18), it can be observed that $\mathbf{H}$ is a diagonal matrix. Hence,

$$\prod_{m=1}^{k} \lambda^2 \Delta \xi_m^{\mathrm{rl}} e^{-\lambda_m \Delta} (2 - \lambda_m \Delta) \geq 0 \tag{3.19}$$

must hold for all $k = 1, \ldots, M$. Since all factors are non-negative, (3.19) is true only if $2 - \lambda_m \Delta$ is non-negative for all $m = 1, \ldots, M$. □

Theorem 2 (TC with optimal strategy, Rayleigh fading)**.** *The optimal p_m^*, denoting the m-th component of $\mathbf{p}_{opt}$, of the optimization problem* (P1) *with $q_m = q_m^{rl}$ in the region $\lambda_m \Delta \leq 2$ are given by*

$$p_m^* = \max\left[0, \frac{1}{\lambda \Delta}\left(1 - \mathscr{W}\left(\frac{\nu^* e}{\lambda \xi_m^{rl}}\right)\right)\right], \quad m = 1, \ldots, M, \tag{3.20}$$

where ν^* is the solution of

$$\sum_{m=1}^{M} \max\left[0, \frac{1}{\lambda \Delta}\left(1 - \mathscr{W}\left(\frac{\nu e}{\lambda \xi_m^{rl}}\right)\right)\right] - 1 \stackrel{!}{=} 0. \tag{3.21}$$

and $\mathscr{W}(\cdot)$ denotes the principal branch of the Lambert-W function.

Proof. The solution follows by solving the standard KKT equations. □

3.3 Numerical evaluation

3.3.1 Suboptimal channel access strategies

In the following, we describe four suboptimal channel access strategies of practical importance: Naïve , best channel only, threshold-based, and min-max optimized threshold-based channel access. Adaptive strategies can be further classified as being *hard*- or *soft*-adaptive: We call a strategy hard-adaptive if all active channels are treated equally, i.e., the access probabilities of active channels do not depend on the external interference. A strategy is soft-adaptive if the access probabilities of active channels can differ.

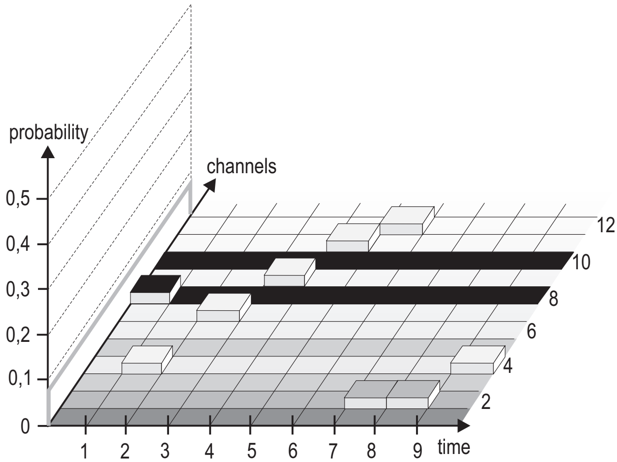

Figure 3.1: Exemplary realizations of naïve (non-adaptive) hopping over 12 channels. Darker channels indicate lower quality, i.e., higher external interference. Channels used for data transmission are denoted by cells.

Naïve non-adaptive channel access

For the naïve strategy, every node selects a channel with equal probability, i.e., $\mathbf{p} = [\frac{1}{M}, \ldots, \frac{1}{M}]^T$. The resulting density in each channel is

$$\lambda_m = \frac{\lambda}{M} \tag{3.22}$$

for all $m \in \mathbb{M}$. This non-adaptive hopping strategy corresponds to standard FH-CDMA. It is illustrated in Fig. 3.1.

Best channel only access

For the best (single) channel only access strategy, only the best available channel, i.e., the channel with the least NSR_m, is used. The corresponding intensity λ_m is given by

$$\lambda_m = \begin{cases} \lambda & , m = \arg\min_n \{\mathrm{NSR}_n | n = 1, \ldots, M\} \\ 0 & , \text{otherwise.} \end{cases} \tag{3.23}$$

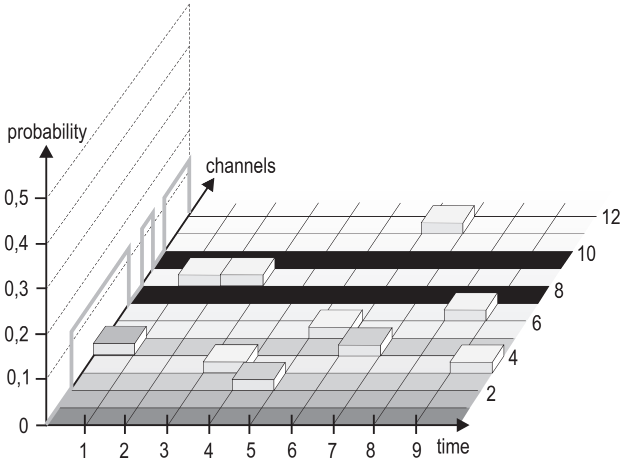

(a) Hard adaptive, threshold-based hopping

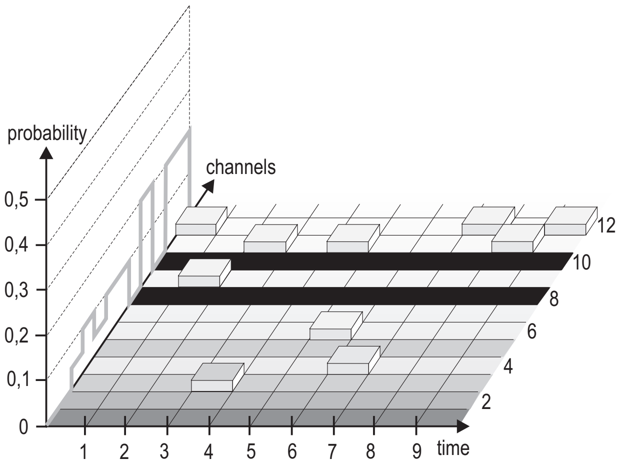

(b) Soft adaptive, optimized threshold-based hopping

Figure 3.2: Exemplary realizations of adaptive hopping strategies over 12 channels. Darker channels indicate lower quality, i.e., higher external interference. Channels used for data transmission are denoted by cells.

According to our classification, the best channel only strategy is hard-adaptive.

Threshold-based channel access

With the threshold based channel access strategy, both the best K channels and all remaining channels with sufficient quality are used. The criterion for a channel m to be active is $\mathrm{NSR}_m \leq \kappa$, where κ denotes the quality threshold. Let the set of active channels be denoted by

$$\mathscr{K} = \{m \in \mathbb{M} : \mathrm{NSR}_m \leq \kappa \vee \mathrm{NSR}_m \,\text{among the}\, K \text{ smallest}\} . \tag{3.24}$$

Then $|\mathscr{K}|$ with $|\mathscr{K}| \geq K$ is the number of active channels, and this channel access strategy assigns transmission density to the channels according to

$$\lambda_m = \begin{cases} \frac{\lambda}{|\mathscr{K}|} & , m \in \mathscr{K} \\ 0 & , \text{otherwise.} \end{cases} \tag{3.25}$$

This hard-adaptive thresholding strategy is comparable to the mechanism implemented in IEEE 802.15.1/802.15.2 [9, 60] and shown in Fig. 3.2(a).

Min-max optimized threshold-based channel access

In this optimized version of threshold-based channel access, the channel access probabilities for the active channels are determined by solving the min-max problem over all *active* channels. Denoting by $\mathscr{K}^c = \mathbb{M} \setminus \mathscr{K}$ the set of all inactive channels, one can write

$$\begin{aligned} \min_{\mathbf{p}} \max_{m} \, & p_m q_m(p_m \lambda) \\ \text{s.t.} \; & p_m \geq 0 \text{ if } m \in \mathscr{K}, \\ & p_m = 0 \text{ if } m \in \mathscr{K}^c, \\ & \|\mathbf{p}\|_1 = 1. \end{aligned}$$

Again, min-max channel allocation ensures constant QoS. A possible outcome of such a soft adaptive scheme is depicted in Fig. 3.2(b). By its construction, this strategy is soft-adaptive.

Parameter	r	β	α	M	$\overline{\text{NSR}}$	κ	K
Value	10	1	4	10	$-5\,$dB	$5\,$dB	3

Table 3.1: Evaluation parameters

3.3.2 Comparison of channel access strategies

For numerical evaluation and comparison of the strategies, we chose NSR to be exponentially distributed, NSR $\sim$ Exp, with expected value $\overline{\text{NSR}} = -5$ dB.[52] The basic parameters are given in Table 3.1, corresponding to a robust WLAN scenario with a medium number of channels and low decoding threshold. The effects of varying these basic model parameters will be examined in simulations. In the non-convex region, that is for high λ and q, the $\mathbf{p}_{\text{opt}}$ were obtained numerically using global optimization heuristics.

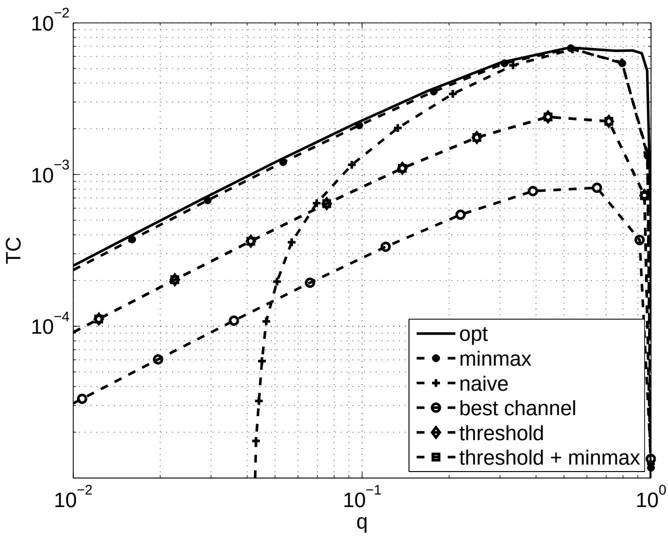

Figure 3.3: Path loss model, transmission capacity for various strategies

[52]Note that the assumption NSR $\sim$ Exp has been made ad hoc. However, the exact external interference statistics do not affect the relative performances of the strategies.

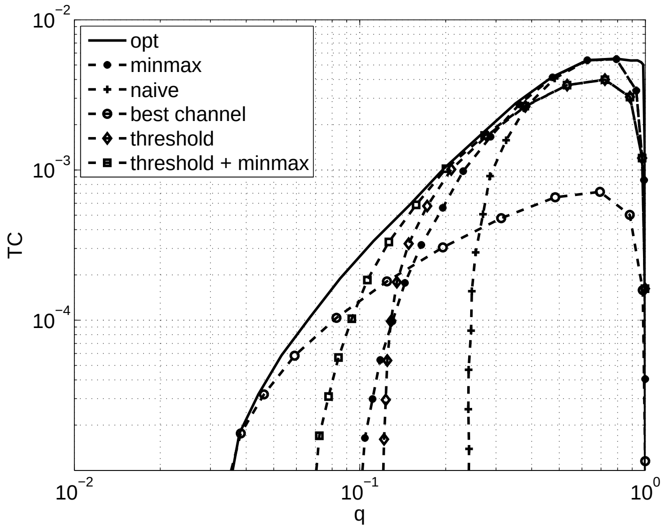

(a) Rayleigh fading model, without fading of external interference

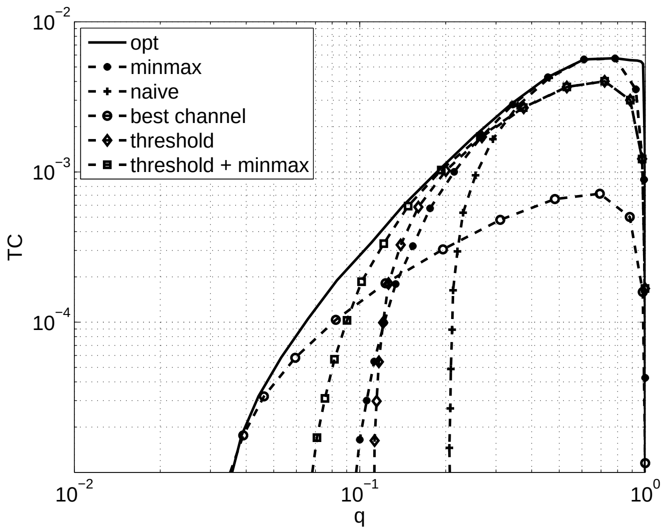

(b) Rayleigh fading model, with fading of external interference

Figure 3.4: Transmission capacity for various strategies

Fig. 3.3 and Fig. 3.4(a) show the TC for the path loss and Rayleigh fading model without fading between receiver and external interference ($G_N = 1$). Comparing the two figures, we observe that the TC for Rayleigh fading is generally lower than for the path loss model which is consistent with findings in the single channel case [28].

The TC for Rayleigh fading with $G_N \sim \text{Exp}(1)$, i.e., Rayleigh fading with expected value 1, is shown in Fig. 3.4(b); the qualitative characteristics of the channel access strategies do not differ from those of Fig. 3.4(a), however, fading of external interference increases the TC slightly; notice, for example, the lower outage probability of the naïve strategy at a TC of 10^{-2} successful transmissions per unit area. The TC with $G_N \sim \text{Exp}(1)$ is increased by approx. 8.5%: If fading between receiver and external interferer is present, the outage probability associated with the external interference is lower than without fading. This can be seen directly by applying the Jensen inequality, $P[\frac{g_1}{g_2} < a] = 1 - E[e^{-g_2 a}] \leq 1 - e^{-E[g_2]a} = 1 - e^{-a}$. Thus, fading between receiver and external interferer is beneficial. Knowledge about the type of this channel can hence be exploited for the calculation of the optimal channel access probabilities in order to increase TC.

Furthermore we observe that the channel access strategies behave qualitatively different in the Rayleigh fading model when compared to the path loss model: all strategies exhibit a non-vanishing outage probability even for $\lambda \to 0$. This is due to the fact that outage still may occur, even for very low densities, due to deep fades.

At low outage probabilities, and hence low λ, the optimal strategy is to choose the best channel since this minimizes the overall outage probability. For the path loss model, this effect is not observed – outage probability is unaffected by the quality of good channels. Here, equally balancing internal and external interference is optimal even when λ becomes arbitrarily small. As a result, the optimal and the min-max strategy yield the same solution at small q, while thresholding (with and without min-max optimization) performs slightly worse because not all “alive” channels are used. It should be noted that the transmission capacity metric does not reveal the performance limit of the latter strategies in the path loss model as it assumes a fixed β. The transmitters could employ adaptive modulation and coding in order to benefit from good channels.[53]

[53] If adaptive modulation and coding is employed by the transmitters in order to benefit from good channels, another metric such as the aggregated Shannon capacity should be used here to compare these strategies for the path loss model in order to accurately reflect the gains.

In the intermediate outage probability region, where internal and external interference are of the same order, we can see that both the naïve and the best channel strategy do not perform well. Here, thresholding, and in particular thresholding with min-max optimization, yield large performance gains over a wide range and show near-optimality. For Rayleigh fading, the performance is even better than the min-max solution.

In the high outage probability (and high node density) region, the naïve strategy quickly approaches the optimal TC before falling off.

Fig. 3.5(a) and 3.5(b) show the average outage probability $q(\lambda)$ as well as the average (empirical) standard deviation of the outage probability, i.e.,

$$\sigma = \sqrt{\frac{1}{N}\sum_{i=1}^{N}(q_i(\lambda,\mathbf{p}_i)-\overline{q})^2} \tag{3.26}$$

where the q_i are realizations of the outage probabilities for a certain strategy with corresponding optimized $\mathbf{p}_i$ and

$$\overline{q} = \frac{1}{N}\sum_{i=1}^{N} q_i(\lambda,\mathbf{p}_i) \tag{3.27}$$

is the average (empirical) outage probability.

For the threshold strategies, only the active channels are considered. It can be observed that σ is nearly constant over a wide range. At (undesirable) high outage probabilities, σ increases fast for the optimal strategy (the bend indicates the end of the convex region) and decreases for the threshold and naïve strategy. At low λ, σ is approximately of the same order as q, which may have a negative effect on QoS guarantees. Note that, for both the min-max and the threshold-based min-max strategy, $\sigma = 0$.

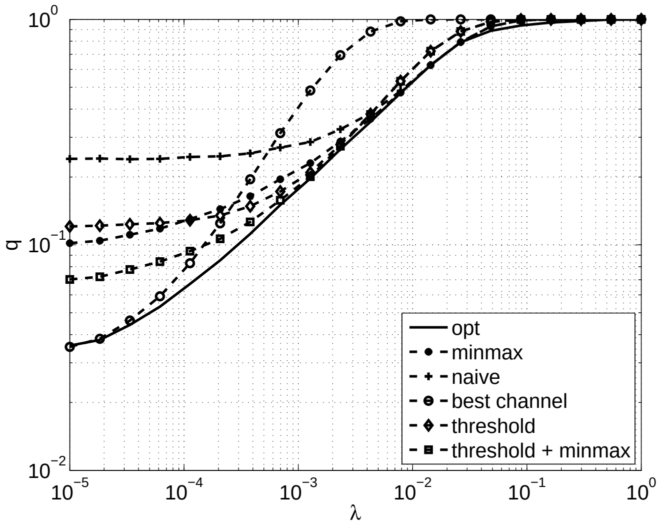

(a) Average outage probability

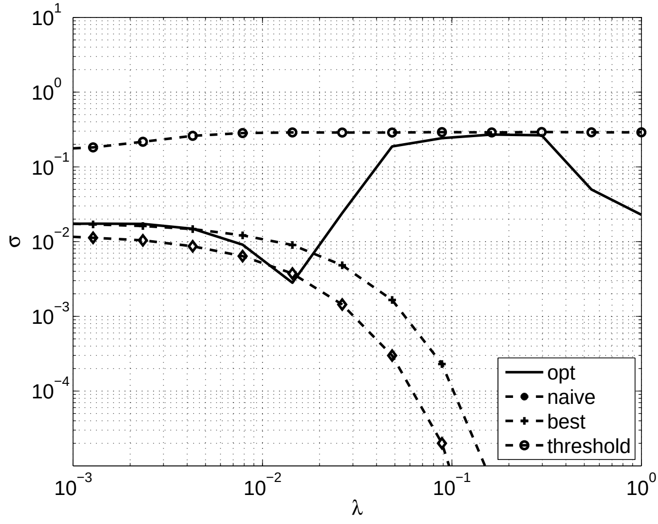

(b) Standard deviation of weighted channel outage probabilities

Figure 3.5: Outage probability and standard deviation as QoS for various strategies (Rayleigh model without fading of external interference)

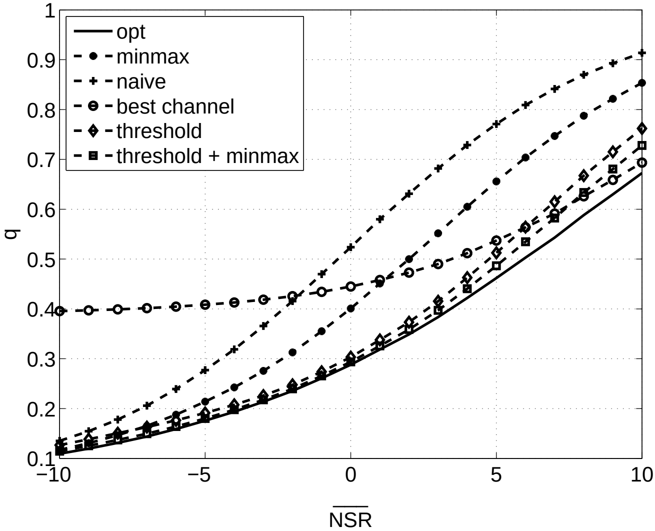

(a) Rayleigh fading model, without fading of external interference

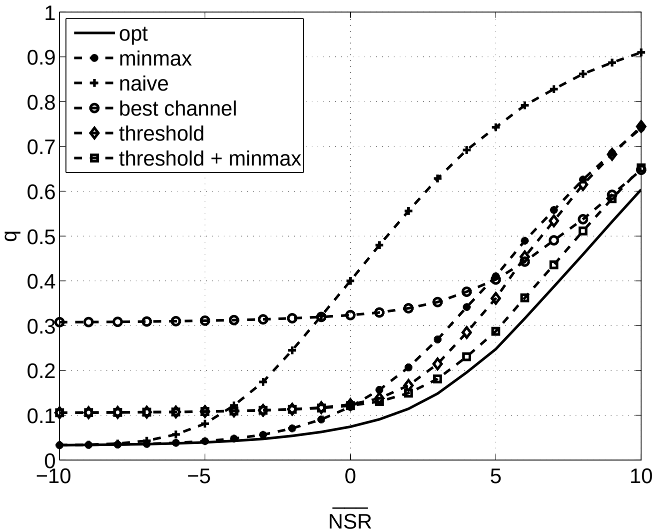

(b) Path loss model

Figure 3.6: Outage probability over $\overline{\text{NSR}}$ for various strategies, $\lambda = 10^{-3}$

Figure 3.6(a) and 3.6(b) show the performance of both models when $\overline{\mathrm{NSR}}$ is varied at a medium node density of $\lambda = 10^{-3}$. With increasing $\overline{\mathrm{NSR}}$ and hence increasing intensity of external interference, the path loss model shows near constant outage probability for all strategies, until a threshold is reached. Fading leads to less threshold-like behavior, as good and bad fades occur for all $\overline{\mathrm{NSR}}$ values. Interestingly, hard-adaptive thresholding and soft-adaptive thresholding show very similar performance in both models and with the given values outperform min-max scheduling over all channels. Comparing hard and soft-adaptive thresholding, a significant gain of soft-adaptive thresholding is only achieved at high $\overline{\mathrm{NSR}}$ values and outage probabilities, which are of small practical importance when operating a network.

The thresholding strategies outperform naïve hopping in the fading model for all $\overline{\mathrm{NSR}}$ values. In the Rayleigh fading model, for low $\overline{\mathrm{NSR}}$ the naïve and the min-max strategy over all channels outperform thresholding. This shows the concentration effect of thresholding: Relatively good channels are excluded at $\kappa = 5\,\mathrm{dB}$ with thresholding, leading to higher internal interference in the remaining channels. If external interference is not the issue, naïve hopping is also the best strategy.

The optimal performance lower bounds the outage probability. One can see that hard and soft-adaptive thresholding show close-to-optimal performance over a wide range of interference levels, especially in the Rayleigh fading model. Soft-adaptive thresholding offers a small gain over hard-adaptive thresholding, especially under high external interference conditions.

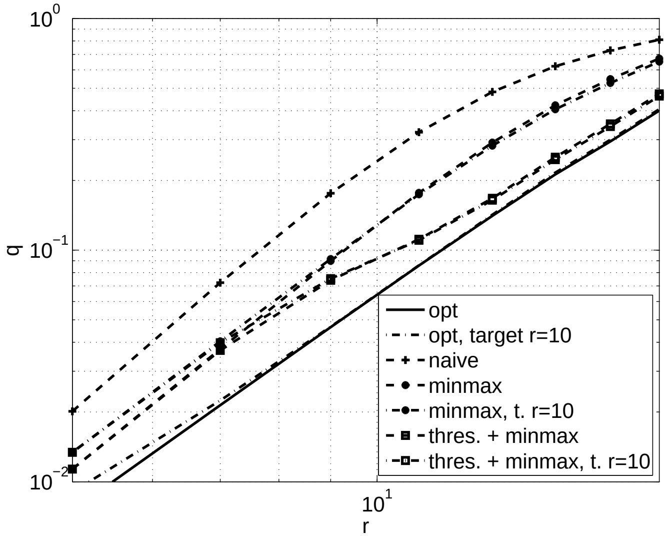

Figure 3.7: Influence of varying transmission distance for a fixed optimization target $r_{\text{opt}} = 10$.

Finally, Fig. 3.7 shows the effect of varying transmission distances r while optimizing the channel access probabilities based on a target transmission distance $r_{\text{opt}} = 10$. In both cases of channel models, outage probability increases only marginally and still remains lower than in the case of the suboptimal solutions.

3.3.3 Implications for protocol design

For protocol design, two conclusions can be drawn from the analysis and comparison of strategies. First, adaptivity does not result in a gain if the node density is high and hence internal interference dominates. In such high density networks, applying a naïve strategy will then yield a close to optimal result. Not included in our system model but of considerable practical importance is the role of communication signaling overhead that will further degrade the performance of adaptive strategies. Especially if the node density is high, it might be preferable to avoid this additional load on the network in favor of a non-adaptive technique.

Second, if the transmitting node density is not extremely high, adaptivity can indeed help: In both the path loss and the Rayleigh model, a min-max strategy, with optional thresholding to exclude bad channels, is a good strategy with the benefit of constant QoS. Interestingly, this holds for all levels of external interference. As long as internal interference is not the limiting factor, adaptivity offers a benefit.

These finding are consistent with the interference avoidance mechanisms currently implemented in IEEE 802.15.1/802.15.2. However, while IEEE 802.15.2 employs hard-adaptive thresholding, a possible small gain can be achieved through soft thresholding. This gain might be greater if time dynamics of interference are considered: A soft adaptive technique can potentially monitor more channels through implicit sensing, i.e., through observation of error rates, and hence adapt faster to a changing interference environment.[54]

3.4 Summary

We derived, for the convex low to medium outage region, analytical outage expressions of the given FH-CDMA system under the influence of external interference for both a Rayleigh fading and path loss model. These expressions can be used to calculate the average outage probabilities as well as the transmission capacities. Suboptimal strategies were compared to those bounds in numerical simulations. As outlined, the implications of the model can be useful in the design stage of wireless network protocols. Future work could focus on finding analytical expressions and bounds for those suboptimal allocation strategies, in order to create an analytical framework for FH-CDMA ad hoc networks under external interference. It could also focus on providing numerical results for different interference fields, i.e., different shapes of q_m. An extension that suggests itself is the combination of locally orthogonal hopping, as described in Chapter 2, and adaptive hopping, for example using a non-homogeneous Poisson approximation, cf. [61].

[54] See also the discussion of implicit and explicit sensing in Chapter 4.

4

MAC design aspects

While the previous chapters analyzed the principal interference trade-offs in frequency hopping code division multiple access (FH-CDMA) ad hoc networks, the objective of this chapter is to describe and compare medium access control (MAC) protocol approaches that implement internal and external interference avoidance mechanisms. Although stochastic geometry is a good tool for modeling global properties of large-scale ad hoc networks, it is still difficult to address MAC design aspects within this model.

In the following section, first a brief overview of the issues encountered in multi-channel MAC protocols and strategies to deal with them is given. We then go on to describe and analyze in a single collision domain a MAC strategy for single transceiver *synchronized* adaptive frequency hopping networks with a high number of channels and nodes. In Section 4.2, we consider internal interference avoidance techniques, while in Section 4.3 the effect of external interference is analyzed.[55]

[55] As in the previous chapters, we differentiate between *frequencies*, *channels* and *hopsets*, see Fig. 2.1. The terms *hopset* and *hopping sequence* are used interchangeably. A frequency is a physical center frequency of a channel. A channel is a pointer to a frequency with an associated bandwidth, and a hopset is a time-indexed set of channels. The term *channel* is also used to describe a snap-shot of a hopset as in *common broadcast channel*.

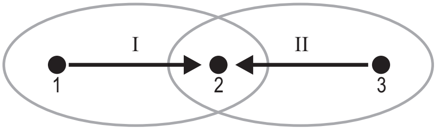

Figure 4.1: The single channel spatial hidden node problem

Prior relevant works are [37], on which we build our analysis, as well as [62]. Both [37] and [62] assume a channel access model that overestimates the performance of a randomly hopping parallel rendezvous MAC, especially if the number of channels and nodes is high. We improve the model and compare the performance of a randomly hopping rendezvous MAC with naïve orthogonal hopping with channel re-use and rendezvous based on multi-level locally orthogonal (MLLO) hopping[56]. We show that the MLLO scheme succeeds at reducing internal interference over traditional approaches. Within the same system model, the gains of external interference avoidance are analyzed in the last section of this chapter. We show under which circumstances external interference avoidance can be beneficial to network throughput.

4.1 Multi-channel MAC issues and classification

4.1.1 Multi-channel hidden node problem

A well known issue in single channel MAC protocol design is the *spatial* hidden node problem, where two transmissions collide at a receiver due to the fact that the transmitting nodes are not able to coordinate their transmissions. This happens because the two nodes are out of transmission range of each other: They could be too far apart or the geometry is such that there is high attenuation between the nodes.

Consider Fig. 4.1, which shows three nodes in two collision domains with two contending links, the latter denoted by Roman numerals. Nodes 1 and 3 are hidden from each other. The (single channel) MAC protocol now has to avoid collisions of packets at node 2. The problem can be mitigated by a

[56]The scheme was also discussed in 2.4, a patent is pending [63].

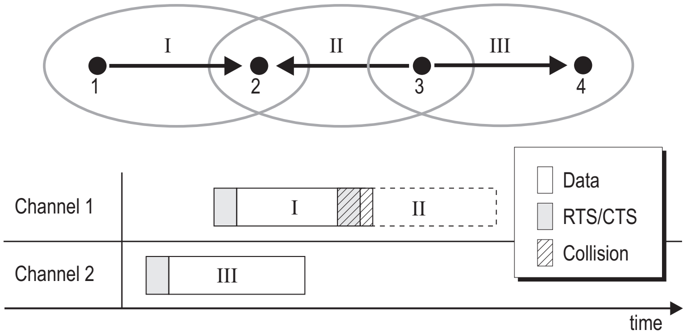

Figure 4.2: The multi-channel hidden node problem

request-to-send (RTS) and clear-to-send (CTS) handshake protocol before data transmission, a technique known as *Carrier Sense Multiple Access/Collision Avoidance* (CSMA/CA). In order to establish link I, an RTS packet is then sent by node 1 and node 2 responds with a CTS packet. This packet includes the duration of the intended transmission and can be overheard by node 3, so that it refrains from accessing the channel until transmission on link I is complete. Conversely, if node 3 happens to start the transmission first to set up link II, the CTS packet will be overheard by node 1. Due to the finite speed of light and the error-prone nature of the wireless medium, a two-way handshake can in practice only mitigate the hidden node problem, but never completely avoid it. Additional measures, such as longer observation times with network-wide synchronization before accessing the medium, can further help to reduce the influence of hidden nodes.

In multi-channel networks, the hidden node problem can become a much greater issue. Consider Fig. 4.2 with four nodes in three collision domains. Assume that, using a traditional RTS/CTS approach, link I is initiated on channel one and node 1 is transmitting while node 3 is busy on channel 2. Once node 3 becomes idle, it tries to initiate a link with node 2 and sends an RTS. This packet collides with the on-going transmission of link I, because node 3 could not overhear the RTS/CTS exchange for link I since it was busy on another channel.

This shows that, in multi-channel networks of single transceiver radios, the multi-channel hidden node problem cannot be mitigated by an RTS/CTS procedure – it cannot be guaranteed that all RTS/CTS handshakes in the neighborhood are overheard because they can be sent on different channels.

4.1.2 MAC strategies

As shown, compared to single channel networks, two factors complicate the design of MAC protocols for multi-channel frequency hopping networks: The multi-channel component does not allow to monitor the channel for transmissions of neighbors, even if the node is in an idle phase. Furthermore, the frequency hopping component induces switching times, during which the node also cannot keep track of the channel status.

The only possibility to mitigate this issue is a common broadcast channel[57] that is accessed from time to time. The way that this common broadcast channel is constituted and used allows multi-channel protocols to be classified. Several principal approaches for organizing the medium access exist [37, 64]:

Synchronous Split Phase protocols have a periodic control and data transmission phase. During the control phase, all nodes meet on a common broadcast channel and negotiate on which channels data transmission should take place. Afterwards, nodes switch channels and return to the control channel after a predefined data transmission period. In synchronous split phase protocols, the control and data phases are synchronized across the whole network. The broadcast channel is used for neighborhood discovery and transmission negotiation.

In *Asynchronous Split Phase* protocols, data transmission is also separated into two phases. The phases are, however, not synchronized network wide. Thus, the load on the broadcast channel is eased but an additional waiting period before transmission is necessary to avoid the multi-channel hidden node problem. An example of this class is the WiFlex protocol proposed by Lee et al. in [64].

Common Hopping is a strategy in which all idle nodes of the network tune to the common broadcast channel. Medium access is negotiated on the channel and data transmission then takes place using a different hopping sequence to

[57] In the terminology of the popular paper on Cognitive Radio by Haykin [18], this common broadcast channel is the necessary *feedback channel* to coordinate spectrum access. In Haykin's words, "cognitive networks" need to be *receiver centric*, as interference occurs only at the receiver.

exchange data. This approach is structurally simple to implement and inherently well suited for use in frequency hopping networks. A disadvantage is the high load on the broadcast channel, leading to a single point of failure.

In *Parallel Rendezvous* protocols, all nodes know the hop sequences of the nodes in their neighborhood. The broadcast channel is used for neighborhood discovery; transmissions are initiated directly with the intended destination node as the hop set is known. It is communicated within the neighborhood over the broadcast channel. Parallel rendezvous is the best suited candidate for robust large scale network applications with frequency hopping. It requires rigorous timing synchronization and local knowledge of the hopping sequences of all possible communication partners. These factors increase protocol complexity but are necessary in a frequency hopping setting. It also makes the network less vulnerable to jamming, since the common broadcast channel is used for neighborhood discovery only. Also, due to the concurrent structure of transmission initiation, parallel rendezvous protocols have been shown to perform better in networks with a high number of channels and nodes than single channel rendezvous protocols [37]. Parallel rendezvous-type multi-channel MAC do not necessarily need to employ frequency hopping[58], but many multichannel MAC protocols suggested in literature rely on frequency hopping to increase robustness and flexibility as the service quality of channels varies. Examples of such protocols are SSCH [65] or McMAC [66], both of which allow simultaneous transmission agreements to improve performance. In these protocols, each node has its own home channel, which may or may not follow a frequency hopping sequence. Nodes visit the home channel of their potential receivers to transmit data.

[58]Capacity loss due to switching times and increased spurious emissions are the price to be paid. Whether frequency hopping is a good choice highly depends on the application.

Protocol class	Use of common channel	MAC hidden node resolution	Suitability for large scale frequency hopping networks
Synchronous Split Phase	Neighborhood discovery and negotiation	yes	low
Asynchronous Split Phase	Neighborhood discovery and negotiation	yes	moderate
Common Hopping	Neighborhood discovery and negotiation	yes	moderate
Parallel Rendezvous	Neighborhood discovery	no	high

Table 4.1: Multi-channel MAC protocol classes, relevant for frequency hopping networks

The disadvantage of parallel rendezvous is that the multi-channel hidden node problem is not inherently resolved. For this reason, parallel rendezvous will find better applicability in scenarios with few hidden nodes. Such a scenario is given if, for example, the majority of links use high transmission power as in tactical military communications. If there are numerous hidden nodes, additional measures to mitigate their influence on performance need to be taken. For these reasons, parallel rendezvous is unlikely to be a good choice for low cost, low power applications such as sensor networks.

Parallel rendezvous is the best option, if a dedicated transceiver for exchanging control information is available. This dedicated channel can then be used to announce successfully established transmissions and hence allows all nodes that share a collision domain to keep track of the network state. This is also an argument for applications that target high cost communication networks.

A *hybrid approach* that clusters nodes into groups that are hidden from each other but have conflicting links can also be a viable option. A single channel rendezvous to mitigate the hidden node problem is then used only for nodes inside that cluster, but not for all nodes in the network, thus easing the burden on the rendezvous channel.

Table 4.1 summarizes the properties of different protocol classes with respect to their applicability to frequency hopping networks.

4.1.3 Interference avoidance on the MAC layer

The primary task of the MAC layer is to organize medium access in a manner that ensures that internal interference is avoided, i.e., in such a way that orthogonal communication channels are provided to links. Also, in multi-channel networks that operate in an environment which includes adverse external interference conditions, the MAC layer has to adapt to changes in the interference landscape to minimize external interference.

The degree of freedom a single communication link in a frequency hopping network has to optimize its performance is the choice of hopping sequence. The MAC layer needs to choose a good hopping sequence assignment, minimizing internal (multiple access) interference and the influence of external interference.

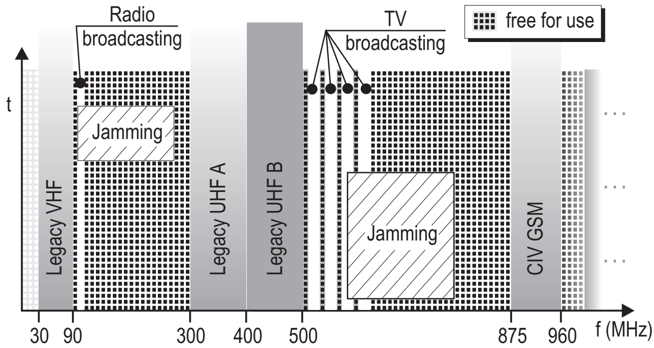

Figure 4.3: Example of a frequency plan

Fig. 4.3 shows a possible situation for the frequency plan of a deployed tactical military communications network[59]. Several frequency bands are permanently excluded from network usage by prior frequency planning. In these bands, legacy systems operate that should not be interfered with. These systems are shown here as Legacy VHF, Legacy UHF A and Legacy UHF B. Furthermore, civilian systems, exemplarily shown here as CIV GSM, should not be interfered with, either. Other frequency bands are free for use, even if their own transmissions interfere with other systems such as TV and radio broadcasting as shown in the sketch. Network nodes can use this spectrum opportunistically for their communication if it is free at their location. Deliberate jamming is also shown: The network needs to adapt to this external interference, e.g., by temporarily excluding the jammed channels from the hop set.

External interference to the network can be caused by deliberate jamming or by transmitters, which are not part of the communication network, e.g., by civilian systems or by other enemy communication systems. The detection of external interference and the discovery of new transmission opportunities – the absence of external interference in certain channels – are carried out via spectrum sensing. From a design perspective, one can differentiate between *implicit sensing* and *explicit sensing*.

Implicit sensing is the monitoring of the per channel packet error rate. Each

[59] We use military communications as an example. Frequency hopping systems in large scale ad hoc networks for other applications operate in a technically similar manner. The frequency ranges will differ, but the mode of operation will be analogical.

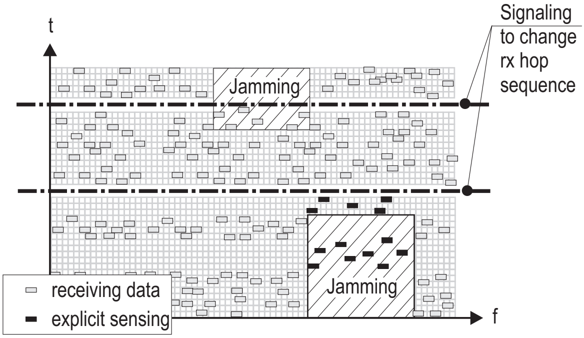

Figure 4.4: Principle of adaptive hopping

network node collects statistics of the errors occurring in transmissions to a certain node in the neighborhood. It monitors the channel link quality to adapt coding and modulation. If the quality of transmissions to a node in the neighborhood varies greatly depending on the channel chosen, the channels experiencing lower SINR values are probably being interfered with.

Explicit sensing is the monitoring of channels during idle periods. The cumulated noise and interference power is measured in the absence of a transmission. Explicit sensing, independent of the sensing algorithm, requires some control over the gain settings in order to be able to attach a physical interference temperature value to the measurement, a fact to be taken into account when designing the RF hardware for such an application. Explicit sensing is also associated with a certain cost, as the node is busy during the sensing phase and not available to receive data.

The combination of both sensing approaches yields an overall view of the spectral occupancy at the location of a node. With implicit sensing, the node can decide which channels to *exclude* from the hopping sequence for optimal performance. With explicit sensing, the node can explore new or monitor previously excluded channels and decide to *include* them to increase the robustness of transmissions. Fig. 4.4 shows the time-frequency plane with the receive channel hop sets of a communication between two nodes. During idle times, the nodes use explicit sensing to explore channels currently not included in their hop set, while implicit sensing is used to eliminate jammed channels from the hop set.

Accessing a certain channel always increases the internal network interference in that channel. Instead of hard limiting, i.e., including or excluding channels in the hop sequence, one can also adapt the channel hopping probabilities: Good channels should be included more frequently than bad channels. Such strategies were examined in Chapter 3. It was found that a good potential strategy is based on a min-max criterion, balancing internal and external interference, leading to equal weighted packet error probabilities in all hopping channels.

To increase overall robustness against jamming, the node should strive

- to maximize the hopping bandwidth, i.e., the spectral distance between the channel with lowest center frequency and the channel with highest center frequency and
- to favor higher frequency ranges over lower frequency ranges if network load allows.

If the hopping bandwidth is maximized, a responsive jammer that monitors the spectrum and allocates interference power to detected transmissions has to cover the maximum bandwidth. The higher the spectral distance, the less likely a responsive jammer will be able to intercept that packet and react with a jamming signal. Furthermore, if the network tends to use channels as high as possible in the operating bandwidth, jamming is hindered by the unfavorable propagation properties and higher attenuation of higher frequencies. Active transmission channels should choose their center frequencies as high as possible, but as low as necessary so as to not impact the point-to-point data rate.

4.2 Avoidance of internal interference

After describing in the previous sections the principal tasks of the MAC layer in multi-channel networks, we will, for the remainder of this chapter, focus on parallel rendezvous-type MAC. Such a MAC approach is the primary choice for military communication applications as illustrated in Fig. 4.3 and Fig. 4.4. Parallel rendezvous-type MAC can be considered for all applications where the price for scalability, i.e., increased complexity, can be afforded. We furthermore assume that measures have been taken to mitigate the multi-channel hidden node problem, for example, by employing a separate dedicated control channel. This allows for approximation of the network MAC performance with a single collision domain model.

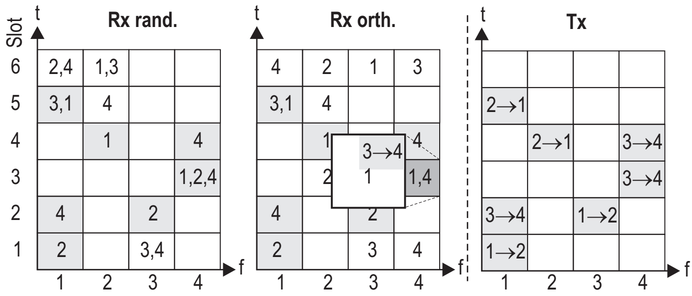

Figure 4.5: Receive and transmit channel hopping for random and orthogonal rendezvous; $M = 4$, $N = 4$. The transmit plane shows on-going transmissions, e.g., $1 \rightarrow 2$ denotes a link from node 1 to node 2. The receive planes show a realization of home channels of idle nodes, overlaid with transmissions. We observe that, for orthogonal hopping, *idle* nodes do not collide on the receive plane, but they can collide with on-going transmissions. E.g., in channel 4, slot 3 (drawn to perspective) the home channel of idle node 1 collides with "$3 \rightarrow 4$".

4.2.1 Parallel rendezvous hopping strategies

In [37], Mo et al. analyzed different classes of multi-channel MAC protocols, including parallel rendezvous protocols. For rendezvous, the authors assumed a pseudo-random hopping home channel strategy to be implemented, e.g., as part of McMAC introduced in [66]. In McMAC, if a link is established, nodes stop hopping to transfer data. When idle, nodes hop according to a pseudo-random sequence. On average, this distributes the transmissions over all channels.

We propose to deviate from the McMAC scheme in two ways in order to increase throughput and robustness:

1. The rendezvous scheme shall be based on orthogonal hopping instead of random hopping to minimize interference, and
2. during data transmission, nodes shall continue to hop according to a sequence taken from an orthogonal transmission hop set[60]. The channel in

[60]Note that, although simple, to the best of the author's knowledge, this extension has not been

which the nodes meet determines the exact transmission sequence. Fig. 4.5 shows a possible receive and transmit hopping sequence according to this doubly orthogonal scheme for $N = 4$ nodes in $M = 4$ channels. For comparison, an example of random hopping rendezvous for the same link sequence is also shown.

Using multi-level locally orthogonal hopping as the home channel hopping scheme improves performance. In the following sections, we compare random hopping rendezvous with rendezvous strategies based on orthogonal hopping, namely orthogonal hopping with channel re-use and multi-level orthogonal hopping. The framework of Mo et al. [37] is used for analysis.

Random hopping

The simplest hopping strategy is pseudo-random hopping in which the next home channel is determined by a pseudo-random sequence. With random hopping, each device picks a seed to generate a different pseudo-random hopping sequence. Nodes follow their "home" hopping sequence when they are idle. As nodes attach their random seeds to every packet they send, their neighboring devices can eventually learn the hopping patterns in a neighborhood. For example, McMAC uses a linear congruential generator $X(t) = 16807 \cdot X(t-1) \bmod (2^{31}-1)$, where $X(t)$ is a pseudo-random number at time t. To map $X(t)$ to channel space, a modulo M operation is applied to $X(t)$, where M is the number of channels. Other similar schemes employing different pseudo-random number generators are thinkable.

Orthogonal hopping

Orthogonal hopping is different from random hopping in that orthogonal sequences are used to minimize receiver side collisions. For our purposes, two sequences $s = (s_1, s_2, \ldots)$ and $s' = (s'_1, s'_2, \ldots)$ are said to be orthogonal if $s_i \neq s'_i$ for all $i = 1, 2, \ldots$. Assume that the number of channels is $M = 3$. Then, two hopping sequences $(1,3,2,1,\ldots)$ and $(3,2,1,2,\ldots)$ are orthogonal.

The maximum number of orthogonal sequences is the same as the number of channels M. When the number of devices N is less than the number of channels, it is possible to keep the home channels of idle nodes collision-free. However, if $N > M$, there is no way to avoid sharing home channels.

suggested in literature.

Orthogonal hopping with channel re-use: A possible solution for sharing home channels is assigning the same hopping sequence s to two or more nodes. This channel re-use scheme arises naturally when allocating hopping sequences such that interference in the network is minimized as considered in Chapter 2: Nodes that are far apart will use the same sequence, while close nodes will use different sequences. Even though our MAC system model does not reflect distance (and hence interference) relationships, we evaluate orthogonal hopping with channel re-use for the purpose of comparison.

Multi-level orthogonal hopping: Another method to address the limited number of orthogonal codes is proposed in Chapter 2.4. It uses multiple sets of orthogonal codes. Each of these sets can be seen as a *layer*, stacked up in multiple levels on top of other. A layer hence comprises M sequences and any two sequences in a layer are orthogonal. For example, for 5 nodes in 3 channels there would be 2 layers, one layer with 3 nodes and another one with 2 nodes. Each layer has an associated pseudo-random sequence. To reduce correlation between layers, all sequences in a layer are pseudo-randomly permutated in each step. In this way, collisions are avoided between nodes in the same layer – thus keeping the benefits of orthogonal hopping – while collisions between nodes in different layers are randomized.

Orthogonal hopping, as will be seen in the following, leads to higher throughput compared to random hopping. This advantage[61] of orthogonal hopping over random hopping stems from the fact that home channels are more evenly distributed while many devices can be listening in a single channel with non-negligible probability using random hopping. With an even distribution of home channels, the probability of receiver contentions decreases. In the following, we compare the different home sequence hopping schemes with a Markov chain model and simulation.

4.2.2 Performance model

The discrete time Markov chain model of [37] is extended to compare different hopping strategies; the model is briefly explained in the following[62]. There are

[61] The possible gains of orthogonal hopping can be achieved if nodes within a collision domain coordinate their home sequences. In ad hoc networks, this can be achieved in a decentralized manner without explicitly coordinating the channel choice as further described Chapter 2.4.

[62] See [37] for further analysis and other relevant references.

N nodes that operate in M channels. In each time slot, an idle node tries to transmit with probability p; the parameter p hence models the overall network load. If an agreement with the intended receiver is made, a packet is transmitted over the following time slots. The packet lengths, given in number of slots, are assumed to be geometrically distributed with mean $1/q$. This implies that each ongoing packet transmission ends independently with probability q in each slot, allowing for a memoryless Markov chain model.

Assuming half-duplex transmission, the state space $\mathscr{S}$ of the Markov chain comprises the number of currently active transmissions[63]:

$$\mathscr{S} = \left\{0, 1, \ldots, \min\left(\left\lfloor \frac{N}{2} \right\rfloor, M\right)\right\}, \tag{4.1}$$

where $\lfloor \cdot \rfloor$ denotes the floor function.

The state changes either if new transmission agreements are made or if transmissions end. Let $S_k^{(i)}$ and $T_k^{(j)}$ denote the probability of i transmissions starting and j transmissions ending when the current state is k. The maximum number of transmissions that can end in the next time slot is k. The transition probability $p_{k,l}$ from state k into state l can then be written as

$$p_{k,l} = \sum_{m=\max\{k-l,0\}}^{k} S_k^{(m+l-k)} T_k^{(m)}. \tag{4.2}$$

The $p_{k,l}$ are the elements of the stochastic transition probability matrix P. From P, one can calculate the steady state distribution vector π by solving $\pi P = \pi$, i.e., by calculating the eigenvector of P associated with eigenvalue 1. An element π_i gives the equilibrium probability of being in state i, i.e., the probability that i transmissions are ongoing. Using the steady state distribution vector π, the total average throughput C can be calculated as

$$C = \sum_{i=0}^{|\mathscr{S}|-1} i\pi_i. \tag{4.3}$$

[63] If the same model is applied to multiple collision domains, the state space has to include all $(n-1)n$ links leading to a total number of $2^{n(n-1)}$ states. Note that directionality also has to be considered, as active links create potential conflicts. These conflicts depend on the network geometry. Furthermore, hidden nodes can create collisions with active links, degrading performance. We see that, without the single domain collision assumption, the model becomes significantly more complex and is limited to a small number of nodes.

The termination probability $T_k^{(j)}$ can be easily computed from the assumption of a geometric packet length distribution. The number of ending transmissions in each time slot follows a Bernoulli distribution with parameter q, since all ongoing transmissions end independently:

$$T_k^{(j)} = \binom{k}{j} q^j (1-q)^{k-j}. \tag{4.4}$$

However, the (success) probability $S_k^{(j)}$ of j new agreements is quite complicated for a parallel rendezvous protocol and is, according to the law of total probability, given by

$$\begin{aligned} S_k^{(j)} = \sum_{a=0}^{N-2k} \sum_{o=0}^{\min(M,a)} \sum_{i=0}^{o} & P\left[A=a\right] P\left[O=o|A=a\right] \\ & P\left[I=i|A=a,O=o\right] P\left[J=j|A=a,I=i,O=o\right] \end{aligned} \tag{4.5}$$

The conditional probabilities are calculated in the following. To have j new connections, these conditions need to be met:

1. The number A of nodes attempting to start a transmission should be equal to or larger than j,
2. the number of ”one-attempt” channels O, i.e., the number of channels where exactly one device tries to initiate a transmission should be at least j,
3. the number of idle one-attempt channels I should be larger than j and
4. the number of idle receivers that are ready to start a new connection in an idle one-attempt channel J should be exactly j.

The probability of a idle nodes wanting to start a transmission, again given the current number of active nodes k, is

$$P\left[A=a\right] = \binom{N-2k}{a} p^a (1-p)^{N-2k-a}. \tag{4.6}$$

The one-attempt probability $P(O=o|A=a)$ depends on the home channel hopping strategy and will be evaluated later for different approaches.

To calculate $P(I=i|O=o,A=a)$, the total number of ways to get exactly i idle one-attempt channels is considered: $\binom{M-k}{i}$ is the number of ways to distribute

i idle one-attempts onto $M-k$ idle channels. $\binom{k}{o-i}$ gives the number of ways to distribute the remaining $o-i$ busy one-attempts to the k busy channels. Finally, $\binom{M}{o}$ is the number of possibilities to distribute o one-attempts to M channels. Hence, the probability that o one-attempt channels are idle[64] is

$$P[I=i|O=o,A=a] = \frac{\binom{k}{o-i}\binom{M-k}{i}}{\binom{M}{o}}. \tag{4.7}$$

Finally, the probability that a given transmitter finds its receiver, i.e., that the intended receiver is not busy or part of the attempting nodes, is approximated by

$$p_s = \frac{N-2k-a}{N-1}, \tag{4.8}$$

that is, we assume that all idle devices are equally busy, i.e., that no node is selected more often than others as a receiver. Accordingly, the probability that j nodes find their receivers and can establish a new connection is

$$P[J=j|I=i,O=o,A=a] = \binom{i}{j} p_s^j (1-p_s)^{i-j}. \tag{4.9}$$

One-attempt probability

The one-attempt probability or $P[O=o|A=a]$ models collisions in parallel rendezvous protocols and has significant impact on the throughput C. Collisions occur if transmitters select

- the same receiver or
- two different receivers with the same home channel.

The latter probability differs depending on the hopping strategies of devices and we would like to compare them for two different strategies: Random hopping and orthogonal hopping.

If the home channels of devices are uniformly distributed over multiple channels, the chance of a receiver collision decreases. In the case of random hopping in which devices select their home channel randomly, the home channels are evenly distributed only *on average*, however, for a given realization, there is a high probability that home channels will overlap. With orthogonal hopping, the receiver channel collision probability can be significantly reduced.

[64] Note that the formula given in [37, Section 3.3] contains a typing error.

Random hopping: With random hopping, each node chooses its current home channel with equal probability from the number of available channels. Collisions can occur due to two events: Transmitters can select the same receiver or two selected receivers have the same home channel[65]. Both collision events are independent.

We calculate the one-attempt probability by conditioning on a certain selection of receivers and a certain selection of home channels.

The probability of a certain outcome $\vec{c}_t = (c_1, c_2, \ldots, c_N)$ of selected receivers is given by

$$P\left[\vec{C}_t = \vec{c}_t | A = a\right] = \binom{a}{c_1, c_2, \ldots, c_N} \left(\frac{1}{N}\right)^a, \tag{4.10}$$

where c_i denotes the number of transmitters choosing node i. Valid outcomes are all $\binom{N+a-1}{a}$ N-compositions[66] of a, i.e., $\sum_{i=1}^{N} c_i = a$, with $c_i \geq 0$.

Analogously, the probability of a certain outcome of receiver home channels $\vec{c}_r = (c_1, c_2, \ldots, c_M)$ is given by

$$P\left[\vec{C}_r = \vec{c}_r | A = a\right] = \binom{a}{c_1, c_2, \ldots, c_M} \left(\frac{1}{M}\right)^a, \tag{4.11}$$

where c_i denotes the number of receivers dwelling in channel i. Valid outcomes are all M-compositions of a.

$\vec{c}_r$ and $\vec{c}_t$ denote the number of transmitters and receivers in a certain channel. For a given combination of $\vec{c}_r$ and $\vec{c}_t$, the number of one-attempts can be calculated by generating all receive channel assignments that yield the same $\vec{c}_r$ and counting the number of one-attempts when throwing balls into bins according to $\vec{c}_t$. Due to symmetry, this can easily be achieved by generating one possible receive channel assignment according to $\vec{c}_r$ and then generating all $a!$ permutations of this assignment. The one-attempt probability $P(O = o | \vec{C}_t = \vec{c}_t, \vec{C}_r = \vec{c}_r)$

[65] The one-attempt probability given in [37] for the parallel rendezvous protocol McMAC is correct for orthogonal hopping and $N \leq M$. It gives an upper bound on the one-attempt probability for random hopping since the probability of receive channel collisions is neglected. For orthogonal hopping and $N > M$, collisions of receive channels have to be taken into account as well. Pawelczak et al. in [62] use the same optimistic model.

[66] The compositions can be efficiently enumerated using the NEXTCOM algorithm described in [67, pp. 46].

is then calculated numerically by counting the number of outcomes with exactly o one-attempts.

To calculate the overall unconditional one-attempt probability for random hopping, the probability of each transmit and receive channel combination needs to be considered:

$$P[O=o|A=a] = \sum_{i=1}^{\binom{N+a-1}{a}} \sum_{j=1}^{\binom{M+a-1}{a}} P\left[\vec{C}_t = \vec{c}_i\right] P\left[\vec{C}_r = \vec{c}_j\right] \\ P\left[O=o|\vec{C}_t = \vec{c}_t, \vec{C}_r = \vec{c}_r\right], \tag{4.12}$$

where the $\vec{c}_i$ and $\vec{c}_j$ run through all possible outcomes for transmitter and receiver collisions.

Orthogonal hopping: Orthogonal hopping assigns one of M orthogonal home channels to nodes. If $N > M$, some nodes have to share a home channel. We distribute the available channels to nodes evenly so that the maximum of the number of nodes that have the same home channel is minimized. Let L denote the number of full layers, i.e., $L = \lfloor \frac{N}{M} \rfloor$.

In the following, let the number of bins with exactly one ball after throwing x balls uniformly into y bins be denoted by $B(y,x)$ and the number of bins with exactly zero balls as $Z(y,x)$. There is no closed-form solution for the probability distribution of $B(y,x)$ and $Z(y,x)$, but they can be calculated by considering a Markov chain, for which the states $(Y_0^{(n)}, Y_1^{(n)})$ describe the number of bins containing zero balls $Y_0^{(n)}$ and exactly one ball $Y_1^{(n)}$ after n throws: The initial state is $(Y_0^{(0)}, Y_1^{(0)}) = (N, 0)$ and the transition probabilities are

$$P\left[(Y_0^{(n+1)}, Y_1^{(n+1)}) = (y_0, y_1) | (Y_0^{(n)}, Y_1^{(n)}) = (y_0, y_1)\right] = 1 - \frac{y_0 + y_1}{N},$$

$$P\left[(Y_0^{(n+1)}, Y_1^{(n+1)}) = (y_0 - 1, y_1 + 1) | (Y_0^{(n)}, Y_1^{(n)}) = (y_0, y_1)\right] = \frac{y_0}{N}$$

and

$$P\left[(Y_0^{(n+1)}, Y_1^{(n+1)}) = (y_0, y_1 - 1) | (Y_0^{(n)}, Y_1^{(n)}) = (y_0, y_1)\right] = \frac{y_1}{N}.$$

First, assume that $N \leq M$. The one-attempt probability $P[O = o|A = a]$ is then given by $P[B(M,a) = o]$.

Now, assume $N > M$. If $N \bmod M = 0$, the one-attempt probability $P[O = o|A = a]$ is also given by $P[B(M,a) = o]$ due to symmetry, as all channels have equal probability of being selected. If $N \bmod M \neq 0$, $R = N \bmod M$ channels are used by $L+1$ nodes, while $M - R$ channels are used by L nodes. The total one-attempt probability can be calculated by considering all possible outcomes of the distribution of attempts to the two partitions R and $M - R$. The probability of having k attempts in the R bins is $\binom{a}{k} p_R^k (1-p_R)^{a-k}$ with $p_R = \frac{R(L+1)}{N}$.

The one-attempt probability for orthogonal hopping is then

$$P[O = o|A = a] = \sum_{o=1}^{a} \sum_{o_1,o_2} \sum_{k=0}^{a} \binom{a}{k} p_R^k (1-p_R)^{a-k} \\ P[B(R,k) = o_1]\, P[B(M-R, a-k) = o_2] \,, \tag{4.13}$$

where the second sum runs over all $\binom{o+1}{o} = o+1$ possible 2-compositions of o one-attempts.

Single attempt collision probability

The probability of collision for a single attempting node with any other node is another metric that can be used to show differences in performance. We compute the probability p_c of collision of a representative receiver given a attempting nodes.

Random hopping: To calculate the collision probability p_c of a representative receiver for random hopping, we consider two mutually exclusive events:

1. At least one of the other $a-1$ attempting devices selects the representative node and
2. none of the other $a-1$ attempting devices selects the representative node.

In the first case, a collision occurs with probability 1 while in the second case, a collision only occurs if the home channel of another receiver is shared with the home channel of the representative node.

The probability of the first event is as simple as $1-\left(1-\frac{1}{N}\right)^{a-1}$. Given the second event of probability $\left(1-\frac{1}{N}\right)^{a-1}$, if we let r be the number of selected receivers out of $N-1$ potential receivers by $a-1$ attempting devices, then it ranges from 1 to $a-1$. This probability is the same as $P[Z(N-1,a-1)=N-r-1]$ or the probability that $N-r-1$ devices are not selected. By multiplying the probability that at least one home channel must overlap, we have the collision probability

$$
\begin{aligned}
p_c = & 1-\left(1-\frac{1}{N}\right)^{a-1}+\left(1-\frac{1}{N}\right)^{a-1} \\
& \sum_{r=1}^{a-1} P\left[Z(N-1,a-1)=N-r-1\right] \\
& \left(1-\left(1-\frac{1}{M}\right)^{r}\right).
\end{aligned} \tag{4.14}
$$

Orthogonal hopping with channel re-use: For orthogonal hopping with channel re-use, some channels are occupied by $L=\lfloor\frac{N}{M}\rfloor$ nodes and the others by $L+1$ nodes. The collision probability $p_{c,\text{re-use}}$ differs depending on whether the representative node is in a channel with L node or $L+1$ nodes. This is given as

$$
p_{c,\text{re-use}} = \begin{cases} p_{c,\text{re-use, high}} = 1-(1-\frac{L}{N})^{a-1}, & \text{if in a channel with } L \text{ devices;} \\ p_{c,\text{re-use, low}} = 1-(1-\frac{L+1}{N})^{a-1} & \text{otherwise.} \end{cases} \tag{4.15}
$$

We again assume an even distribution of available channels to nodes so that the maximum of the number of nodes that have the same home channel is minimized. We can see that the collision probability of some devices is higher than that of others in this scheme, which can be considered to be unfair.

Multi-level orthogonal hopping: In multi-level orthogonal hopping, the layers are scrambled to retain orthogonality within the layer but, at the same time, distribute the possible conflicts evenly across all nodes. Again, we assume that the layers are filled from the bottom. With multi-level hopping, a node in a full layer will experience a collision with the probability

$$p_{c,\mathrm{ML}} = \frac{R}{M}\left(1-\left(1-\frac{L+1}{N}\right)^{a-1}\right)+\left(1-\frac{R}{M}\right)\left(1-\left(1-\frac{L}{N}\right)^{a-1}\right), \tag{4.16}$$

and with probability $p_{c,\mathrm{ML}} = p_{c,\text{re-use}}$ if it is in the last layer. Here again, $R = N \bmod M$ and $L = \lfloor \frac{N}{M} \rfloor$.

Note that there are other possible approaches to distributing conflicts evenly among nodes and hence achieving fairness. In fact, it is simple to design a repeated hopping sequence that achieves this deterministically without randomization by distributing conflicts in time direction. On the other hand, the proposed multi-layer approach has the advantage of being flexible in the sense that nodes do not have to adapt their home hopping sequences once another node joins or leaves the network. It is also possible within this scheme to increase fairness further by balancing the layers, i.e., by assigning each layer the same number of nodes.

4.2.3 Numerical results

In the following, we evaluate the system model numerically and analyze the dependencies of various variables. It has been shown that the model closely approximates the performance of real implementations of parallel-rendezvous type MAC, see e.g. [37, 66].

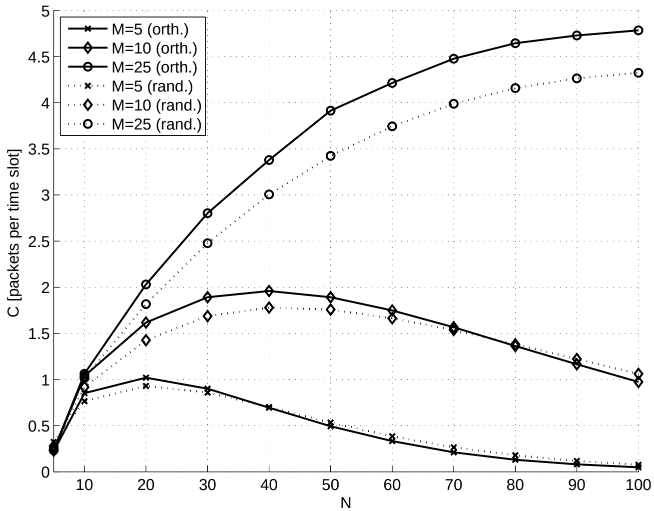

Figure 4.6: Throughput versus number of nodes for $p = 0.3$, $q = 1$.

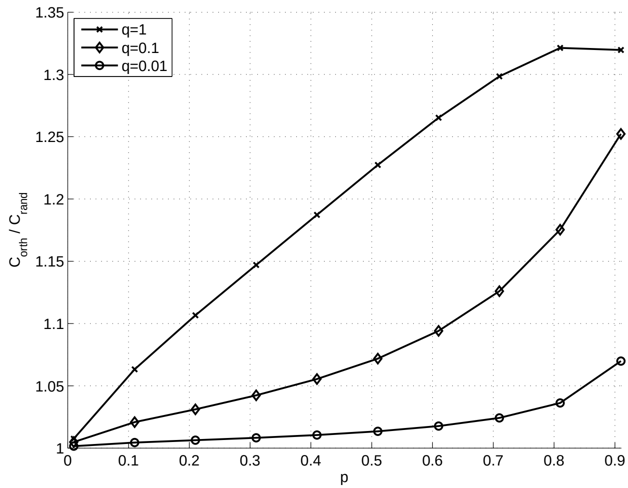

Figure 4.7: Relative increase in throughput versus p for $M = 25$, $N = 50$.

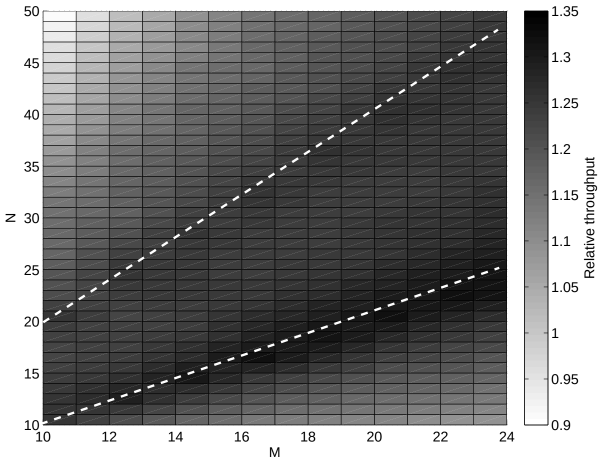

Figure 4.8: Relative increase in throughput for $p = 0.6$, $q = 1$.

Throughput improvements

Fig. 4.6 shows the total average normalized throughput C for orthogonal hopping and random hopping. A notable gain of orthogonal hopping can be seen for a larger number of channels. For a fixed number of channels M and a given network load p, there is a saturation point after which throughput decreases due to congestion collapse. A specific MAC implementation needs to make sure that the back-off mechanisms adapt the overall traffic so that congestion does not occur. Interestingly, after saturation in the congestion collapse regime for large N, orthogonal hopping becomes slightly worse than random hopping. Orthogonal hopping distributes the transmission attempts evenly; therefore collisions happen in all channels. For random hopping there is a chance that nodes will collide only in a few channels, leading to a (slightly) higher throughput.

Fig. 4.7 gives the relative increase of orthogonal hopping over random hopping in percent versus the network load p. A notable gain can be achieved for short average transmission durations, i.e., small $1/q$, and a high load of the network, i.e., larger p. For long average packet durations and low network load, orthogonal hopping does not offer a significant benefit. If the packet durations are long, the impact of the time needed to establish a successful rendezvous becomes negligible. Moreover, for low network load, the probability of one-attempts is also high for random hopping.

Fig. 4.8 shows the relative increase in throughput over N and M. Also shown are lines indicating $N = M$ and $N = 2M$. If $N = M$, the relative increase is maximal due to the fact that transmitter-side collisions have the greatest effect, for $N = 2M$ this effect is also visible. If the number of nodes significantly exceeds the number of channels and the network is operated in the congestion collapse regime, the gain eventually becomes smaller than 1 as was already observed in Fig. 4.6.

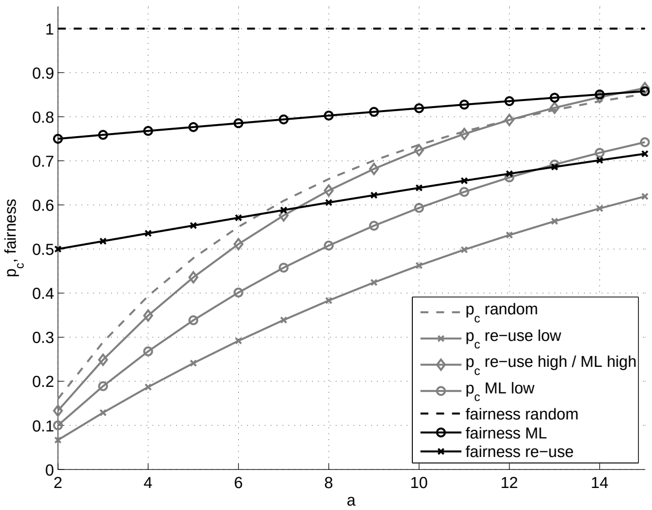

Figure 4.9: Collision probability for a single node p_c and fairness versus a for different strategies, $M = 10$, $N = 15$.

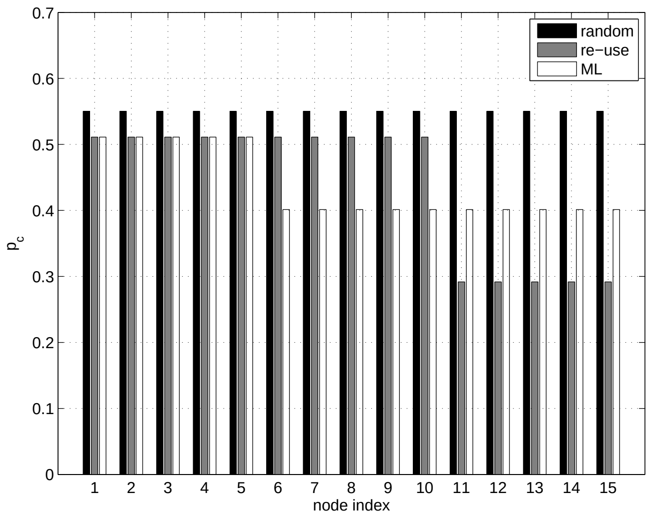

Figure 4.10: Collision probability for all nodes for different strategies, $a = 4$, $M = 10$, $N = 15$.

	Random	Orthogonal with channel re-use	Multi-level orthogonal
Collisions	Random with all nodes	Deterministic with neighbors re-using the same channel	Random with neighbors from other layers
Fairness	1	Worst case ($L = 1$, $a = 2$, $R = M/2$): 0.5	Worst case: 0.75

Table 4.2: Qualitative summary of collision behavior of home channel hopping strategies

Fairness and single attempt collision probability

Fig. 4.9 shows the collision probabilities of a single connection as well as the fairness for each strategy. Fairness is defined as the ratio of the collision probabilities of nodes from a full layer to the collision probability of nodes from the last (non-full) layer, i.e., $p_{c,\text{low}}/p_{c,\text{high}}$.

For the re-use strategy, there are $R(L+1)$ nodes experiencing a higher probability of collision, whereas for the multi-level strategy this is the case for only R nodes. To illustrate this, Fig. 4.10 shows the collision probability for all nodes with four attempting devices, i.e., $a = 4$. As can be seen, the multi-layer hopping yields better fairness than the re-use strategy.

Tab. 4.2 summarizes the behavior.

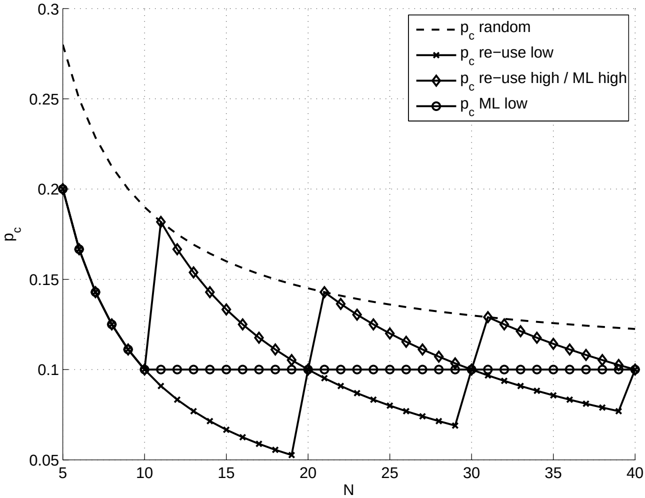

Figure 4.11: Collision probability of a single connection with $a = 2$, $M = 10$.

The dependency on the number of nodes is plotted in Fig. 4.11. If all layers are filled, i.e., $R = 0$ at $N = 10, 20, 30, \ldots$, both re-use and MLLO strategies inhibit a collision probability of 0.1. If the last layer is not filled completely, the unfairness, i.e. the distance between the collision probabilities of the node in the last layer and any other, is greater for re-use rendezvous than for MLLO rendezvous. Random hopping is fair, but yields a higher collision probability for any number of nodes.

4.3 Avoidance of external interference

The findings of Chapter 3 suggest that selective interference avoidance by means of excluding certain channels from the hop sequence can be a good strategy in the practical regime of low to medium outage. For the MAC design, it follows that a hard-decision strategy, i.e., a strategy that includes good channels and excludes bad channels from the hop sequence, can be sufficient for good performance. Such a strategy can also easily be combined with orthogonal hopping.

In the following, we will therefore evaluate the influence of external interference on an adaptive parallel rendezvous MAC that employs bad channel avoid-

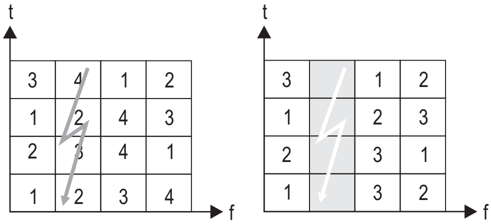

(a) Non-avoiding (b) Avoiding

Figure 4.12: Protocol approaches

ance. To this end, we extend the Markov model to include a simple binary external interference model. While the system model in the previous section assumed a collision-free transmission during data transfer, collisions with interferers now have a major influence. They can happen during rendezvous, but also reduce the overall data throughput of the network.

We aim to compare two protocol approaches, illustrated in Fig. 4.12(a) and 4.12(b):

- A non-avoiding protocol, that simply deals with bad channels by retransmission, and

- an avoidance protocol that excludes bad channels from transmission.

In [62], Pawelczak et al. consider a similar model in an overlay (opportunistic) spectrum access scenario. Of interest are the interrelations between a primary spectrum user and an opportunistic secondary spectrum user. To model these interrelations, an architecture with per slot channel sensing is assumed. Modeling of per slot channel sensing requires the incorporation of primary user false alarm and detection rates. Hence, the model emphasizes the trade-off between interference to the primary user and secondary user throughput and focuses on the short-term influence of channels occupied by the primary user. Here, we assume that – in the case of the collision-avoidance protocol – channel sensing is carried out accurately in larger time scales and that the signaling overhead required to communicate the resulting information throughout the collision domain is negligible. This assumption holds if the interference environment changes slowly, the model hence describes the long term effects of external interference on MAC throughput.

4.3.1 Performance model

The model of Section 4.2.2 needs to be extended to include the influence of bad channels. Let $F < M$ denote the number of bad channels. It is assumed that the set of bad channels does not change for the purposes of our analysis and that, in the case of the interference avoiding protocol, all nodes know which channels are not usable.

Non-avoiding protocol

Bad channels have a two-fold influence on the performance. First, the rendezvous probability is reduced, since two nodes might (unsuccessfully) try to meet in a bad channel. Second, during data transfer, a packet might be corrupted due to collision with a bad channel.

The modified rendezvous probability, taking bad channels into account, is

$$p_{s'} = \left(1 - \frac{F}{M}\right) \frac{N - 2k - a}{N - 1}\,. \tag{4.17}$$

Overall, we then have for j nodes (cf. (4.9)):

$$P\left[J = j | I = i, O = o, A = a\right] = \binom{i}{j} p_{s'}^{j} (1 - p_{s'})^{i-j}\,. \tag{4.18}$$

If a connection is established and the packet transmission is on-going, the pseudo-random hopping component results in a collision probability per slot of $\frac{F}{M}$. We assume that, if a slot is corrupt, the corrupted part of the packet has to be retransmitted in the next slot. This is a best-case performance estimate as it neglects the overhead associated with a practical retransmission protocol. The modified termination probability, see (4.4), is then

$$T_k^{(j)} = \binom{k}{j} q'^{j} (1 - q')^{k-j} \tag{4.19}$$

with

$$q' = \left(1 - \frac{F}{M}\right) q\,. \tag{4.20}$$

Bad channels hence extend the effective packet length by a factor of $\frac{M}{M-F}$.

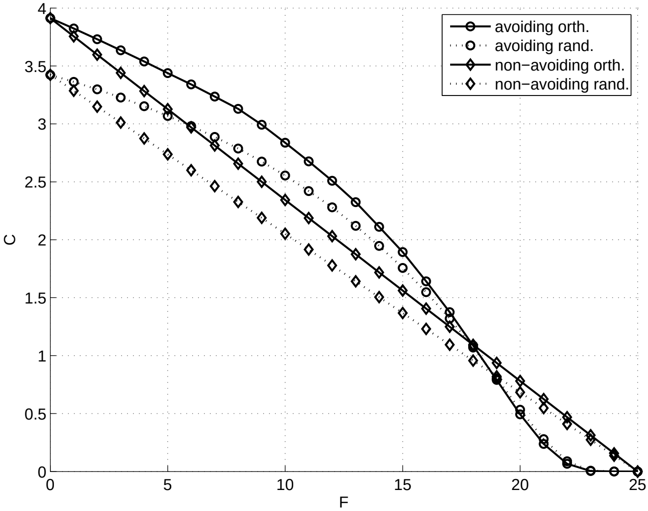

Figure 4.13: Throughput versus number of bad channels for $N = 50$, $M = 25$, $p = 0.3$, $q = 1$.

When calculating the total average normalized throughput from the steady state distribution, see (4.3), the influence of bad packets has to be taken into account. The total average normalized throughput for the non-avoiding protocol is the throughput without bad channels weighted with the probability of collision. It is given by

$$C = \left(1 - \frac{F}{M}\right) \sum_{i=0}^{|\mathscr{S}|-1} i\pi_i \,. \tag{4.21}$$

Collision-avoidance protocol

If the network locally flags all bad channels, the influence on the system model is very simple: The number of usable channels is reduced to $M' = M - F$, otherwise the system model is left unmodified.

4.3.2 Numerical results

Fig. 4.13 shows the throughput versus the number of bad channels for both protocol approaches, with random hopping rendezvous and orthogonal hop-

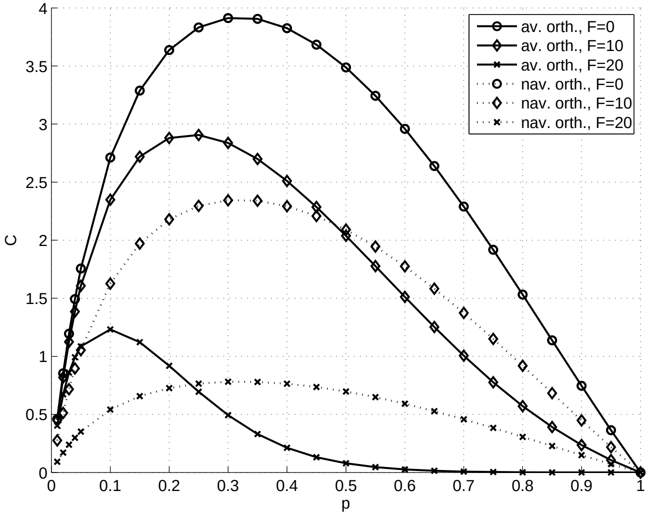

Figure 4.14: Throughput for orthogonal hopping over p, $q = 1$, $M = 25$, $N = 50$, for an avoiding (av.) and a non-avoiding (nav.) protocol

ping rendezvous. As can be seen, the decline in throughput is linear for the non-avoiding protocol, a fact to be expected from the system model: For a given F, M and N, $p_{s'}$ and q' are constant and do not affect the rendezvous probability. The linear term $\frac{F}{M}$ in (4.21) is thus the only dependency of F. The throughput of the interference avoiding protocol is non-linear and provides a gain up until $F = 18$ channels are unusable. For a very high number of bad channels, the avoiding protocol leads to lower throughput for a fixed load p, as the network is driven into congestion. Adaptivity does not pay off in this case.

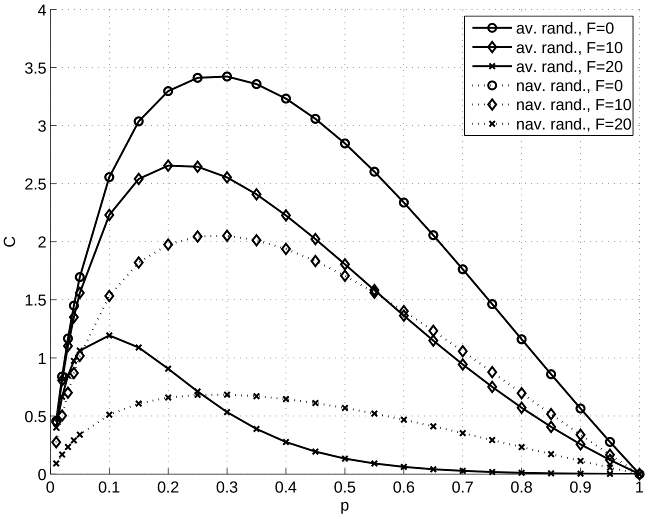

Figure 4.15: Throughput for random hopping over p, $q = 1$, $M = 25$, $N = 50$, for an avoiding (av.) and a non-avoiding (nav.) protocol

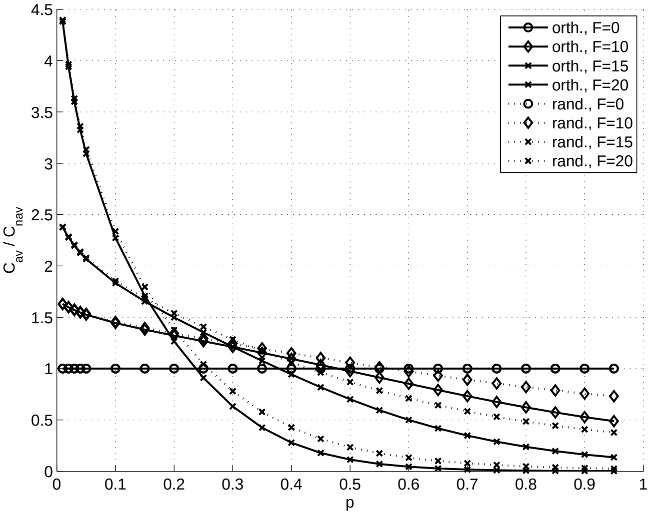

Figure 4.16: Relative throughput over p, $q = 1$, $M = 25$, $N = 50$. For $p = 1$, the throughput is zero for all approaches.

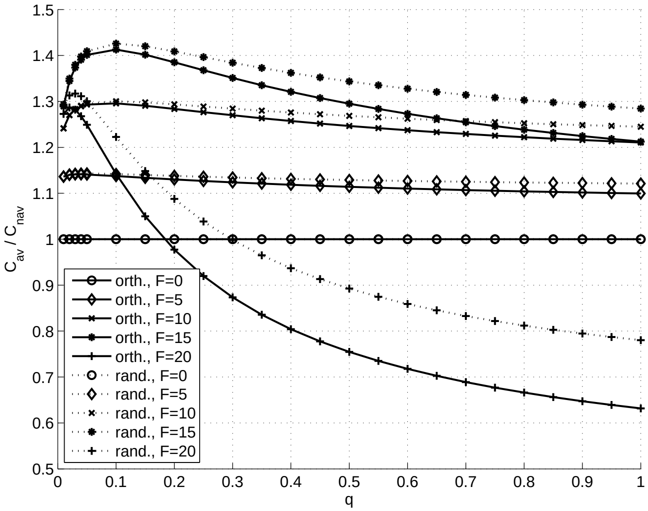

Figure 4.17: Relative throughput over q, $p = 0.3$, $M = 25$, $N = 50$.

Fig. 4.14 shows this situation for orthogonal hopping and Fig. 4.15 for random hopping. For $F = 0$ the curves for the avoiding and the non-avoiding approach coincide. For orthogonal hopping rendezvous, the higher the number of bad channels, the lower the optimum p for which throughput is maximal. The effect is not visible for the non-avoiding approach. Here, transmission attempts always concern the same number of channels M and a ”concentration effect” on fewer channels does not occur. The network does not need to adapt its back-off mechanism, regardless of the number of bad channels.

The relative throughput over network load p is shown in Fig. 4.16. The interference avoiding protocol shows highest relative gains under low network load. Furthermore, random hopping rendezvous benefits slightly more than orthogonal hopping.

In Fig. 4.17 the relative throughput is plotted over q to show the dependencies on the transmission termination probability q, corresponding to an average packet length of $1/q$. Interestingly, for a given number of bad channels F, while overall throughput decreases with shorter packet length, there is an optimum packet length that maximizes the relative gain. Especially for a higher number of bad channels, interference avoidance only increases throughput for small q, i.e., long average packet lengths.

Improvement	**Condition for significant gains over non-adaptive scheme**	**Costs**
MLLO hopping rendezvous	High number of channels, short packets, high load	Local negotiation over hopping sequences
External interference avoidance	Low number of bad channels, longer packets, low load	Local signaling of bad channels, negotiation of hopping sequence

Table 4.3: Summary of the gains and costs of interference avoidance approaches

4.4 Summary

Having described design issues in multi-channel MAC conceptually, a new rendezvous scheme based on multi-level orthogonal hopping for parallel rendezvous multi-channel MAC was proposed and analyzed. Its performance was compared to other popular schemes, i.e., with random hopping and channel reuse hopping, which naturally arise in a frequency hopping setting. The results indicate that orthogonal hopping rendezvous provides gains, especially if the traffic pattern comprises a high volume of short packets to different destination nodes. In such networks, rendezvous is the performance bottleneck and avoiding collisions on the MAC layer during transmission negotiation to avoid internal interference is paramount.

Within the same system model, we also compared a non-avoiding ”dumb” transmission protocol with an interference avoiding protocol approach. The interference avoiding protocol proves to be superior and offers high gains in most practical operating regimes. Only if the network is operated under very high loads and congestion occurs, interference avoidance is not beneficial.

We have shown through simulation and analysis under which conditions the throughput of adaptive ”smart” internal and external interference avoidance techniques can be superior to non-adaptive schemes. On the downside, external interference avoidance, in particular, requires some additional degree of communication between the nodes and it needs to be noted that our analysis did not consider signaling overhead. The costs for an MLLO scheme in parallel rendezvous MAC are negligible, as the hopping sequences of all neighbors need to be known within a neighborhood anyway. Local negotiation is hence necessary even for a non-adaptive scheme.[67] Table 4.3 summarizes the findings. Considering that the implementation costs of MLLO hopping and interference avoidance can be small and that the adaptive behavior can be created on top of a non-adaptive MAC as an optional feature, protocol designers for frequency hopping networks should consider including mechanisms that facilitate adaptivity when aiming for maximum robustness.

Our analysis is limited to a single collision domain. The extension to multi-collision domains is highly desirable in order to capture effects on the MAC layer throughput caused by hidden and exposed nodes; this remains as future research.

[67] See also Chapter 2, adaptation can be carried our in a distributed fashion.

5

Conclusion

> All models are wrong but some are useful.
>
> *George E. P. Box*

We conclude with a short summary of the previous chapters, restating the main results. Furthermore, the limitations of their applicability are discussed and an outline of further possible research directions is given.

5.1 Contribution

In the introductory Chapter 1, the applications of frequency hopping systems with very large operating bandwidth and their combination with multi-channel medium access control (MAC) protocols in wireless networks were outlined. Current hardware combined with smart sensing techniques makes it possible to use large discontinuous swathes of spectrum to operate wireless networks, adapting to free spectrum and avoiding interferers. The modeling of the performance of such frequency hopping code division multiple access (FH-CDMA) networks is a challenging task; a recent approach is based on stochastic geometry. Stochastic geometry can be used to analyze the interference field of random networks, reducing the model complexity by averaging over all possible spatial configurations.

Chapter 2 dealt with the principal performance limits of FH-CDMA with local frequency division multiple access (FDMA) scheduling. The optimization was cast as a random vertex coloring problem and bounds on outage probability and transmission capacity were given. Next, multi-level locally orthogonal (MLLO) hopping was introduced as a practical method for local scheduling in ad hoc networks. A distributed algorithm capable of finding a proper channel assignment was derived. MLLO avoids the hotspot problems of local FDMA scheduling with spatial re-use, where hopping sequences can deterministically collide. Interference is hence more evenly spatially distributed and network performance improved.

Chapter 3 considered the influence of external interference within a similar system model as the one considered in Chapter 2. Within that model, the optimum channel assignment was derived that balances internal interference and external interference for the convex region of the optimization problem in a path loss and Rayleigh fading model. The performance of the resulting hopping strategies was compared to various suboptimal strategies such as non-adaptive hopping and min-max allocation with constant quality of service. It was found that adaptivity offers a benefit only at low to medium node densities and that a good suboptimal strategy is based on hard exclusion of bad channels (thresholding) with optimal min-max allocation to balance the load of active channels.

Multi-channel MAC operation is a necessity in large scale wireless networks. In Chapter 4, the challenges of multi-channel MAC were outlined and interference avoidance techniques for parallel rendezvous-type MAC evaluated by means of a Markov chain model. It was found that internal interference avoidance has its merits, especially if the number of channels as well as the network load are high and the packets are short. In other words, internal interference avoidance is beneficial if the rendezvous process dominates the performance. In parallel rendezvous multi-channel MAC, the costs of adapting the hopping sequences are small, as communication and distribution within a neighborhood is required even for non-adaptive schemes. External interference avoidance has benefits especially if the number of bad channels is low, a fact mirroring the findings of Chapter 3.

In summary, a spatial interference model for the physical layer of adaptive FH-CDMA systems was given and the principal gains that can be achieved through adaptation were shown. A lesson learned is that adaptivity is not always needed, and not always beneficial – the application and interference relationships within a network have to be considered. Furthermore, a practical algorithm to reduce internal interference, multi-level orthogonal hopping, was given and non-traditional adaptive hopping techniques to minimize external interference were proposed. Interference reduction techniques were also evaluated in a Markov MAC model and implementation issues were discussed.

5.2 Limitations of simple geometrical and Markov models

The presented results are, of course, limited by the validity of their respective system models. Care must be taken as to their applicability in practical scenarios because network performance is heavily influenced by the assumed spatial configuration. A core assumption of the first two chapters, the homogeneous Poisson point process geometry, is valid only if the network nodes can be assumed to be uniformly distributed in a given area and the number of nodes within that area follows a Poisson distribution. This model holds for large wireless networks in homogeneous space, but this is a situation that is rarely found in nature. People and vehicles, and hence mobile transmitters, tend to follow roads, avoid obstacles and create clusters. All of these effects are not covered by the model. Extending the results to inhomogeneous, spatially correlated point processes is a possible straightforward extension, but will, in most cases, result in analytically intractable models. This, however, does not necessarily mean that the stochastic geometry approach to modeling is useless in itself, as valuable insight might be gained using numerical methods to evaluate the network performance. The underlying trade-offs will, however, not be directly accessible through simple analytical expressions.[68]

The MAC model is principally limited by its lack of consideration of time dynamics and delay as well as the simplistic homogeneous traffic model in a single collision domain. While the physical layer performance is dominated by network geometry, the MAC layer performance also heavily depends on the traffic pattern. The MAC model is a good tool for analyzing the rendezvous probabilities in multi-channel MAC and the presented trade-offs, but it cannot

[68] An example is [68, 69], where sensing mechanisms in frequency hopping ad hoc networks are analyzed with the help of a stochastic geometry model. The results are mainly not given as closed-form expressions, but rely on numerical evaluations.

be used to directly calculate throughput in practical networks with asymmetric traffic patterns.

Models are valuable for deriving design guidelines. However, once systems of interacting systems exceed a certain complexity threshold, engineers have to rely on computer based simulations and, ultimately, field tests to gain insight into the overall performance.[69] With the presented results, we hope to have provided some novel design insights for frequency hopping networks. A frequency hopping network protocol designed with the principles outlined in this thesis in mind will show good performance. Any implementation, however, will have to be evaluated with extensive simulations.

5.3 Current developments

The application of stochastic geometry to wireless networks and the simple MAC model presented are just one way of dealing with the multi-dimensional complexities of arbitrary wireless networks that classical information theory cannot handle. Shannon theory relies on unbounded delay to achieve error-free coding. As Andrews et al. outline in their position paper [21], a good network theory must take into account delay and reliability, temporal and spatial dynamics, and incorporate the role of necessary overhead messaging and feedback between nodes. They argue for development of new theories that describe the *functional* capacity of networks under practical constraints. Finding a general theory that describes all aspects of any network is, indeed, likely to be a too ambitious goal. However, finding and extending statistical theories that allow insights into the expected performance of networks (as opposed to worst case or best case scenarios) are very valuable. A promising avenue of future research could lie in adapting ideas from statistical physical models, where modeling of interactions in systems with many particles has a long history, to network information theory.

[69] For wireless software radio networks an interesting approach deemed *Wireless Networks In-the-Loop* combines development and simulation [70, 71]. The key idea is to provide a transparent RF interface that can be used in simulation and for real hardware. With this approach it is possible to simulate all aspects of wireless networking without creating dedicated simulations.

A

Appendix - Stochastic Geometry

The following definitions and theorems that are used in Chapters 2 and 3 are compiled from [47]. For terms and definitions from basic probability theory necessary for understanding see, e.g., [55, 72].

A *point process* Φ is a random variable with realizations $\phi = \{x_n\}$ of points in $\mathbb{R}^d$. We write $\Phi(B)$ for the number of points of Φ in Borel set $B \subseteq \mathbb{R}^d$, i.e., B denotes some union of bounded subsets of $\mathbb{R}^d$. ϕ needs to be locally finite, i.e., each bounded subset of $\mathbb{R}^d$ only contains a finite number of points. A more formal definition of a point process is given in [47, p. 99]. For our purposes, only the Poisson point process and its properties as defined below are of interest.

For a point process Φ, we write $\Phi = \{x_n\}$ in short to highlight the structure of the random variable Φ as a collection of random variables $\{x_n\}$.[70]

A point process $\Phi = \{x_n\}$ is *stationary*, if $\Phi' = \{x_n + s\}$ has the same distribution as Φ for all $s \in \mathbb{R}^d$: The statistics are invariant to translation.

[70]Note that in the above definition of Φ the $\phi = \{x_n\}$ are realizations of Φ, while when writing $\Phi = \{x_n\}$ they denote random variables.

The *intensity measure* of a point process Φ is defined by

$$\Lambda(B) = E\left[\Phi(B)\right] = \int \phi(B)P(d\phi)\,. \tag{A.1}$$

for all Borel sets $B \subseteq \mathbb{R}^d$. The intensity measure gives the expected number of points of Φ in B. For a stationary point process, it holds that $\Lambda = \lambda\,\nu_d$, where $\nu_d(\cdot)$ is the Borel-Lebesgue measure in $\mathbb{R}^d$ (i.e., $\nu_d(B)$ is the d-dimensional volume of B). λ is called the *intensity* of the process.

Definition (Marked point process)**.** *A marked point process is a point process that has marks m_n attached to every point x_n. The marks can also be random, i.e., the m_n can be drawn from some mark distribution.*

Definition (Binomial point process)**.** *A Binomial point process of n points is a point process that is formed by n independent points uniformly distributed over the same compact set W.*

Definition (Poisson point process)**.** *A Poisson point process is a point process that satisfies the following conditions:*

1. *Poisson statistics: The number of points in every bounded Borel set B has a Poisson distribution with mean $\Lambda(B)$:*

$$P\left[\Phi(B) = m\right] = \exp(-\Lambda(B))\frac{\left[\Lambda(B)\right]^m}{m!}, m = 0, 1, \ldots \tag{A.2}$$

2. *Independent scattering: The number of points in disjoint Borel sets form independent random variables.*

A Poisson point process is *homogeneous*, if the number of points of Φ in a bounded Borel set B only depends on the volume of B (and not on its shape).

Independent homogeneous Poisson point processes Φ_a and Φ_b with intensities λ_a and λ_b have the following properties:

1. Stationarity;
2. Additivity: The point process made up of all points of Φ_a and Φ_b, i.e., $\Phi_a + \Phi_b$ is a homogeneous Poisson point process of intensity $\lambda_a + \lambda_b$;
3. Independent thinning: If points are independently removed from Φ_a with probability p, the removed points form a homogeneous PPP with density $(1-p)\lambda_a$.

Of these properties, only stationarity requires homogeneity of the Poisson point process.[71]

Theorem (Slivnyak's theorem: Reduced Palm distribution of a Poisson point process)**.** *The reduced Palm distribution $P^{!x}$ of a Poisson point process with distribution P is*

$$P^{!x} = P\,. \tag{A.3}$$

In other words, the Palm distribution of a Poisson point process given a point at x without counting it is equal to the distribution of the Poisson point process. Informally, the distribution of a Poisson point process is not changed if we condition it on the presence of an arbitrary point. For a proof see [47, p. 95].

[71] Note that for non-Poisson processes, homogeneity does not imply stationarity.

B

Appendix - Graph Theory

The following definitions and theorems that are used in Chapter 2 are compiled from [73]. For a proof of Brooks theorem see [73, p. 122] or the original paper by Brooks [45].

Definition (Graph)**.** *A graph G is an ordered triple (E_G, V_G, ψ_G) of E_G edges, V_G vertices and an incidence function ψ_G that associates each edge of E_G with an unordered pair of vertices from V_G.*

A graph is

- *simple* if does not contain any loops (i.e., an edge starting and ending at the same vertex) or any multiple edges,
- *connected* if there is a path along the edges from any vertex to any other vertex,
- *complete* if any vertex is connected to any other vertex,
- *cyclic* if the graph has a path, i.e., a way through the graph along the edges, that has the same start and end vertex.

Definition (Vertex degree)**.** *The* vertex degree *is the number edges that a vertex has. The* maximum vertex degree Δ *of a graph is the maximum vertex degree of all vertices of the graph.*

Definition (k-vertex Graph coloring)**.** *A k-vertex coloring of a simple graph G is an assignment of k colors to the vertices of G.*

A coloring is *proper* if no two distinct adjacent vertices have the same color. G is k-(vertex)-colorable if a proper k-coloring of G exists.

Definition (Chromatic number)**.** *The chromatic number* χ *of G is the minimum k for which G is k-colorable. If* $\chi = k$*, G is said to be k-chromatic.*

Theorem (Brooks' theorem)**.** *If G is a connected simple graph, and is neither an odd cycle (i.e., a cyclic graph with an odd number of edges) nor complete graph, then* $\chi \leq \Delta$*. Otherwise,* $\chi = \Delta + 1$.

Acronyms

ADC Analog-to-Digital Converter

CMOS Complementary Metal Oxide Semiconductor

CDMA Code Division Multiple Access

CSMA/CA Carrier Sense Multiple Access/Collision Avoidance

DC Direct Current

DSSS Direct Sequence Spread Spectrum

FCC Federal Communications Commission

FDMA Frequency Division Multiple Access

FH Frequency Hopping

GSM Global System for Mobile Communications

ISM Industrial, Scientific and Medical

IEEE Institute of Electrical and Electronics Engineers

KKT Karush-Kuhn-Tucker

LTE Long Term Evolution

MAC Medium Access Control (Layer)

MAI Multiple Access Interference

MLLO Multi-Level Locally Orthogonal (Hopping)

NSR Noise-to-Signal Ratio

PHY Physical (Layer)

PPP Poisson Point Process

QoS Quality of Service

RF Radio Frequency

SDR Software-Defined Radio

SINR Signal-to-Interference-and-Noise Ratio

SHF Super High Frequency

SNR Signal-to-Noise Ratio

TC Transmission Capacity

TDMA Time Division Multiple Access

UHF Ultra High Frequency

VHF Very High Frequency

WLAN Wireless Local Area Network

Bibliography

This work contains material from prior conference and journal publications [1–6], ©2010 - 2012 IEEE. Reprinted, with permission. Specifically, Chapter 2 is based on [1–3], Chapter 3 on [4, 5] and Chapter 4 contains material from [6].

[1] J. P. Elsner, R. Tanbourgi, and F. Jondral, "On the Transmission Capacity of Wireless Multi-Channel Ad Hoc Networks with local FDMA scheduling," in *International Congress on Ultra Modern Telecommunications and Control Systems*, Moscow, Russia, Oct. 2010.

[2] J. Elsner, R. Tanbourgi, and F. Jondral, "A Note on Local Receive Channel Scheduling versus Transmit Channel Scheduling in Wireless Multi-Channel Ad Hoc Networks," in *International Conference on Computer and Information Application*, Tianjin, China, Dec. 2010.

[3] J. P. Elsner, R. Tanbourgi, and F. Jondral, "Multiple Access Interference Mitigation Through Multi-Level Locally Orthogonal FH-CDMA," in *The 2011 Military Communications Conference*, Baltimore, Maryland, USA, Nov. 2011.

[4] J. P. Elsner, R. Tanbourgi, J. Schmid, and F. K. Jondral, “Hopping Strategies for Adaptive FH-CDMA Ad Hoc Networks under External Interference,” in *IEEE International Conference on Communications*, Ottawa, Canada, Jun. 2012.

[5] ——, “Hopping strategies for adaptive frequency hopping networks with Poisson point process geometry under external interference,” *IEEE Transactions on Wireless Communications*, submitted, under review.

[6] J. P. Elsner, J. Mo, and F. Jondral, “Multi-Channel Medium Access Control: Multi-Level Orthogonal Hopping Rendezvous,” *IEEE Communications Letters*, vol. 16, no. 8, pp. 1220–1223, Aug. 2012.

[7] “3GPP Long Term Evolution,” Release 8. [Online]. Available: http://www.3gpp.org/LTE

[8] “IEEE Standard for Information Technology-Telecommunications and Information Exchange Between Systems-Local and Metropolitan Area Networks-Specific Requirements - Part 11: Wireless LAN Medium Access Control (MAC) and Physical Layer (PHY) Specifications,” *IEEE Std 802.11-2007 (Revision of IEEE Std 802.11-1999)*, Dec. 2007.

[9] “IEEE 802.15.1 WPAN Task Group.” [Online]. Available: http://ieee802.org/15/pub/TG1.html

[10] “IEEE 802.15.4 WPAN Task Group.” [Online]. Available: http://ieee802.org/15/pub/TG4.html

[11] C. E. Shannon, “A Mathematical Theory of Communication,” *Bell System Technical Journal*, pp. 379–423, 623–656, Jul., Oct. 1948. [Online]. Available: http://cm.bell-labs.com/cm/ms/what/shannonday/shannon1948.pdf

[12] B. Razavi, *RF Microelectronics*. Prentice Hall PTR, 1998.

[13] M. Ingels, V. Giannini, J. Borremans, G. Mandal, B. Debaillie, P. Van Wesemael, T. Sano, T. Yamamoto, D. Hauspie, J. Van Driessche, and J. Craninckx, “A 5 mm^2 40 nm LP CMOS Transceiver for a Software-Defined Radio Platform,” *IEEE Journal of Solid-State Circuits*, vol. 45, no. 12, pp. 2794 –2806, Dec. 2010.

[14] “Ettus Research LLC, USRP product line.” [Online]. Available: http://www.ettus.com

[15] J. P. Elsner, C. Koerner, and F. K. Jondral, “Centralized Modeling of the Communication Cpace for Spectral Awareness in Cognitive Radio Networks,” *ACM SIGMOBILE Mobile Computing and Communications Review*, vol. 13, no. 2, Apr. 2009.

[16] “Federal Communications Commision, White Space Database Administration.” [Online]. Available: http://www.fcc.gov/encyclopedia/white-space-database-administration

[17] F. Jondral, “Cognitive Radio: A Communications Engineering View,” *IEEE Wireless Communications*, vol. 14, no. 4, pp. 28–33, Aug. 2007.

[18] S. Haykin, “Cognitive Radio: Brain-empowered Wireless Communications,” *IEEE Journal on Selected Areas in Communications*, vol. 23, no. 2, pp. 201–220, Feb. 2005.

[19] J. P. Elsner, C. Mohr, and F. K. Jondral, “Capacity Regions of Multi-Channel Ad Hoc Networks,” in *IEEE Vehicular Technology Conference*, San Francisco, USA, Sep. 2011.

[20] S. Toumpis and A. Goldsmith, “Capacity Regions for Wireless Ad Hoc Networks,” *IEEE Transactions on Wireless Communications*, vol. 2, no. 4, pp. 736 – 748, Jul. 2003.

[21] J. Andrews, S. Shakkotai, R. Heath, N. Jindal, M. Haenggi, R. Berry, D. Guo, M. Neely, S. Weber, S. Jafar, and A. Yener, “Rethinking Information Theory for Mobile Ad Hoc Networks,” *IEEE Communications Magazine*, Dec. 2008.

[22] P. Gupta and P. Kumar, “The Capacity of Wireless Networks,” *IEEE Transactions on Information Theory*, vol. 46, no. 2, pp. 388–404, Mar. 2000.

[23] M. Grossglauser and D. Tse, “Mobility Increases the Capacity of Adhoc Wireless Networks,” *IEEE/ACM Transactions on Networking*, vol. 10, no. 4, pp. 477–486, Aug. 2002.

[24] P. Kyasanur and N. H. Vaidya, “Capacity of MultiChannel Wireless Networks: Impact of Channels, Interfaces and Interface Switching Delay,” University of Illinois at Urbana-Champaign, Tech. Rep., Oct. 2006, extended and revised version of MobiCom 2005 paper. [Online]. Available: http://www.crhc.illinois.edu/wireless/papers/capacity_mobicom_long_revised.pdf

[25] M. Haenggi, "Outage, Local Throughput, and Capacity of Random Wireless Networks," *IEEE Transactions on Wireless Communications*, vol. 8, no. 8, pp. 4350–4359, Aug. 2009.

[26] M. Haenggi and R. K. Ganti, "Interference in Large Wireless Networks," *Foundations and Trends in Networking*, vol. 3, pp. 127–248, Feb. 2009. [Online]. Available: http://dx.doi.org/10.1561/1300000015

[27] F. Baccelli and B. Blaszczyszyn, "Stochastic Geometry and Wireless Networks, Volume 1+2: Theory and Applications," *Foundations and Trends in Networking*, vol. 3, no. 3-4, pp. 249–449, 2009.

[28] S. Weber, J. Andrews, and N. Jindal, "An Overview of the Transmission Capacity of Wireless Networks," *IEEE Transactions on Communications*, vol. 58, no. 12, pp. 3593–3604, Dec. 2010.

[29] S. Weber and J. G. Andrews, "Transmission Capacity of Wireless Networks," *Foundations and Trends in Networking*, vol. 5, no. 2–3, pp. 109–281, 2012.

[30] J. Andrews, R. Ganti, M. Haenggi, N. Jindal, and S. Weber, "A Primer on Spatial Modeling and Analysis in Wireless Networks," *IEEE Communications Magazine*, vol. 48, no. 11, pp. 156 –163, Nov. 2010.

[31] J. Andrews, S. Weber, and M. Haenggi, "Ad Hoc Networks: To Spread or not to Spread," *IEEE Communications Magazine*, vol. 45, no. 12, pp. 84–91, Dec. 2007.

[32] M. K. Simon, J. K. Omura, R. A. Scholtz, and B. K. Levitt, *Spread Spectrum Communications Handbook.* McGraw-Hill, 1994, revised edition.

[33] P. Popovski, H. Yomo, and R. Prasad, "Strategies for Adaptive Frequency Hopping in the Unlicensed Bands," *IEEE Wireless Communications*, vol. 13, no. 6, pp. 60–67, Dec. 2006.

[34] ——, "Dynamic Adaptive Frequency Hopping for Mutually Interfering Wireless Personal Area Networks," *IEEE Transactions on Mobile Computing*, vol. 5, pp. 991–1003, 2006.

[35] L. Stabellini, L. Shi, A. Al Rifai, J. Espino, and V. Magoula, "A new Probabilistic Approach for Adaptive Frequency Hopping," in *IEEE 20th International Symposium on Personal, Indoor and Mobile Radio Communications*, Sep. 2009, pp. 2147–2151.

[36] S. Kumar, V. Raghavan, and J. Deng, "Medium Access Control protocols for Ad Hoc Wireless Networks: A survey," *Elsevier Ad Hoc Networks*, vol. 4, no. 3, pp. 326–358, May 2006.

[37] J. Mo, H.-S. W. So, and J. Walrand, "Comparison of Multichannel MAC Protocols," *IEEE Transactions on Mobile Computing*, vol. 7, no. 1, pp. 50–65, Jan. 2008.

[38] N. Geng and W. Wiesbeck, *Planungsmethoden für die Mobilkommunikation: Funknetzplanung unter realen physikalischen Ausbreitungsbedingungen*, 1st ed. Springer Verlag, Sep. 1998, in German.

[39] H. Holma and A. Toskala, *LTE for UMTS: Evolution to LTE-Advanced*, 2nd ed. John Wiley & Sons, Mar. 2011.

[40] S. Weber, X. Yang, J. Andrews, and G. de Veciana, "Transmission Capacity of Wireless Ad Hoc Networks with Outage Constraints," *IEEE Transactions on Information Theory*, vol. 51, no. 12, pp. 4091–4102, Aug. 2005.

[41] A. Hasan and J. Andrews, "The Guard Zone in Wireless Ad Hoc Networks," *IEEE Transactions on Wireless Communications*, vol. 6, no. 3, pp. 897–906, Mar. 2007.

[42] S. Weber, J. Andrews, X. Yang, and G. de Veciana, "Transmission Capacity of Wireless Ad Hoc Networks With Successive Interference Cancellation," *IEEE Transactions on Information Theory*, vol. 53, no. 8, pp. 2799–2814, Aug. 2007.

[43] R. Tanbourgi, J. Elsner, and F. Jondral, "Lowering Outage Probability in Ad Hoc Networks by Nearest Neighbor FDMA Scheduling," in *IEEE Wireless Communications and Networking Conference 2011*, Cancun, Mexico, Mar. 2011.

[44] N. Jindal, J. Andrews, and S. Weber, "Bandwidth Partitioning in Decentralized Wireless Networks," *IEEE Transactions on Communications*, vol. 7, no. 12, pp. 5408–5419, Dec. 2008.

[45] R. Brooks, "On Colouring the Nodes of a Network," *Mathematical Proceedings of the Cambridge Philosophical Society*, Apr. 1941.

[46] J. Mo, "Performance Modeling of Communication Networks with Markov Chains," *Synthesis Lectures on Communication Networks*, 2010.

[47] D. Stoyan, W. Kendall, and J. Mecke, *Stochastic Geometry and its Applications*, 2nd ed. Wiley, 1995.

[48] A. Baddeley, "Spatial Point Processes and their Applications," in *Stochastic Geometry: Lectures given at the C.I.M.E. Summer School held in Martina Franca, Italy, September 13–18, 2004*, ser. Lecture Notes in Mathematics 1892 (subseries: Fondazione C.I.M.E., Firenze), A. Baddeley, I. Bárány, R. Schneider, and W. Weil, Eds. Springer Verlag, 2006, pp. 1–75.

[49] M. Haenggi, "On Distances in Uniformly Random Networks," *IEEE Transactions on Information Theory*, vol. 51, no. 10, pp. 3584–3586, Oct. 2005.

[50] W. K. Hale, "Frequency Assignment: Theory and Applications," *Proceedings of the IEEE*, vol. 68, no. 12, pp. 1497–1514, Dec. 1980.

[51] G. Chakraborty, "An Efficient Heuristic Algorithm for Channel Assignment Problem in Cellular Radio Networks," *IEEE Transactions on Vehicular Technology*, vol. 50, no. 06, pp. 1528–1539, Nov. 2001.

[52] R. J. Waters, "Graph Colouring and Frequency Assignment," Ph.D. dissertation, University of Nottingham, Nov. 2005. [Online]. Available: http://etheses.nottingham.ac.uk/135/1/waters-thesis.pdf

[53] M. Garey and D. Johnson, *Computers and Intractability: A Guide to the Theory of NP-completeness*, ser. Series of books in the mathematical sciences. W.H. Freeman, 1979.

[54] K. Briggs, L. Song, and T. Prellberg, "A Note on the Distribution of the Maximum of a Set of Poisson Random Variables," *preprint*, Mar. 2009. [Online]. Available: http://front.math.ucdavis.edu/0903.4373

[55] A. Rényi, *Wahrscheinlichkeitsrechnung mit einem Anhang über Informationstheorie*, 6th ed. Berlin: VEB Deutscher Verlag der Wissenschaften, 1979, in German.

[56] D. J. Leith and P. Clifford, "Convergence of Distributed Learning Algorithms for Optimal Wireless Channel Allocation," in *IEEE Conference on Decision and Control*, San Diego, USA, Dec. 2006.

[57] K. R. Duffy, N. O'Connell, and A. Sapozhnikov, "Complexity Analysis of a Decentralised Graph Colouring Algorithm," *Inf. Process. Lett.*, vol. 107, no. 2, pp. 60–63, 2008.

[58] A. Babaei, M. Haenggi, A. P., and B. Jabbari, "Interference Statistics of a Poisson Field of Interferers with Random Puncturing," in *The 2011 Military Communications Conference*, Baltimore, Maryland, USA, Nov. 2011.

[59] T. Ibaraki and N. Katoh, *Resource Allocation Problems: Algorithmic Approaches*. The MIT Press, 1988.

[60] "IEEE 802.15 Coexistence Task Group 2 (TG2) for Wireless Personal Area Networks." [Online]. Available: http://ieee802.org/15/pub/TG2.html

[61] R. Tanbourgi, J. P. Elsner, H. Jaekel, and F. K. Jondral, "Lower Bounds on the Success Probability for Ad Hoc Networks with Local FDMA Scheduling," in *Spatial Stochastic Models for Wireless Networks (SpaSWiN'11)*, Princeton, NJ, USA, May 2011.

[62] P. Pawelczak, S. Pollin, H.-S. So, A. Bahai, R. Prasad, and R. Hekmat, "Performance Analysis of Multichannel Medium Access Control Algorithms for Opportunistic Spectrum Access," *IEEE Transactions on Vehicular Technology*, vol. 58, no. 6, pp. 3014–3031, Jul. 2009.

[63] J. Elsner and R. Tanbourgi, "Mehrebenenfrequenzsprungverfahren zur interferenzreduzierten Kommunikation in einem Ad-Hoc-Netzwerk," German patent application DE 10 2011 015 095.1, Mar. 25, 2011.

[64] J. Lee, J. Mo, M. T. Trung, J. Walrand, and W. H.-S. So, "Design and Analysis of a Cooperative Multichannel MAC Protocol for Heterogeneous Networks," *IEEE Transactions on Vehicular Technology*, vol. 59, no. 7, pp. 3536–3548, Sep. 2010.

[65] P. Bahl, R. Chandra, and J. Dunagan, "SSCH: Slotted Seeded Channel Hopping for Capacity Improvement in IEEE 802.11 ad-hoc Wireless Networks," in *Proceedings of the 10th annual international conference on mobile computing and networking*, ser. MobiCom '04. New York, NY, USA: ACM, Sep. 2004.

[66] W. H.-S. So, J. Walrand, and J. Mo, "McMAC: A Parallel Rendezvous Multi-Channel MAC Protocol," in *IEEE Wireless Communications and Networking Conference*, Hong Kong, China, Mar. 2007.

[67] A. Nijenhuis and H. S. Wilf, *Combinatorial Algorithms*. Academic Press Inc., 1978. [Online]. Available: http://www.math.upenn.edu/~wilf/website/CombAlgDownld.html

[68] R. Tanbourgi, J. P. Elsner, H. Jaekel, and F. K. Jondral, “Adaptive Frequency Hopping in Ad Hoc Networks with Rayleigh Fading and Imperfect Sensing,” *IEEE Wireless Communications Letters*, Jun. 2012.

[69] ——, “Optimizing Practical Adaptive Frequency Hopping and Medium Access Control in Ad Hoc Networks,” in *Spatial Stochastic Models for Wireless Networks (SpaSWiN’12)*, Paderborn, Germany, May 2012.

[70] J. Elsner, M. Braun, S. Nagel, K. Nagaraj, and F. Jondral, “Wireless Networks In-the-Loop: Software Radio as the Enabler,” in *Software Defined Radio Forum Technical Conference*, Washingtion, D.C., USA, Dec. 2009.

[71] S. Koslowski, M. Braun, J. Elsner, and F. K. Jondral, “Wireless Networks In-the-Loop: Emulating an RF front-end in GNU Radio,” in *Software Defined Radio Forum European Reconfigurable Radio Technologies Workshop*, Mainz, Germany, Jun. 2010.

[72] F. Jondral and A. Wiesler, *Wahrscheinlichkeitsrechnung und stochastische Prozesse*, 2nd ed. Stuttgart: B. G. Teubner, 2002, in German.

[73] J. A. Bondy and U. S. R. Murty, *Graph Theory with Applications*. North-Holland, 1976, fifth printing, 1982.

Supervised theses

While employed at the Communication Engineering Lab of the Karlsruhe Institute of Technology, the following student theses and projects were supervised.

Martin Braun	*Applications of Compressed Sensing in a Cognitive Radio context* (Diplomarbeit)
Kshama Nagaraj	*GNU Radio SPEEX – digital narrow band voice transmission* (Studienarbeit)
Kshama Nagaraj	*Wireless Network In-The-Loop: Software Radio as the enabler* (Master thesis)
Gerald N. Baier	*Implementing Thomson's Multitaper Method in GNU Radio* (Bachelor thesis)

Reinhard Gentz	*Abschätzungen und numerische Berechnung von Interferenzverteilungen Poisson'scher Punktprozesse* (Bachelor thesis)
Christian Mohr	*Einfluss von Frequency Division Multiple Access auf die Übertragungskapazität von ad hoc Netzwerken* (Master thesis)
Moritz Krüger	*Implementierung eines parametrischen AR-Spektralschätzers nach der LS-Kovarianzmethode* (Bachelor thesis)
Jörg Schmid	*Modellierung der Kapazität drahtloser mehrkanaliger Ad-hoc-Netze mit Methoden der stochastischen Geometrie* (Diplomarbeit)
Francisco de Borja Ortiz de la Orden	*A Multiple Collision Domain Model for Multi-Channel MACs* (Master thesis)
Felix Wunsch	*Implementation of a DRM+ transmitter in the GNU Radio software radio framework* (Bachelor thesis)

Index

Sponsorship

The author's research visit to the *Network Economics, Management and Optimization Lab* headed by Professor Jeonghoon Mo at Yonsei University, Seoul, Korea, was supported by the Karlsruhe House of Young Scientists (KHYS) and the Communications Engineering Lab of KIT.